Recombinant Electron Donors and Acceptors to and From Reaction Center Particles, and Light Dependent Menaquinone Reduction in Isolated Membranes of Heliobacterium Modesticaldum

by

Trevor Kashey

A Dissertation Presented in Partial Fulfillment
of the Requirements for the Degree
Doctor of Philosophy

Approved February 2015 by the
Graduate Supervisory Committee:

Kevin Redding, Chair
Petra Fromme
Giovanna Ghirlanda

ARIZONA STATE UNIVERSITY

MAY 2015

ABSTRACT

The Heliobacterial reaction center (HbRC) is generally regarded as the most primitive photosynthetic reaction center (RC) known. Even if the HbRC is structurally and functionally simple compared to higher plants, the mechanisms of energy transduction preceding, inside the core, and from the RC are not totally established. Elucidating these structures and mechanisms are paramount to determining where the HbRC is in the grand scheme of RC evolution. In this work, the function and properties of the solubilized cyt c553, PetJ, were investigated, as well as the role HbRC localized menaquinone plays in light-induced electron transfer, and the interaction of the Nif-specific ferredoxin FdxB with reaction center particles devoid of bound FA/FB proteins. In chapter 2, I successfully express and purify a soluble version of PetJ that functions as a temperature dependent electron donor to P800+. Recombinant PetJ retains the spectroscopic characteristics of membrane-bound PetJ. The kinetics were characteristic of a bimolecular reaction with a second order rate of 1.53 x 104 $M^{-1}s^{-1}$ at room temperature and a calculated activation energy of 91 kJ/mol. In chapter 4, I use reverse phase high-performance liquid chromatography (HPLC) to detect the light-induced generation of Menaquinol-9 (MQH2) in isolated heliobacterial membranes. This process is dependent on laser power, pH, temperature, and can be modified by the presence of the artificial electron acceptor benzyl viologen (BV) and the inhibitors azoxystrobin and terbutryn. The addition of the bc complex inhibitor azoxystrobin decreases the ratio of MQ to MQH2. This indicates competition between the HbRC and the bc complex, and hints toward a truncated cyclic electron flow pathway. In chapter 5, the Nif-Specific ferredoxin

FdxB was recombinantly expressed and shown to oxidize the terminal cofactor in the HbRC, FX^{-}, in a concentration-dependent manner. This work indicates the HbRC may be able to reduce a wide variety of electron acceptors that may be involved in specific metabolic processes.

DEDICATION

I want to dedicate this work to Dr. James Tuohy. He was awesome enough to take a risk and accept me as a student in his molecular biology course before I was even old enough to drive myself to the building the class was held in. Dr. T was patient with my incessant rudimentary questions, ridiculous obsession with hypothetical scenarios, and general classroom antics. He fostered my curiosity more than anyone else in my life combined. It is because of him that I will be a lifelong student of the biochemical sciences and do my best to educate anyone willing to listen. I guess my mom was pretty cool to drive me to these classes, too. I love you mom.

ACKNOWLEDGMENTS

I came into contact with Kevin Redding during a tough time in my life, and his child-like love of fundamental science helped pull me out of my slump, subsequently prompting me to harass him until he let me work in his laboratory. He is quite simply the best educator, both theoretical and applied, that I have ever come into contact with. One day, I hope to be one quarter of the scientist he is. I need to thank my lab manager, Patricia Baker, for being a fantastic role model and a great resource for just about anything I could need. Her patience with user manuals has single handedly prevented me from throwing every machine out the window at least once. Lastly, I want to thank Chris Gisreal for being the friend I needed when the sky may as well have been falling, and may his exceptional work ethic inspire other budding scientists to be the best they can be. I am appreciative of all the members of the Redding lab, past and present, I have learned from you all.

TABLE OF CONTENTS

CHAPTER Page

CHAPTER Page

LIST OF TABLES

LIST OF FIGURES

CHAPTER 1

GENERAL INTRODUCTION

General Photosynthesis:

Photosynthesis is a progression of redox reactions where light is harnessed and converted into chemical energy that powers metabolic processes in living organisms. The individuality of the system's implementation is determined by the biochemical requirements of the cell. Thus, the details can vary greatly. The most highly studied variation of photosynthesis is oxygenic photosynthesis (*1*).

Photosynthesis can be broken down into the light and the dark reactions. Simply put, in the light reactions, radiative energy from absorbed photons is converted into chemical energy in the cell, mostly in the form of Adenosine Triphosphate (ATP) and Nicotinamide Adenine Dinucleotide Phosphate (NADPH) (*1*).Once these compounds are created, they are used in the dark reactions to synthesize biomolecules from CO_2 for longer-term storage of chemical energy (*1*).

There are also several variations of photosynthesis that do not result in oxygen production, commonly referred to as anoxygenic photosynthesis. Globally, the mechanisms for photosynthesis between systems vary greatly, but the process of light energy conversion is strikingly similar (*1*).

General Reaction Center Function:

Photon energy transduction is a three-step process. The first step is the absorption of the photon by pigments in the reaction center complex or attached antenna (*1*). Light harvesting pigments absorb the light and energy eventually moves toward the reaction center core. The energy is transferred from pigment to pigment as excited states. In step two, the primary electron donor, or "special pair" (P) of chlorophylls receives the exciton, becoming a strong reductant (*1*). The special pair can thus reduce an adjacent acceptor pigment (A) within the core to make the initial charge-separated state ($\mathbf{P^+A^-}$). In the third step, the charge-separated state is stabilized by subsequent electron transfer from the primary acceptor to the secondary acceptor and the to the tertiary acceptor, etc. These acceptors are placed at discrete distances and bound in specific orientations, and have redox potentials tuned to expedite transfer between them(*1*). The amino acids that line the binding pockets of the cofactors provide the specific microenvironments to facilitate this process. The cofactors are arranged such that the energy of the subsequent charge-separated states declines after each transfer, effectively directing the electron away from the core and ultimately to mobile carriers that can provide reducing equivalents to other metabolic pathways (e.g. CO2 fixation). As a result of the multi-transfer process, the system loses free energy, the distance from the primary donor is increased, and the stability (and lifetime) of the charge-separated state is increased (*1*).

The types of cofactors that serve as cofactors within the reaction center core are the basis for classifying reaction centers. Reaction centers in the Type I category have a bound iron-sulfur cluster as the terminal electron acceptor. Reaction centers in the Type II category have a mobile quinone as the terminal electron acceptor. Organisms that

participate in oxygenic photosynthesis have Photosystem I and Photosystem II that work sequentially to split water and reduce $NADP^+$ (*1*).

Type II Reaction centers:

As far as bacteria go, there are two known groups that work with type II reaction centers, green non-sulfur bacteria and purple bacteria. Interestingly, both of these groups use the type II reaction center exclusively(*1*). In a photochemical event, the reaction center will stabilize a charge-separated state within the photosynthetic membrane. After which, it facilitates a double reduction event, converting quinone to hydroquinone. The electrons that the RC uses to catalyze this reaction are repleted by the exogenous ferrocytochrome c_2. The conversion of quinone to hydroquinone (quinol) goes handedly with the efflux of protons from the cytoplasm to the RC to facilitate the reduction. After the double reduction event, the quinol migrates from the binding pocket through the periplasm and eventually becomes reoxidized back to quinone by the membrane integrated cytochrome bc_1 complex(*2*). The oxidation event from the cytochrome leaves the protons to diffuse into the periplasm, and the remaining electrons are used to reduce cytochrome c_2. This quinone cycling phenomenon provides the electrochemical gradient necessary to facilitate the synthesis of ATP, which takes place in the third and final step, the ATP synthase complex (*1*).

The function of photosystem II is to split water and produce plastoquinol. The reaction center polypeptide count varies from between groups. Eukaryotic photosystem II

contains up to 25 subunits, while the cyanobacterial photosystem II reaction center contains 21 polypeptides (*1*). The secondary electron donors and acceptors are bound in the main subunits D1 and D2. The special pair in photosystem II is made up of two chlorophyll a molecules (P680). The adjacent acceptor to P680 is a pheophytin molecule (chlorophyll without magnesium). From here, the pheophytin reduces two quinones (Q_A and Q_B) in a sequential manner. Both Q_A and Q_B are stable in their binding pockets in the radical state. Once a secondary charge separation has occurred and a second electron gets funneled through the RC Q_b is reduced. Following, the plastoquinol is ejected into the membrane. When (reduced) plastoquinol leaves the binding pocket, (oxidized) plastoquinone re-fills the Q_B site; the cytochrome b_6f complex oxidizes the plastoquinol molecule that leaves the binding pocket(*1*). Ultimately, this creates the proton flux required for the biosynthesis of ATP. The act of splitting water provides reducing equivalents for the newly oxidized $P680^+$ photosystem II, while the electron that is harvested from the plastoquinol is kicked back to an electron donor such as cytochrome c_6 or plastocyanin and act as the donors to photosystem I (*1*).

Type I Reaction Centers:

Unlike the situation with the type 2 RCs, Photosystem I (PSI) of oxygenic phototrophs is the best-characterized member of the type I RCs and much less is known about the type I RCs of anoxygenic phototrophs. Photosystem I uses an absorbed photon to both reduce ferredoxin and oxidize plastocyanin (or cyt *c*). This light-driven plastoquinone:ferredoxin

oxidoreductase contains twelve subunits, and contain an impressive 110+ cofactors (*3*), a bulk of which are bound to PsaA and PsaB, which form the core of the protein. Photosystem I also has a special pair of chlorophylls (*a* and *a'* respectively) acting as the primary donor in the core (dubbed P_{700}). Once a photon is absorbed by the antenna, the excited state energy makes its way to P_{700} initiating electron transfer within the photosystem I core. After P_{700} acquires the excited state energy it donates an electron to an adjacent chlorophyll *a* molecule (A_0). This creates the charge-separated state between P_{700}^+ (primary donor) and A_0^- (primary acceptor) (*3*). Phylloquinone (A_1) acts as the secondary acceptor, being reduced by A_0^-. Lastly, an electron is transferred from A_1^- to a series of three [4Fe-4S] clusters. First, the electron is transferred to F_X, a [4Fe-4S] cluster located at the interface of PsaA and PsaB, then afterwards to F_A and F_B. Interestingly, F_A and F_B are harbored in a separate ferredoxin-like subunit called PsaC (*3*). This will have interesting implications for studies of the heliobacterial type I reaction center. Once the electron is transferred to F_B it is donated to a mobile ferredoxin. This ferredoxin has a potential low enough to reduce $NADP^+$ to NADPH by virtue of the ferredoxin:$NADP^+$ oxidoreductase enzyme (*3*). Another important event worth discussing (and expounded upon later) is what happens during this process when there is the absence of both an electron donor to P_{700}^+ (such as cytochrome c_6 and plastocyanin) and an electron acceptor for F_B^-. When the reaction center lacks these two participants, the system will recombine, setting itself back to a neutral state (*4*). The rate of charge recombination is dependent on which cofactor the electron is residing. The further the cofactor is from P_{700}^+, the longer the back reaction will take (*4*).

Worth noting, In 2010, Muller et al. (*5*) did a study on photosystem I in *Chlamydomonas reinhardtii* where the amino acids providing hydrogen bonds to the ec3 chlorophylls were mutated, on both branches. Not only did the point mutations tune the directionality of electron transfer, biasing a particular branch, but it corroborated an electron transfer model in PSI in which ec2 is the primary electron donor. This would make the first radical pair $ec2^{+}/ec3^{-}$ followed by the generation of $P_{700}^{+}/ec3^{-}$.

Heliobacteriaceae (*6*) , *Chlorobiaceae* (*7*), and acidobacteria(*8*) are the only bacterial groups known that exclusively contain a Type 1 reaction center. Interestingly, they are also all homodimeric, in contrast to the heterodimeric PSI. The chlorobium reaction center (RC) core is a homodimer made up of two PscA polypeptides. The PscA homodimer binds roughly 22 chlorophyll molecules, along with the special pair P840 (thought to be a pair bacteriochlorophyll *a'* (*9*)), the primary acceptor A_0 (chlorophyll *a* 670 (*10*)), and an endogenous [4Fe-4S] cluster F_X (*11*). Likewise, *H. modesticaldum* also utilizes chlorophyll *a* as its A_0 pigment. However, it is not utilized anywhere else in these organisms. As with PSI, the process of charge separation and electron transfer begins after the antennae pigments capture a photon and transfer the excitation energy to P840. P840* then donates an electron to A_0, creating the initial charge-separated state $P840^{+}A_0^{-}$ (*3*). From here, it would seem that A_0^{-} reduces the [4Fe-4S] cluster F_x directly without the use of a quinone intermediate. F_x^{-} then reduces the [4Fe-4S] clusters F_A and F_B (*3*), which are bound by the PscB polypeptide. Unlike PSI, the role of the quinone is not yet understood in the homodimeric type I RCs. This type I RC also contains a membrane bound cytochrome (*12*) (PscC) that acts as a reductant for $P840^{+}$ along with the Fenna-

Mathews-Olson protein, which acts as an antenna complex (with approximately 40 bacteriochlorophyll *a* molecules) linking to the chlorosome antenna complex (*13*). All of these subunits work together in order to provide reductive power to produce NADPH (*14*).

Compared to PSI, there is a paucity of information regarding the heliobacterial RC (HbRC) . The total number of subunits is still under debate. However, the HbRC core consists of nothing more than the PsaA homodimer.

Heliobacterial Discovery and Classification:

In 1981, *Heliobacterium chlorum* was discovered during a series of soil enrichment experiments that were meant to isolate nitrogen-fixing bacteria under photoheterotrophic conditions (*15*). Serendipitously, sulfate was added to the medium and became reduced to sulfide, selecting against purple bacteria that would typically grow in the medium. A brown-green biofilm formed on the plates, and this ultimately was identified as a new kind of phototroph, leading to the introduction of the *Heliobacteriaceae* bacterial family

Heliobacteria are wholly anaerobic. When exposed to oxygen and light, their unique pigment, bacteriochlorophyll *g*, will isomerize into chlorophyll *a* (turning from brownish to green) and they will die (*15*). True to the original enrichment medium, further study also indicated that heliobacteria are (photo)heterotrophs, growing better in the presence of light but requiring a reduced carbon source (*15*). Heliobacteria are

capable of heterotrophic growth in the dark (*16*). During fermentative growth in the dark, the doubling time of the organism is notably increased, while the carbon source that will allow growth is essentially limited to pyruvate and similar organic acids (*16*).

In reports of all current heliobacterial species, they have always been characterized as photoheterotrophs (*15, 17-20*). Heliobacteria are mostly dependent on carbon sources such as acetate, lactate, butyrate, and pyruvate (*21, 22*). After Kimble et al. tested 13 different heliobacterial species (Including *H. modesticaldum*), the metabolism of organic compounds is certainly light dependent and is limited to lactate and pyruvate while growing in the dark (*16, 22*). According to the sequenced genome of *Heliobacterium modesticaldum*, key enzymes in every known carbon fixation pathway are missing (*23*).

Heliobacteria use the reductive power of photosynthesis to aid in their capacity to fix nitrogen. The nature of some of the organisms in this group (e.g. H. *modesticaldum)* would suggest a symbiotic nature between heliobacteria, and possibly a grain plant like rice, where heliobacteria provide nitrogen compounds and the plant provides reduced carbon sources(*24*). Being isolated in fertile soil coupled with the capacity to fix nitrogen would lead to a reasonable hypothesis that these bacteria play an important role in the local ecology. Nitrogen fixation is a very energy intensive process requiring 16 ATP and 8 low-potential electrons to biosynthesize two ammonia molecules per dinitrogen (N_2). The type 1 RC of heliobacteria has the capacity to use light to create the means, such as ferredoxin, that are reducing enough to facilitate nitrogen fixation. Heliobacteria

can fix nitrogen in the dark, but it is far less efficient, and requires pyruvate to facilitate it (*24*).

It is now known that all of the pigments involved in photosynthetic electron transfer are exclusively located within the $PshA_2$ homodimer (*25*). Along with bacteriochlorophyll *g*, heliobacteria are also unique among the phototrophs in that they lack an external antennae complex(*26*). The complete lack of external pigment binding antennae complexes combined with the homodimeric structure would support the idea that the heliobacterial photosynthetic apparatus is primitive.

Heliobacterial Reaction Center:

Interestingly, the gene encoding the PshA protein is located in the genome adjacent to other open reading frames that encode pigment-producing enzymes and is not next to other proteins that facilitate electron transfer (*23*). The adjacent genes code for carotenoid and bacteriochlorophyll synthesis pathways. Secondarily it is also close to genes encoding subunits of the cytochrome *bc* complex (*23*).

one of the unique characteristics in heliobacteria is the use of bacteriochlorophyll *g.* This pigment is a tautomer of chlorophyll *a* with a vinyl group at position 3, and also structurally similar bacteriochlorophyll *b* (ethylene at position 8 and II ring saturated) (*27*). Once bacteriochlorophyll *g* is exposed to oxygen in the presence of light, the saturated ring isomerizes and becomes spectroscopically comparable to chlorophyll *a*(*27*). This conversion also occurs in the presence of acid in the absence of oxygen (*28*).

This type of chlorophyll may have an interesting selective advantage in its environment by being able to capture both near-infrared and near-ultraviolet light (*27*). Bacteriochlorophyll g' makes up the primary donor (P800) in the HbRC. The pair was originally named P798 due to the maximal bleaching at that wavelength after light exposure in *Heliobacterium chlorum* (*29*). With a redox potential of ~+225 mV, it is of the lowest known potential of any RC (*29*).

The primary acceptor of P800, A_0, bleaches at 670 nm upon formation of the $P_{800}^{+}A_0^{-}$ state, and this bleaching then decays with a lifetime of ~700 ps (*30*). A_0, although spectroscopically similar to chlorophyll *a* was actually 8^1hydroxy-chlorophyll *a* with a farnesyl tail (*31*). This similarity may also hint at an evolutionary link between the two types of photosystems (*32*). The homodimeric construction of the reaction center would suggest that A_0 is identical on each branch and that the utilization of each pathway is 50/50.

Menaquinone is the only quinone used by heliobacteria. The menaquinone population varies only by the length of the tail, commonly with lengths of 7, 8, 9, and 10 isoprene units (*33*). Menaquinone-9 is by far the dominant pigment in *H. modesticaldum* (*25*). Green sulfur bacteria use menaquinone-7, and menaquinone-10 has been detected in Chloroflexus (*34*). This may reflect that anaerobes tend to use menaquinone and aerobes use ubiquinone (*35*) or other quinones, such as phylloquinone (*36*)due to the difference in redox potentials. Menaquinones are lower potential, so they would be more suited to anaerobic environments (*37*). In the membrane, there are approximately 5 menaquinones per reaction center when normalized to 22 Bchl *g*. There are 1.5-2 menaquinones in each

isolated reaction center, and the yield can vary between preparations (*25*). The literature regarding the MQ in the HbRC is equivocal about its role. Photoaccumulation of semimenaquinone was first observed in *Hc. mobilis* and *H. chlorum* (*38, 39*). However, removal of the quinone via extraction techniques does not interfere with forward electron transport processes (*40*). It is unlikely that the quinone in heliobacteria has no role, but it may not play a part in forward electron transfer. There is little reason for a pigment to be included in the reaction center and not have some purpose.

The 4Fe-4S cluster (F_X), when compared to photosystem I, the binding pocket for F_X would be most likely located at axis of symmetry between the homodimer. Not surprisingly, this area has a largest sequence identity with photosystem I (*41*). The physical and biochemical characteristics of F_X make its direct study using EPR arduous, as it is both buried in the homodimer, very reducing, and the optical spectra of iron-sulfur proteins are unremarkable. A shoulder in the 400-430 nm region is the only signature characteristic in the spectra(*42*). Overlapping spectra of other pigments in their excited states make resolving F_X difficult. Even though these complications exist, difference spectra in the visible region show signature Fe/S cluster shouldered peak around 430 nm(*43*)

The presence of F_X is supported by spectroscopic studies. After PshB is removed, when particles are exposed to light, there is a charge recombination with P_{800}^+ that has a lifetime of about 20 ms (*43*) which is corroborated by a 15ms lifetime via Heinnickel et al. (*44*). When the P_{800}^+ portion of the spectrum was subtracted, it left the otherwise featureless spectrum with a shoulder between 400 and 500 nm, with the maximum

absorption point at 430 nm; the differential extinction coefficient at that maxima was calculated to be between 10 and 11 mM^{-1} cm^{-1} (*43*) which is comparable to the Fe/S clusters in PSI (*45*).

Currently published literature shows conflicting EPR data when comparing both membranes and purified particles. Heinnickel et al. had illuminated HbRC sans PshB at room temperature and reported monophasic kinetics with a lifetime of 15 ms. Mossbauer spectroscopy confirmed all iron in the HbRC cores were existing as $[4Fe\text{-}4S]^{2+}$ clusters. When the HbRC particles were illuminated in the presence of dithionite the iron was shown to exist in a $[4Fe\text{-}4S]^{1+}$ state. X-band EPR measurements on photoaccumulated HbRC samples pre-reduced with dithionite at 77K produced a spectrum akin to the [4Fe-4S] nitrogenase iron protein with a spin 3/2 state (*46*).

Miyamoto et al. showed a light-minus-dark difference spectrum in pre-reduced HbRC (containing F_A/F_B) samples at 5k. The signal produced was assigned to a photoreducible, fast relaxing, F_X cluster in a spin 1/2 state. Interestingly, these results could not be replicated once the F_A/F_B clusters were removed.

John Cowgill of our lab performed EPR at 77K on dithionite reduced HbRC (pH 6 and 10) and dithionite reduced carbonate washed membranes, and the spectrum was assigned to a spin 3/2 which corroborates the data from Heinnickel et al. (*46*). Moreover, his electrochemical and photochemical studies found the midpoint potential to be -372 mV and -502 mV respectively. Regardless of the differing values, they are both significantly more reducing than F_X in PSI. A higher reduction potential would stabilize a

reduced F_X, and this would explain the longer lifetime of the $P_{800}^+ F_X^-$ state as compared to PSI (*44, 47*).

The F_A/F_B clusters are held in a loosely bound polypeptide called PshB. The analogous subunit in photosystem I is PsaC (*48*). However, PsaC is strongly associated with photosystem I(*49*), while PshB can dissociate under relatively mild conditions (*44*).

PsaC is a PSI subunit that contains the F_A/F_B clusters. It interacts with the PsaA/PsaB core on the stromal side of the membrane adjacent to F_X (*50*). The extended C-terminus is thought to be in involved with preliminary docking to PsaB via the hydrogen bonds that are made by the C-terminus of PsaC to PsaB (*51*). A full deletion of the C-terminal end on PsaC prevents assembly in the native conformation(*49*). After initial docking via hydrogen bonds from the C-terminus, PsaC binds tightly PSI due to 10 ionic interactions that share C_2-symmetry split evenly between PsaA and PsaB and 3 asymmetric hydrogen bonds between a superficial portion PsaB and the C-terminus of PsaC (49). Once PsaC has oriented itself onto PsaA and PsaB, PsaD connects with all three peptides. PsaD overlaps the bound C-terminal portion of PsaC whilst adhering to PsaA and PsaB (*50*). PsaD forces PsaC into its native position and provides the platform for ferredoxin interaction while simultaneously promoting complex stability(*52*).

An interesting point about the mobile acceptor hypothesis is that there is actually a paralogous gene to *pshb* (HM1_1462); adjacently placed in a dicistronic operon (HM1_1461) (*23*). Both genes code for a 54 amino-acid dicluster ferredoxin with a sequence identity of 62%. It was hypothesized that because of sequence identity, and conservation of the dual CxxCxxCxxxC motif, that the functional characteristics of these

proteins would be similar. After recombinant expression and purification of HM1_1462 and HM1_1461, these proteins were shown to accept electrons from the HbRC cores, which is dependent on ionic strength (*53*). It is unclear whether the purpose of the paralog is to increase the acceptor pool, provide reducing equivalents to specific proteins in separate parts of the cell's biochemistry, or possibly provide a less oxygen sensitive alternative (*54*). The protein dosage hypothesis seems reasonable, but transcriptomic analysis shows a 5-fold difference in expression for PshB I compared to PshB II in typical growth conditions (unpublished data). Moreover, there are no features that are analogous to the C-terminal loop or the PsaD clamp, both of which are integral in robust adherence of PsaC to the PsaA/PsaB heterodimer (*49*) . The lifetime of the $P800^{+}F_X^{-}$ charge-separated state is actually an order of magnitude longer than the analogous state in PSI (*55*). The longer-lived charge separated state may give time for the soluble electron carriers to dock, accept electrons, and then dissociate and diffuse away.

EPR data in membranes show that F_A/F_B are visible under liquid nitrogen and intense light, and each is individually distinguishable (*48*). Similar to F_X, procuring optical information on F_A/F_B is difficult. There is little to optically distinguish F_A/F_B and F_X. As discussed above, purified particles from heliobacteria do not show the presence of F_A/F_B. Further study showed that the purification of the reaction center causes F_A/F_B to dissociate (*44*). Moreover, lack of an extended C-terminal loop to guide correct orientation, and a PsaD analog to stabilize docking opposes the permanent subunit hypothesis. Lastly, PshB is part of an operon that contains (now named) PshBII (*23*). This is a paralogous F_A/F_B containing protein with high sequence homology to PshB

(*23*). When incubated with reaction center particles, it can act in the place of PshB. PshBII is likely acting as an alternative acceptor *in vivo* (*53*). Also interesting, the heliobacterial reaction center has been shown to interact with cyanobacterial flavodoxin completely independent of F_A/F_B (*56*).

The last pigment to the heliobacteria family is their endogenous diapocarotenoids. 4,4-diaponeurosporene is a thirty carbon acyclic carotenoid with 9:1 conjugated to non-conjugated bonds (*57*). This pigment is the entirety of the carotenoid population in the cell (*57*). As compared to other phototrophic organisms, heliobacteria contain a small amount of carotenoid (*15*). Currently, there is no evidence supporting active involvement of 4,4-diaponeurosporene in any cellular process. The singular carotenoid found in the isolated HbRC is also interesting, not only due to the strange stoichiometry (since the reaction center is a homodimer), but because there is no known involvement in any process(*58*). It is not unrealistic to assume that the carotenoid way work as a pigment that affords photoprotection, possibly in the presence of oxygen (*15*) (*59*) (*47*).

Membrane-attached Cytochrome in Heliobacteria:

Cytochromes are a diverse group of proteins, and all are involved in electron transfer processes. These proteins are normally associated with complexes and integrated into membranes outside of the cytosol. Among the heliobacterial family, the dominant membrane-anchored cytochromes have similar amino acid sequences, with particularly high homology in the redox-active domain of the protein (*60*). The membrane-anchored

proteins are monoheme *c*-type cytochromes (*61*). There are no soluble cytochromes in heliobacteria, and identifying the specific donors to the special pair is difficult because all the *c*-type cytochromes have and alpha-band absorption in the same 553 nm range. The cytochromes retain their activity in isolated membranes (*61*). In the case of cyt c_{553} the alpha band is located at 553 nanometers while in its reduced form (*61*). Interestingly, this cytochrome is not integrated into the membrane via transmembrane helices, but a thioether-linked diacylglyceride (DAG) attached to the N-terminus (*61*). Cytochrome c_{553} is a protein responsible for re-reducing $P800^{+}$. There is no selective pressure to maintain tight binding, as there is in soluble cytochromes. The dependence of soluble cytochromes and electrostatic interactions is likely so the protein can orient itself from a longer range (*60*).

Soluble cytochromes are much quicker to bind than they are to dissociate (*62*). Observations of light induced changes in heliobacterial membrane cytochrome included a bleaching event at 553 nm that is the addition of 3 exponential decays with half-times of 4 ms 18 ms and a long lived component. The first component is assigned to recombination of the special pair, the second component is assigned to reduction of the membrane associated cytochrome c_{553} and the third is associated with a slow reduction by ascorbate (Figure 3.5). Forward electron transfer is faster in whole cells than it is in isolated membranes (*63*). Currently characterized cytochromes in heliobacteria are implicated in direct and indirect reduction of P_{800}^{+} (*61, 64, 65*). In whole cells of heliobacteria, the cytochrome c_{553} re-reduces the special pair in less than a millisecond (*63*). The 18 kDa (membrane attached) and the 50 kDa cytochrome *c*'s are involved with

reduction of P_{800}^{+}. The 18 kDa cytochrome c_{553}, PetJ, is the most abundant cytochrome protein in the cell interactions with two other peptides making the cytochrome c_{553} complex (*61*).

Heliobacterial cytochrome *bc* complex

The cytochrome *bc* complex in heliobacteria is an integral protein complex in facilitating cyclic electron transfer and producing the proton gradient for ATP production. They are transmembrane quinol oxidizing enzymes that reduce one-electron carriers in the periplasm. The putative genes that have been labeled code for four subunits are: The Rieske iron sulfur protein (PetC), the diheme cytochrome *c* (PetA), and subunit IV (PetD) (*23*). Cytochrome *b* has been shown to be a cytochrome b_6 like protein (*66*). Inhibitor studies show that the heliobacterial *bc* complex is sensitive to the inhibitor stigmatellin, which inhibits the Q_O site (*64*). It's possible that the cytochrome *bc* complex is comparable to the cytochrome b_6f complex in cyanobacteria, however, instead of the cytochrome *f* found in the b_6f complex heliobacteria use a diheme cytochrome *c* (*67*). This is a change in the cytochrome c_1 that bacterial bc_1 complexes use (*68*). Analysis of modeled structures and sequence alignments show integral properties: it is predicted to be an alpha-helix rich protein with a globular structure and contains an N-terminal transmembrane helix akin to cytochrome c_1 (*68*). Secondly, the heme binding domains on both termini share high sequence similarity making it a cytochrome c_4-type polypeptide. These are diheme cytochromes possibly came from a gene duplication, creating two

heme binding domains that resemble a typical type I monoheme cytochrome (*68*). The subunit containing the diheme cytochrome *c* differentiates the heliobacterial complex from other anoxygenic photosynthetic bacteria, and the function is not yet fully understood.

REFERENCES

1. R. E. Blankenship, *Molecular Mechanisms of Photosynthesis*. (Blackwell Science Ltd, Oxford, 2002), pp. 321.

2. J. Deisenhofer, H. Michel, Nobel lecture. The photosynthetic reaction centre from the purple bacterium Rhodopseudomonas viridis. *Embo J* **8**, 2149-2170 (1989).

3. K. Brettel, W. Leibl, Electron transfer in photosystem I. *Biochimica Et Biophysica Acta-Bioenergetics* **1507**, 100-114 (2001).

4. V. P. Shinkarev, B. Zybailov, I. R. Vassiliev, J. H. Golbeck, Modeling of the P700+ charge recombination kinetics with phylloquinone and plastoquinone-9 in the A1 site of photosystem I. *Biophysical Journal* **83**, 2885-2897 (2002).

5. M. G. Müller, C. Slavov, R. Luthra, K. E. Redding, A. R. Holzwarth, Independent initiation of primary electron transfer in the two branches of the photosystem I reaction center. *Proc Natl Acad Sci U S A* **107**, 4123-4128 (2010).

6. S. Neerken, J. Amesz, The antenna reaction center complex of heliobacteria: composition, energy conversion and electron transfer. *Biochimica et Biophysica Acta* **1507**, 278-290 (2001).

7. G. Hauska, T. Schoedl, H. Remigy, G. Tsiotis, The reaction center of green sulfur bacteria. *Biochimica et Biophysica Acta* **1507**, 260-277 (2001).

8. D. A. Bryant *et al.*, Candidatus Chloracidobacterium thermophilum: an aerobic phototrophic Acidobacterium. *Science* **317**, 523-526 (2007).

9. G. Hauska, T. Schoedl, H. Remigy, G. Tsiotis, The reaction center of green sulfur bacteria. *Biochimica et Biophysica Acta* **1507**, 260-277 (2000).

10. M. Kobayashi *et al.*, The primary electron acceptor of green sulfur bacteria, bacteriochlorophyll 663, is chlorophyll a esterified with D2,6-phytadienol. *Photosynthesis Research* **63**, 269-280 (2000).

11. M. Büttner *et al.*, The photosystem I-like P840-reaction center of green S-bacteria is a homodimer. *Biochimica et Biophysica Acta* **1101**, 154-156 (1992).

12. J. S. Okkels *et al.*, A membrane-bound monoheme cytochrome c551 of a novel type is the immediate electron donor to P840 of the Chlorobium vibrioforme photosynthetic reaction center complex. *Journal of Biological Chemistry* **267**, 21139-21145 (1992).

13. H. P. Permentier *et al.*, Reaction center complexes of green sulfur bacteria. *Photosynthesis: Mechanisms and Effects, Proceedings of the International Congress on Photosynthesis, 11th, Budapest, Aug. 17-22, 1998* **1**, 527-530 (1998).

14. G. Hauska, T. Schoedl, H. Remigy, G. Tsiotis, The reaction center of green sulfur bacteria(1). *Biochimica et Biophysica Acta* **1507**, 260-277 (2001).

15. H. Gest, J. L. Favinger, Heliobacterium chlorum, an anoxygenic brownish-green bacterium containing a `new' form of bacteriochlorophyll. *Arch Microbiol* **136**, 11-16 (1983).

16. L. K. Kimble, A. K. Stevenson, M. T. Madigan, Chemotrophic growth of heliobacteria in darkness. *FEMS Microbiol Lett* **115**, 51-55 (1994).

17. L. K. Kimble, L. Mandelco, C. R. Woese, M. T. Madigan, Heliobacterium modesticaldum, sp. nov., a thermophilic heliobacterium of hot springs and volcanic soils. *Arch Microbiol* **163**, 259-267 (1995).

18. P. Beer-Romero, H. Gest, Heliobacillus mobilis, a peritrichously flagellated anoxyphototroph containing bacteriochlorophyll g. *FEMS Microbiology Letters* **41**, 109-114 (1987).

19. A. K. Stevenson, L. K. Kimble, C. R. Woese, M. T. Madigan, Characterization of new phototrophic heliobacteria and their habitats. *Photosynthesis Research* **53**, 1-12 (1997).

20. I. A. Bryantseva, V. M. Gorlenko, E. I. Kompantseva, L. A. Achenbach, M. T. Madigan, Heliorestis daurensis, gen. nov. Sp. Nov., An alkaliphilic rod-to-coiled-shaped phototrophic heliobacterium from a siberian soda lake. *Arch Microbiol* **172**, 167-174 (1999).

21. M. T. Madigan, J. G. Ormerod, Taxonomy, physiology and ecology of heliobacteria. *Advances in Photosynthesis* **2**, 17-30 (1995).

22. M. W. Pickett, M. P. Williamson, D. J. Kelly, An enzyme and 13C-NMR of carbon metabolism in heliobacteria. *Photosynth Res.* **41**, 75-88 (1994).

23. W. M. Sattley *et al.*, The genome of Heliobacterium modesticaldum, a phototrophic representative of the Firmicutes containing the simplest photosynthetic apparatus. *J Bacteriol* **190**, 4687-4696 (2008).

24. L. Kimble, M. T. Madigan, Nitrogen fixation and nitrogen metabolism in heliobacteria. *Archives of Microbiology* **158**, 155-161 (1992).

25. I. Sarrou *et al.*, Purification of the photosynthetic reaction center from *Heliobacterium modesticaldum*. *Photosynth Res* **111**, 291-302 (2012).

26. J. Amesz, The antenna-reaction center complex of heliobacteria. *Advances in Photosynthesis* **2**, 687-697 (1995).

27. H. Brockmann, A. Lipinski, Bacteriochlorophyll g. A new bacteriochlorophyll from Heliobacterium chlorum. *Arch Microbiol* **136**, 17-19 (1982).

28. M. Kobayashi *et al.*, Light-independent isomerization of bacteriochlorophyll g to chlorophyll a catalyzed by weak acid in vitro. *Analytica Chimica Acta* **365**, 199-203 (1998).

29. R. C. Prince, H. Gest, R. E. Blankenship, Thermodynamic properties of the photochemical reaction center of Heliobacerium chlorum. *FEBS Lett* **182**, 345-349 (1985).

30. A. M. Nuijs, R. J. Van Dorssen, L. N. M. Duysens, J. Amesz, Excited states and primary photochemical reactions in the photosynthetic bacterium Heliobacterium chlorum. *Proceedings of the National Academy of Sciences of the United States of America* **82**, 6965-6968 (1985).

31. E. J. Van de Meent *et al.*, Identification of 81-hydroxychlorophyll a as a functional reaction center pigment in heliobacteria. *Biochimica et Biophysica Acta* **1058**, 356-362 (1991).

32. E. J. van de Meent, M. Kobayashi, C. Erkelens, P. A. van Veelen, J. Amesz, Identification of 8^1-hydroxychlorophyll *a* as a functional reaction center pigment in heliobacteria. *Biochim Biophys Acta* **1058**, 356-362 (1991).

33. A. Hiraishi, Occurrence of menaquinone is the sole isoprenoid quinone in the photosynthetic bacterium *Heliobacterium chlorum*. *Arch Microbiol* **151**, 378-379 (1989).

34. M. B. Hale, R. E. Blankenship, R. C. Fuller, Menaquinone is the sole quinone in the facultatively aerobic green photosynthetic bacterium *Chloroflexus aurantiacus*. *Biochim Biophys Acta* **723**, 376-382 (1983).

35. A. Vermeglio, Secondary electron transfer in reaction centers of Rhodopseudomonas sphaeroides. Out-of-phase periodicity of two for the formation of ubisemiquinone and fully reduced ubiquinone. *Biochim Biophys Acta* **459**, 516-524 (1977).

36. H.-U. Schoeder, W. Lockau, Phylloquinone copurifies with the large subunit of photosystem I. *FEBS Lett.* **199**, 23-27 (1986).

37. R. E. Blankenship *et al.*, Primary photochemistry in the facultative green photosynthetic bacterium Chloroflexus aurantiacus. *J Cell Biochem* **22**, 251-261 (1983).

38. J. T. Trost, D. C. Brune, R. E. Blankenship, Protein sequences and redox titrations indicate that the electron acceptors in reaction centers from heliobacteria are similar to photosystem I. *Photosynthesis Research* **32**, 11-22 (1992).

39. I. P. Muhiuddin, S. E. J. Rigby, M. C. W. Evans, J. Amesz, P. Heathcote, ENDOR and Special TRIPLE Resonance Spectroscopy of Photoaccumulated Semiquinone Electron Acceptors in the Reaction Centers of Green Sulfur Bacteria and Heliobacteria. *Biochemistry* **38**, 7159-7167 (1999).

40. F. A. M. Kleinherenbrink, J. Amesz, Stoichiometries and rates of electron transfer and charge recombination in *Heliobacterium chlorum*. *Biochimica et Biophysica Acta* **1143**, 77-83 (1993).

41. U. Liebl *et al.*, Single core polypeptide in the reaction center of the photosynthetic bacterium Heliobacillus mobilis: structural implications and relations to other photosystems. *Proceedings of the National Academy of Science, U.S.A.* **90**, 7124-7128 (1993).

42. F. A. Kleinherenbrink, H. C. Chiou, R. LoBrutto, R. E. Blankenship, Spectroscopic evidence for the presence of an iron-sulfur center similar to Fx of Photosystem I in Heliobacillus mobilis. *Photosynthesis Research* **41**, 115-123 (1994).

43. F. A. M. Kleinherenbrink, H.-C. Chiou, R. LoBrutto, R. E. Blankenship, Spectroscopic evidence for the presence of an iron-sulfur center similar to FX of photosystem I in *Heliobacillus mobilis*. *Photosynthesis Research* **41**, 115-123 (1994).

44. M. Heinnickel, G. Shen, R. Agalarov, J. H. Golbeck, Resolution and reconstitution of a bound Fe-S protein from the photosynthetic reaction center of Heliobacterium modesticaldum. *Biochemistry* **44**, 9950-9960 (2005).

45. K. G. Parrett, T. Mehari, P. G. Warren, J. H. Golbeck, Purification and properties of the intact P-700 and Fx-containing Photosystem I core protein. *Biochim Biophys Acta* **973**, 324-332 (1989).

46. M. Heinnickel, R. Agalarov, N. Svensen, C. Krebs, J. H. Golbeck, Identification of F_X in the Heliobacterial Reaction Center as a [4Fe-4S] Cluster with an S = 3/2 Ground Spin State. *Biochemistry* **45**, 6756-6764 (2006).

47. J. T. Trost, R. E. Blankenship, Isolation of a photoactive photosynthetic reaction center-core antenna complex from *Heliobacillus mobilis*. *Biochemistry* **28**, 9898-9904 (1989).

48. W. Nitschke, P. Setif, U. Liebl, U. Feiler, A. W. Rutherford, Reaction center photochemistry of *Heliobacterium chlorum*. *Biochemistry* **29**, 11079-11088 (1990).

49. B. Jagannathan, J. H. Golbeck, Understanding of the binding interface between PsaC and the PsaA/PsaB heterodimer in photosystem I. *Biochemistry* **48**, 5405-5416 (2009).

50. P. Jordan *et al.*, Three-dimensional structure of cyanobacterial photosystem I at 2.5 A resolution. *Nature* **411**, 909-917. (2001).

51. M. L. Antonkine *et al.*, Assembly of protein subunits within the stromal ridge of photosystem I. Structural changes between unbound and sequentially PS I-bound polypeptides and correlated changes of the magnetic properties of the terminal iron sulfur clusters. *J Mol Biol* **327**, 671-697 (2003).

52. P. Fromme, H. Bottin, N. Krauss, P. Setif, Crystallization and electron paramagnetic resonance characterization of the complex of photosystem I with its natural electron acceptor ferredoxin. *Biophysical Journal* **83**, 1760-1773 (2002).

53. S. P. Romberger, C. Castro, Y. Sun, J. H. Golbeck, Identification and characterization of PshBII, a second F_A/F_B-containing polypeptide in the photosynthetic reaction center of *Heliobacterium modesticaldum*. *Photosynth Res* **104**, 293-303 (2010).

54. A. Hatano, K. Inoue, D. Deo, H. Sakurai, Isolation and partial characterization of two ferredoxins from the photosynthetic bacterium Heliobacillus mobilis. *Journal of Photoscience* **9**, 388-390 (2002).

55. I. R. Vassiliev, M. L. Antonkine, J. H. Golbeck, Iron-sulfur clusters in type I reaction centers. *Biochimica Et Biophysica Acta-Bioenergetics* **1507**, 139-160 (2001).

56. S. P. Romberger, J. H. Golbeck, The F_X iron-sulfur cluster serves as the terminal bound electron acceptor in heliobacterial reaction centers. *Photosynth Res* **111**, 285-290 (2012).

57. S. Takaichi *et al.*, The major carotenoid in all known species of heliobacteria is the C30 carotenoid 4,4'-diaponeurosporene, not neurosporene. *Arch Microbiol* **168**, 277-281 (1997).

58. M. Heinnickel, J. H. Golbeck, Heliobacterial photosynthesis. *Photosynth Res* **92**, 35-53 (2007).

59. E. J. van de Meent, F. A. M. Kleinherenbrink, J. Amesz, Purification and properties of an antenna-reaction center complex from heliobacteria. *Biochimica et Biophysica Acta* **1015**, 223-230 (1990).

60. T. S. Kashey, J. B. Cowgill, M. D. McConnell, M. Flores, K. E. Redding, Expression and characterization of cytochrome c_{553} from *Heliobacterium modesticaldum*. *Photosynth Res* **120**, 291-299 (2014).

61. I. Albert, A. W. Rutherford, H. Grav, J. Kellermann, H. Michel, The 18-kDa cytochrome c_{553} from *Heliobacterium gestii*: gene sequence and characterization of the mature protein. *Biochemistry* **37**, 9001-9008 (1998).

62. D. W. Lee, Y. Ozturk, A. Osyczka, J. W. Cooley, F. Daldal, Cytochrome bc1-cy fusion complexes reveal the distance constraints for functional electron transfer between photosynthesis components. *J Biol Chem* **283**, 13973-13982 (2008).

63. H. Oh-oka, M. Iwaki, S. Itoh, Electron donation from membrane-bound cytochrome *c* to the photosynthetic reaction center in whole cells and isolated membranes of *Heliobacterium gestii*. *Photosynthesis Research* **71**, 137-147 (2002).

64. D. M. Kramer, B. Schoepp, U. Liebl, W. Nitschke, Cyclic electron transfer in *Heliobacillus mobilis* involving a menaquinol-oxidizing cytochrome *bc* complex and an RCI-type reaction center. *Biochemistry* **36**, 4203-4211 (1997).

65. W. Nitschke *et al.*, Membrane-bound c-type cytochromes in Heliobacillus mobilis. Characterization by EPR and optical spectroscopy in membranes and detergent-solubilized material. *European Journal of Biochemistry* **242**, 695-702 (1996).

66. A. L. Ducluzeau, E. Chenu, L. Capowiez, F. Baymann, The Rieske/cytochrome *b* complex of Heliobacteria. *Biochim Biophys Acta* **1777**, 1140-1146 (2008).

67. H. Yue, Y. Kang, H. Zhang, X. Gao, R. E. Blankenship, Expression and characterization of the diheme cytochrome *c* subunit of the cytochrome *bc* complex in *Heliobacterium modesticaldum*. *Arch Biochem Biophys* **517**, 131-137 (2012).

68. S. Junemann, P. Heathcote, P. R. Rich, On the mechanism of quinol oxidation in the bc1 complex. *J Biol Chem* **273**, 21603-21607 (1998).

CHAPTER 2

EXPRESSION AND CHARACTERIZATION OF CYTOCHROME C553 FROM HELIOBACTERIUM MODESTICALDUM

Published as:

Kashey, T. S., J. B. Cowgill, M. D. McConnell, M. Flores and K. E. Redding (2014). "Expression and characterization of cytochrome c_{553} from *Heliobacterium modesticaldum*." Photosynth Res **120**(3): 291-299.

ABSTRACT

Cytochrome c_{553} of *Heliobacterium modesticaldum* is the donor to P_{800}^{+}, the primary electron donor of the heliobacterial reaction center (HbRC). It is a membrane-anchored 14-kDa cytochrome that accomplishes electron transfer from the cytochrome *bc* complex to the HbRC. The *petJ* gene coding cyt c_{553} was cloned and expressed in *Escherichia coli* with a hexahistidine tag replacing the lipid attachment site to create a soluble donor that could be made in a preparative scale. The recombinant cytochrome had spectral characteristics typical of a *c*-type cytochrome, including an asymmetric α-band, and a slightly red-shifted Soret band when reduced. The EPR spectrum of the oxidized protein was characteristic of a low-spin cytochrome. The midpoint potential of the recombinant cytochrome was +217 ± 10 mV. The interaction between soluble recombinant cytochrome c_{553} and the HbRC was also studied. Re-reduction of photooxidized P_{800}^{+} was accelerated by addition of reduced cytochrome c_{553}. The kinetics were characteristic of a bimolecular reaction with a second order rate of 1.53×10^4 $M^{-1}s^{-1}$ at room temperature. The rate manifested a steep temperature dependence, with a calculated activation energy

of 91 kJ/mol, similar to that of the native protein in *Heliobacillus gestii* cells. These data demonstrate that the recombinant soluble cytochrome is comparable to the native protein, and likely lacks a discrete electrostatic binding site on the HbRC.

Introduction

Heliobacteria are phototrophic *Firmicutes* with a homodimeric type 1 (FeS-type) reaction center. They do not have a peripheral antennae system, and are unique in that they use bacteriochlorophyll *g* as the major pigment in their reaction center (RC). The heliobacterial RC (HbRC) shares similarities with the RC of green sulfur bacteria and photosystem I of higher plants. The cofactor arrangements in these RCs are thought to be similar, although the core polypeptides do not share high levels of sequence identity beyond their topological arrangement in the membrane (*7, 69*). Heliobacteria are strict anaerobes (*70*), like many of the bacteria in the order *Clostridiales*, and can grow in the dark fermentatively. They are not autotrophic and use simple organic acids like pyruvate as carbon and electron sources.

Cytochromes are a diverse family of proteins involved in electron transfer, and are made by all eukaryotes and most prokaryotes. Typically, these proteins are associated with protein complexes bound to membranes. Among the *Heliobacteria,* the major membrane-anchored cytochromes have similar primary structures with high homology in the functional domain. These membrane-anchored cytochromes are monoheme *c*-type cytochromes, and are fully functional in isolated membranes. In the reduced form, they have an α-band centered at 553 nm, as is typical for *c*-type cytochromes. Although it is attached to the membrane, the primary structure of cyt c_{553} gave no indications of

transmembrane helices. Instead, mass spectroscopy data indicated an N-terminal modification at Cys23, where a diglyceride is attached via a thioether linkage (*61*) . The heme-binding motif is on the C-terminus (*61*), separated from the N-terminus by a ~40-residue Pro/Ala-rich sequence likely to be unstructured. The stoichiometry of cyt c_{553} to HbRC was measured to be around 5-6 per RC in *Heliobacillus mobilis* (*71*). The isolated reaction center from *Heliobacterium modesticaldum* contains no bound cytochrome (*25*).

The cyt c_{553} serves as the direct reductant of P_{800}^{+} in whole cells and membranes of *Heliobacterium gestii* with a redox potential of +215 mV (*61*), only slightly more negative than the calculated redox potential of +240 mV in P_{800}^{+} in *H. mobilis* (*71*). In whole cells of *Heliobacterium chlorum*, the electron transfer rate from cyt c_{553} to P_{800}^{+} is about 300 μs, while in membranes it is considerably slower at ~3 ms (*29*). Electron transfer from cyt c_{553} to P_{800}^{+} in membranes showed a strong dependence on both temperature and divalent cations. This is consistent with the anchoring of cyt c_{553} in the membrane and its collisional mode of action.

A system was developed to express cyt c_{553} from *H. modesticaldum* in *E. coli* cells. The gene was restructured to remove the lipid attachment site and replace it with a hexahistidine tag to create a fully soluble electron donor to P_{800}^{+}. The recombinant product was characterized in detail to ensure it retained the properties of the native protein. These data show that the expressed cyt c_{553} is on par with the native cytochrome and is functional for future studies.

EXPERIMENTAL PROCEDURES

Construction of recombinant His$_6$-tagged cyt c_{553}: The recombinant cytochrome c_{553} was designed by taking the predicted mature gene product and replacing the diacylglycerol attachment site (Cys23) with a hexahistidine tag. The OmpA signal-sequence (MKKTAIAIAVALAGFATVAQA) was placed upstream of the hexahistidine tag. Cleavage by signal peptidase would result in a polypeptide with an amino terminus of AHHHHHHSSSS rather than (diacylglycerol)-CSSSS in the native protein (see Fig. 2.1). The synthesized sequence (Genscript) was cloned into pET30a (Novagen) using the Nde1 and Xho1 restriction sites, which were introduced at the 5' and 3' ends of the synthesized DNA, respectively. The resulting plasmid, called pET30a-*petJ*, replaces the multicloning site of pET30a with the synthetic H_6-*petJ* gene, putting it under control of the T7 promoter.

Strain construction and protein expression: The pET30a-*petJ* and pRGK333 (*72*) plasmids were co-transformed into BL21(DE3) cells (Invitrogen) and grown on Luria-Bertani (LB) plates supplemented with 100 mg L^{-1} ampicillin (Sigma-Aldrich) and 75 mg L^{-1} kanamycin (Fisher Scientific). A single colony was picked to inoculate a 50-mL starter culture. Cells were grown aerobically in LB media (Difco) containing 100 mg L^{-1} ampicillin and 75 g L^{-1} kanamycin by shaking at 250 rpm at 37 ^{o}C. The overnight culture was diluted 1:100 into 4 L of LB the following morning. Cells were grown to an OD600 of 0.5. At this point, d-aminolevulinic acid (d-ALA; Goldbio) was added to 1 mM to support heme synthesis, and isopropyl β-D-1-thiogalactopyranoside (IPTG) was added at 300 μM to induce synthesis of both H_6-PetJ and the cytochrome maturation machinery.

After 3 hours, cells were harvested by centrifugation for 10 min at 5000x g and the cell pellet was stored at -20 ^{o}C.

Purification of cyt c_{553} and HbRC: Cells were thawed on ice and resuspended with 2 pellet volumes of wash buffer (50 mM sodium phosphate, 300 mM NaCl, pH 7.4) and sonicated with a Microson XL 2000 on ice for 5 rounds of 1 minute at 50% power with 30 seconds between each round. The cell lysate was centrifuged at 25000x *g* for 30 minutes at 4 °C, and the supernatant was re-spun under the same conditions. The resulting supernatant was passed through a 0.22-μm filter. Clarified extract from 4 L of culture was loaded onto a column containing 1.5 mL His60 Ni superflow (Clontech), which was then washed with 20 volumes of wash buffer, followed by 20 volumes of wash buffer + 3 mM imidazole. The cytochrome was eluted with 10 column volumes of wash buffer + 300 mM imidazole. The red fraction was collected and concentrated with VivaSpin20 5-kDa molecular weight cut-off centrifugal filters (Sartorius) followed by buffer exchange in the centrifugal filters with 50 mM MOPS (pH 7.0).

The HbRC from *H. modesticaldum* was purified as described (*25*). The native cytochrome c_{553} was collected as the flow-through fraction from the carboxymethyl-Sepharose ion-exchange column during purification of the HbRC from *H. modesticaldum*, followed by concentration in 5-kDa molecular weight cut-off centrifugal filters .

Mass spectrometry: Native and recombinant cytochrome c_{553} (both 200 μm) were diluted 1:10 in saturated sinapinic acid. Mass spectra were recorded on an Applied

Biosystems DE-STR MALDI-TOF operating on electron reflector mode at 25000 V and a laser rep rate of 20 Hz.

UV-visible spectroscopy: The UV-visible reduced minus oxidized difference spectrum of recombinant cyt c_{553} was collected by subtracting the spectrum of fully oxidized protein (purified and stored in air) from that of a fully reduced sample (after addition of excess sodium dithionite). Spectra were collected on a Perkin Elmer Lamba35 spectrometer.

Electrophoresis and staining for protein or heme: A 20% BisTris-SDS-polyacrylamide gel was loaded with solubilized native and recombinant cyt c_{553} samples corresponding to 125 ng of heme (calculated from spectra of reduced samples). The gels were run at 175 V and rinsed in de-ionized water for 5 minutes. For heme staining, the gel was soaked in 12.5% tricholoroacetic acid for 30 minutes, washed in de-ionized water for 30 minutes, and then soaked in a solution of 4 mM *o*-dianisidine, 10% acetic acid, 10% 0.5 M sodium citrate (pH 4.4) and 0.1% hydrogen peroxide. After development of heme-containing polypeptides, the gel was washed in de-ionized water and photographed. For silver staining of polypeptides, the protocol of (*73*) was used.

Redox titration of recombinant cyt c_{553}: Recombinant cytochrome c_{553} at 200 μM in a buffer containing 50 mM MOPS (pH 7.0) and 150 mM NaCl was allowed to become fully reduced by exposure to an atmosphere of ~3% H_2 in N_2 for several days at room temperature. The redox potential of the sample was monitored with a digital auto-range multi-meter (VWR) with flexible platinum and silver electrodes as the anode and cathode, respectively. The solution was slowly rendered more oxidizing by addition of

small amounts of potassium ferricyanide while monitoring the potential and taking the spectrum after the potential had stabilized following each addition. The use of mediators led to technical difficulties with our voltage measurements. Extra care was taken with the addition of potassium ferricyanide. The amount of reduced cytochrome c_{553} was estimated by the absorption of the a-band at 553 nm. (Each spectrum was fitted as a weighted sum of the spectra of fully oxidized and fully reduced cyt c_{553} in order to quantify the reduced/oxidized ratio.)

Transient absorption spectroscopy: Transient absorbance spectroscopy was performed with a JTS-10 transient spectrometer (Bio-Logic). Purified HbRC samples were diluted to 0.5 μM in a buffer containing 50 mM MOPS (pH 7.0), 5 mM $MgSO_4$, 10 mM ascorbate, 5 mM benzyl viologen (BV) and 0.03% *n*-dodecyl β-D-maltoside, and were loaded into a sealed anaerobic cuvette (1-cm pathlength). A baseline was taken for 1.2 s before excitation and linear regression was used to subtract any baseline shift. A frequency doubled Nd:YAG laser (Surlite Mini-Lite, Continuum) delivered a 6-ns saturating flash (20 mJ at 532 nm) to generate the P_{800}^+ cation. The redox state of the special pair was probed with 10-μs LED flashes centered at 803 nm, commencing 350 μs after the laser flash. Placing a 532-nm notch filter and a 780-nm high-pass filter in front of both the reference and measurement detectors minimized effects of the actinic flash. Recombinant cyt c_{553} was added up to 108 μM. For the temperature-dependence experiments, the cuvette was equilibrated at temperatures varying from 10-40 ^oC for 5 minutes before absorption traces were collected. For each transient experiment, the decay

of P_{800}^{+} was fit to the sum of 3 exponential decay components, with the equation of $y = A_1^{(x/t1)} + A_2^{(x/t2)} + A_3^{(x/t3)}$.

EPR spectroscopy: Continuous wave electron paramagnetic resonance (EPR) spectra were recorded at the EPR facility of University of Arizona. The magnetic field modulation frequency was 100 kHz with a field modulation of 2 mT peak-to-peak. The microwave power was 0.2 mW, the microwave frequency was 9.337 GHz and the temperature was 6 K.

EPR spectra were simulated using EasySpin (v 4.5.0), a computational package developed by Stoll and Schweiger and based on Matlab (The MathWorks, Natick, MA, USA). The model used for the EPR simulations considered a single low-spin Fe^{3+} ion (S = 1/2). The fitting parameters were the *g* values (g_x, g_y and g_z) and the line widths (ΔB_x, ΔB_y and ΔB_z).

RESULTS

Expression and purification of recombinant cyt c_{553}

The native cyt c_{553} from *H. gestii* was found to be attached to a diacylglycerol molecule via a thioether linkage to Cys23, which becomes the N-terminal residue after translocation and cleavage of the signal peptide (*61*). Mass spectroscopic analysis (data not shown) of the cyt c_{553} from *H. modesticaldum* was consistent with the same type of N-terminal modification (*25*). We replaced the native signal peptide and Cys23 with the signal peptide of OmpA followed by the sequence AHHHHHH. This would result in replacement of Cys23 with AH_6 after signal peptide cleavage. We did not expect this change to have a large influence upon the structure of the cyt c_{553}, beyond rendering it

soluble, as the first ~40 residues of these polypeptides are not well conserved between *H. gestii* and *H. modesticaldum*, beyond a propensity for Pro, small (Ala and Ser) and charged (Lys, Asp, Glu) residues (Fig. 2.1). This is consistent with the primary role of this sequence being an unstructured link between the membrane integration site at the N-terminus and the C-terminal cytochrome domain.

The synthetic gene, codon-optimized for *E. coli*, was expressed using the T7 promoter in BL21(DE3) cells, in which T7 RNA polymerase can be induced by addition of IPTG. In order to maximize expression of the recombinant cyt *c*, we co-expressed the *ccmA-H* genes (cytochrome biogenesis system I) (*72*). H_6-tagged cytochrome was purified from the clarified lysate by immobilized metal affinity chromatography (IMAC; see Experimental Procedures). Purified protein contained a 280/410 ratio of 1.5, and a calculated yield of 4.6 mg protein per liter, with an overall recovery rate of 37%.

UV-visible spectroscopy

The spectrum of cyt c_{553} reduced by dithionite is characterized by the appearance of an α-band peaking at 553 nm and a broad β-band centered at 524 nm (Fig. 2). The Soret band peaks at 412 nm in the oxidized state and at 417 nm in the reduced state (Online Resource 1). These properties are identical to those of cyt c_{553} from *H. gestii* (*61*), and are typical for *c*-type cytochromes.

Electrophoretic and mass spectrometric analyses

Recombinant and native cytochromes were loaded on an SDS-PAGE gel on the basis of equal heme (as estimated by the spectrum of reduced protein). The native and recombinant proteins had apparent molecular masses of 13 kDa and 14 kDa, respectively. The slightly higher mobility of the native protein is probably due to its slightly shorter sequence and binding of SDS to the attached lipid moiety. The gels were stained for protein (Fig. 3A) or for heme (Fig. 3B). Their equivalent staining intensity indicates that the heme is covalently attached in the recombinant cyt c_{553} with identical stoichiometry to that of the native protein (*i.e.* 1:1). The lack of other silver-staining bands in the recombinant protein preparation demonstrates that IMAC was sufficient to purify it to homogeneity.

The native cyt c_{553} prep contained 4 additional bands in the 30-42 kDa range, which are resolved poorly in (Fig. 2.3); none of them stain for heme (Fig. 3B), as seen before (*25*). The prep in *H. gestii* had a similar cohort of additional polypeptides, and it was suggested that these formed a complex with the cytochrome (*61*). However, mass spectrometric analysis of these polypeptides from *H. modesticaldum* revealed them to be ABC transporters (*25*). Thus, they are unlikely to be involved with the function of cyt c_{553}, despite their tendency to co-purify with it.

Mass spectrometric analysis of the recombinant cyt c_{553} was consistent with covalent attachment of heme to the polypeptide. We obtained a mass of 14041 ± 14 Da, compared to an expected mass of 14023 Da (Data not shown).

EPR spectroscopy of native and recombinant cyt c_{553}

The oxidized native cyt c_{553} exhibited a low-temperature EPR spectrum typical of a low-spin cytochrome (Fig. 2.4), with *g*-values of 3.05, 2.235, and 1.36 (Table 2.1). Reduction by ascorbate eliminated this spectrum entirely. These *g*-values are very similar to those reported for the g_x and g_y values (3.048 and 2.238, respectively) for the cytochrome from *H. gestii* by (*61*), although they were unable to observe the low-field trough shown in this work. The recombinant protein behaved identically, although the *g*-tensor was slightly less anisotropic, with *g*-values of 2.97, 2.285, and 1.435 (Fig. 2.4, Table 2.1).

Redox titration of recombinant cyt c_{553}

A potentiometric titration was performed to determine the midpoint potential (E_m) of the recombinant cyt c_{553}. The spectrum of the cytochrome solution was measured as the potential was varied. The potential of the sample was lowered by addition of small amounts of potassium ferricyanide and was monitored with an electrode. After the potential had stabilized, the spectrum was taken. Spectra were fit as a weighted sum of the spectra of the fully oxidized and fully reduced protein, to estimate the fraction of reduced cytochrome. When fit to the Nernst equation, the titration plot (Fig 2.5) was consistent with a single titrating species with n=1 (single electron oxidation/reduction) and E_m = +217 ± 0.6 mV versus NHE. This is very similar to the value obtained for the native cyt c_{553} from *H. gestii* (*61*).

Reduction of purified HbRC by recombinant cyt c_{553}

Transient spectroscopy was used to test the ability of the soluble recombinant cyt c_{553} to function as an electron donor to the HbRC ($P_{800}^{+} + c_{553}^{red} \rightarrow P_{800} + c_{553}^{ox}$). Mixtures containing the HbRC and cyt c_{553} with ascorbate as electron donor and benzyl viologen (BV) as electron acceptor were loaded anoxically into sealed cuvettes and the oxidation state of P_{800} was monitored with 10–μs flashes at 803 nm. The HbRC was excited with a saturating laser flash at 532 nm, which resulted in instantaneous bleaching of P_{800} (within the timescale of the measurement) as P_{800} was photooxidized, followed by decay of the bleaching as P_{800}^{+} was reduced (Fig. 2.6A). The decay of P_{800}^{+} was fit to the sum of 3 exponential decay components. The fastest component (~15 ms) representing ~10% of the decay is assigned to charge recombination of the $P_{800}^{+}F_X^{-}$ state (*25, 74*), and is attributed to HbRCs from which the electron does not escape to BV. The slowest component (>3 s) is assigned to the slow reduction of P_{800}^{+} by ascorbate.

After addition of cyt c_{553}, a component of intermediate rate appeared, which can be attributed to P_{800}^{+} reduction by cyt c_{553}. As the concentration of cyt c_{553} was increased, this component increased in amplitude at the expense of the slow component; it represented ~75% of the decay at the highest concentrations tested. Addition of a fourth component did not increase the quality of the fit (data not shown). The calculated rate of reduction of P_{800}^{+} by cyt c_{553} is plotted against cyt c_{553} concentration in Figure 2.6B. Based on this, we estimate the second order rate for this reaction ($P_{800}^{+} + c_{553}^{red} \rightarrow P_{800} + c_{553}^{ox}$) to be $1.53 \times 10^{4}\ M^{-1}s^{-1}$ at 22 °C.

In membranes of *H. gestii*, the rate of P_{800}^{+} reduction by the native c_{553} was strongly dependent upon temperature and Mg^{2+} concentration (*63*). We wished to see if these were

characteristic of the intrinsic HBRC:cyt *c* interaction or of the attachment of cyt c_{553} to the membrane. The temperature dependence of P_{800}^+ reduction by c_{553} was assessed by varying the temperature from 10 to 40 ^oC and measuring the kinetics of P_{800}^+ reduction as before. The reduction of P_{800}^+ by cyt c_{553} was found to be highly temperature dependent, with a 40-fold increase in rate over the 30 °C span of measurement. The apparent activation energy calculated by an Arrhenius plot was 91 kJ/mol (Fig. 2.7). This is very similar to what was seen in membranes from *H. gestii* (*63*). In contrast, however, the rate of P_{800}^+ reduction by the soluble recombinant c_{553} was invariant over a Mg^{2+} concentration ranging from 5 μM to 50 mM (data not shown).

DISCUSSION

Our analysis of the native cyt c_{553} from *H. modesticaldum* revealed no differences between it and the protein from *H. gestii* in terms of heme attachment, UV-visible spectrum, or EPR spectrum (*61*), confirming that the orthologs from these two species are very similar. One would expect this, given the high sequence conservation in their cytochrome domains (74 out of the 80 C-terminal residues; see Fig. 1). Based on its visible and EPR spectra, reduction potential, and other properties, the recombinant cyt c_{553} is almost identical to the native proteins of *H. modesticaldum* and *H. gestii*. This confirms our hypothesis that the N-terminus would be a good place to insert the hexahistidine tag without altering the properties of the cytochrome.

We observed very few differences between the native and recombinant cyt c_{553}, beyond the slower rate of P_{800}^+ reduction by the recombinant protein, which was almost two orders of magnitude slower than the native cyt c_{553} in membranes (*63*). We attribute the

higher rate to the incorporation of native cyt c_{553} in membranes, and this is unsurprising, as the effective concentration of cyt c_{553} in membranes would be much higher than what we can obtain with the recombinant protein in solution; in addition, it may be constrained to interact with the RC in ways that tend to be more productive for electron transfer between them. Consistent with this, we found that the solubilized native protein was also very slow at reducing the purified HbRC, although we were unable to test it at as high a concentration as we did with the recombinant protein (data not shown). Oh-Oka (*63*) observed a ~4-fold increase in the P_{800}^{+} reduction rate upon addition of $MgCl_2$ to membranes in the range of 0.3 – 3 mM. This effect of divalent cations on electron donation rate is somewhat similar to what had been seen with the interaction of plastocyanin and P_{700}^{+} (*75*). However, we saw no difference in the rate of electron donation from soluble cyt c_{553} to P_{800}^{+} in the range of 0.005–50 mM $MgCl_2$ using the soluble version of cyt c_{553} (data not shown). Therefore, the dependence of this rate upon divalent cations must be an effect upon membranes and unrelated to the interface between cyt c_{553} and the HbRC.

The cyt c_{553} of *H. modesticaldum* seems to fall in line with other small *c*-type cytochromes of similar function. *Rhodobacter sphaeroides*, *Chlorobaculum tepidum*, and *H. gestii* all contain *c*-type cytochromes that donate to their respective RCs. These cytochrome all have low-spin hemes (*61, 76, 77*) and share similar spectral characteristics, including an asymmetric α-band, and a slightly red-shifted Soret band when reduced (*61, 78, 79*); (Figure 2.2). They also have similar midpoint potentials, all being within the range of +170 to +220 mV. Thus, the cyt c_{553} of *H. modesticaldum*

seems very much like the other heliobacterial *c*-type cytochromes, which are themselves fairly typical members of this family. Furthermore, the EPR parameters obtained in this work for both native and recombinant cyt c_{553} of *H. modesticaldum* suggest that they belong to the family of low-spin ferriheme proteins containing two histidines as axial ligands. The small differences in the observed *g*-values (Table 2.1) likely reflect slightly different orientations of such ligands.

The interaction of cyt c_{553} with the HbRC of *H. modesticaldum* is very similar to that seen in other type-I photosynthetic RC systems. Interestingly, the cytochromes in *Chlorobium* and *Heliobacteria* have midpoints that give a relatively small gap in potential when compared to the special pair of the corresponding organism. The gap in *Chlorobaculum tepidum* may be as small as 45 mV (*80*), while it is 55 mV and 50 mV in *Heliobacterium chlorum* (*81*) and *Heliobacillus mobilis* (*71*), respectively. Given the highly conserved nature of the photosynthetic proteins within *Heliobacteria,* it is likely that the gaps in potential are similar for *H. modesticaldum* and *H. gestii*. Even the donor proteins for Photosystem I, plastocyanin and cyt c_6, typically have a gap of less than 100 mV with respect to the special pair (*82*). These ranges likely indicate the minimum driving force for an electron transfer rate that does not limit overall electron flow, while optimizing energy conservation. The activation energies of electron transfer from the *c*-type cytochrome to its native RC are also similar, with E_a = 91 kJ mol^{-1} for *H. gestii* (*63*) and E_a = 101 kJ mol^{-1} for *C. tepidum* (*83*) in their native context. We determined an activation energy of 88 kJ mol^{-1} when using the soluble version of *H. modesticaldum* c_{553} (Fig. 2.7). The theoretical isoelectric points were calculated from the functional portion

of the mature protein (the signal sequence and transmembrane helices were omitted to approximate the functional portion of the protein). In addition, the cysteine residues involved in heme binding were replaced in the calculations by glutamic acids to more appropriately simulate the propionates on the heme. The fully matured recombinant cyt c_{553} has a calculated pI of 7.8. The cyt c_{553} proteins from different heliobacteria are: *H. gestii* (7.1), *H. modesticaldum* (native) (7.3), and *H. mobillis* (5.9). The soluble cytochrome from *R. sphaeroides* has a calculated (pI=6.1) The cytochrome of the green sulfur bacterium *C. tepidum* (pI=9.4) has a slightly more basic isoelectric point, perhaps indicating a larger dependence on electrostatic interactions for optimal cooperation with the acceptor. In both the chlorobial and purple bacterial systems, the cytochrome is pre-bound to the reaction center, while in the heliobacterial system the cytochrome seems to depend on a collisional mode for electron transfer. The lack of membrane tether in the recombinant cytochrome is likely the dominant factor influencing the disparity in electron transfer rate when compared to the native cytochrome. Cytochromes that are soluble in their native state share a stronger dependence with electrostatic interaction in order to orient correctly from a longer range, as they are faster to associate and slower to dissociate (*84*). When tethered to the membrane, cyt c_{553} is limited to 2-Dimensional movement and does not need to be dependent electrostatic interaction to correctly orient itself with P_{800}^{+}. In membranes, the rate of electron transfer from cyt c_{553} to P_{800}^{+} in *Heliobacteria* is ~3 ms (*63*), much slower than that seen with *R. sphaeroides* (20-40 μs) (*79*) or *C. tepidum* (110 μs) (*85*). Although the rate is greatly increased when the reaction is measured in whole cells of *H. gestii* (300 μs) (*63*), the order of magnitude difference is

maintained when compared to the electron transfer kinetics of *C. tepidum* (7 μs) (*7*), and *R. sphaeroides* (1 μs) (*86*).

REFERENCES

7. G. Hauska, T. Schoedl, H. Remigy, G. Tsiotis, The reaction center of green sulfur bacteria. *Biochimica et Biophysica Acta* **1507**, 260-277 (2001).

25. I. Sarrou *et al.*, Purification of the photosynthetic reaction center from *Heliobacterium modesticaldum*. *Photosynth Res* **111**, 291-302 (2012).

29. R. C. Prince, H. Gest, R. E. Blankenship, Thermodynamic properties of the photochemical reaction center of Heliobacerium chlorum. *FEBS Lett* **182**, 345-349 (1985).

61. I. Albert, A. W. Rutherford, H. Grav, J. Kellermann, H. Michel, The 18-kDa cytochrome c_{553} from *Heliobacterium gestii*: gene sequence and characterization of the mature protein. *Biochemistry* **37**, 9001-9008 (1998).

63. H. Oh-oka, M. Iwaki, S. Itoh, Electron donation from membrane-bound cytochrome *c* to the photosynthetic reaction center in whole cells and isolated membranes of *Heliobacterium gestii*. *Photosynthesis Research* **71**, 137-147 (2002).

69. H. Oh-oka, Type 1 reaction center of photosynthetic heliobacteria. *Photochem Photobiol* **83**, 177-186 (2007).

70. M. T. Madigan, J. G. Ormerod, in *Anoxygenic Photosynthetic Bacteria,* R. E. Blankenship, M. T. Madigan, C. E. Bauer, Eds. (Kluwer Academic Publishers, Dordrecht, The Netherlands, 1995), pp. 17-30.

71. W. Nitschke, U. Liebl, K. Matsuura, D. M. Kramer, Membrane-Bound c-Type Cytochromes in Heliobacillus mobilis. In Vivo Study of the Hemes Involved in Electron Donation to the Photosynthetic Reaction Center. *Biochemistry* **34**, 11831-11839 (1995).

72. R. E. Feissner *et al.*, Recombinant cytochromes c biogenesis systems I and II and analysis of haem delivery pathways in Escherichia coli. *Mol Microbiol* **60**, 563-577 (2006).

73. J. H. Morrissey, Silver stain for proteins in polyacrylamide gels: a modified procedure with enhanced uniform sensitivity. *Anal Biochem* **117**, 307-310 (1981).

74. M. Heinnickel, G. Shen, J. H. Golbeck, Identification and characterization of PshB, the dicluster ferredoxin that harbors the terminal electron acceptors F(A) and F(B) in *Heliobacterium modesticaldum*. *Biochemistry* **46**, 2530-2536 (2007).

75. N. Tamura, S. Itoh, Y. Yamamoto, M. Nishimura, Electrostatic Interaction between Plastocyanin and P700 in the Electron Transfer Reaction of Photosystem I-Enriched Particles. *Plant and Cell Physiol.* **22**, 603-612 (1981).

76. F. Drepper, P. Mathis, Structure and function of cytochrome c2 in electron transfer complexes with the photosynthetic reaction center of Rhodobacter sphaeroides: optical linear dichroism and EPR. *Biochemistry* **36**, 1428-1440 (1997).

77. C. Azai, Y. Tsukatani, S. Itoh, H. Oh-oka, C-type cytochromes in the photosynthetic electron transfer pathways in green sulfur bacteria and heliobacteria. *Photosynth Res* **104**, 189-199 (2010).

78. H. Oh-oka, M. Iwaki, S. Itoh, Membrane-bound cytochrome c_z couples quinol oxidoreductase to the P840 reaction center complex in isolated membranes of the green sulfur bacterium *Chlorobium tepidum*. *Biochemistry* **37**, 12293-12300 (1998).

79. P. L. Dutton, K. M. Petty, H. S. Bonner, S. D. Morse, Cytochrome c2 and reaction center of Rhodospeudomonas spheroides Ga. membranes. Extinction coefficients, content, half-reduction potentials, kinetics and electric field alterations. *Biochim Biophys Acta* **387**, 536-556 (1975).

80. N. Okumura, K. Shimada, K. Matsuura, Photo-oxidation of membrane-bound and soluble cytochrome c in the green sulfur bacterium Chlorobium tepidum. *Photosynthesis Research* **41**, 125-134 (1994).

81. R. C. Prince, H. Gest, R. E. Blankenship, Thermodynamic properties of the photochemical reaction center of Heliobacerium chlorum. *FEBS Letters* **182**, 345-349 (1985).

82. A. Nakamura, T. Suzawa, Y. Kato, T. Watanabe, Species dependence of the redox potential of the primary electron donor p700 in photosystem I of oxygenic photosynthetic organisms revealed by spectroelectrochemistry. *Plant Cell Physiol* **52**, 815-823 (2011).

83. H. Oh-oka, M. Iwaki, S. Itoh, Viscosity dependence of the electron transfer rate from bound cytochrome c to P840 in the photosynthetic reaction center of the green sulfur bacterium *Chlorobium tepidum*. *Biochemistry* **36**, 9267-9272 (1997).

84. Y. Ozturk *et al.*, Soluble variants of Rhodobacter capsulatus membrane-anchored cytochrome cy are efficient photosynthetic electron carriers. *J Biol Chem* **283**, 13964-13972 (2008).

85. H. Oh-oka *et al.*, Highly purified photosynthetic reaction center (PscA/cytochrome c551)2 complex of the green sulfur bacterium *Chlorobium limicola*. *Biochemistry* **34**, 13091-13097 (1995).

86. S. Wang, X. Li, J. C. Williams, J. P. Allen, P. Mathis, Interaction between cytochrome c2 and reaction centers from purple bacteria. *Biochemistry* **33**, 8306-8312 (1994).

TABLES

Parameters[a]	Source of cytochrome c_{553}	
	Native	Recombinant
g_z	3.050	2.970
g_y	2.235	2.285
g_x	1.360	1.435
ΔB_z (MHz)	530	490
ΔB_y (MHz)	600	510
ΔB_x (MHz)	850	800

[a] The simulation parameters were the following: the three g-values, g_x, g_y, and g_z, and the three line widths, ΔB_x, ΔB_y, and ΔB_z

Table 2.1: Summary of Parameters Used in the Simulations of EPR X-Band Spectra of Cytochrome c_{553} from *H. modesticaldum*

FIGURES

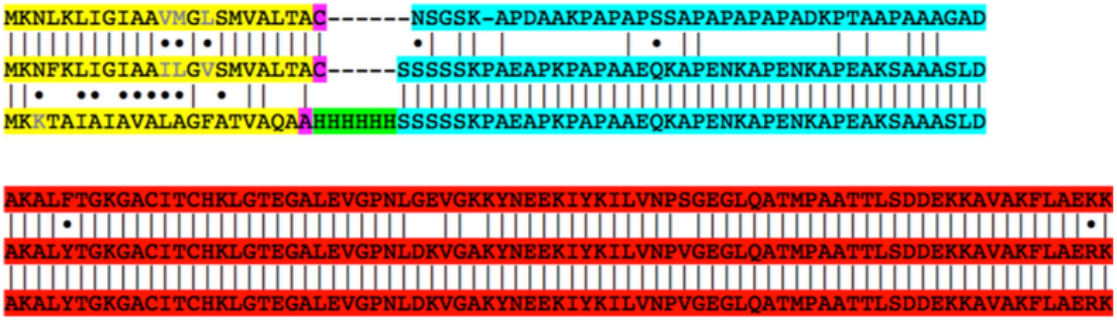

2.1: Alignment of Cyt c553 from H. gestii (Top Sequence) and H. modesticaldum (Middle Sequence) Along With the Recombinant H. modesticaldum Cyt c553 (Bottom Sequence). Highlighting indicates the signal sequence (yellow), N-terminal residue of mature protein (magenta), linker region (cyan), and cytochome domain (red). The recombinant cyt c553 uses the signal sequence of OmpA (yellow) and contains a hexahistidine tag (green). The linker domains are poorly conserved between H. gestii and H. modesticaldum beyond a propensity for Pro and Ala.

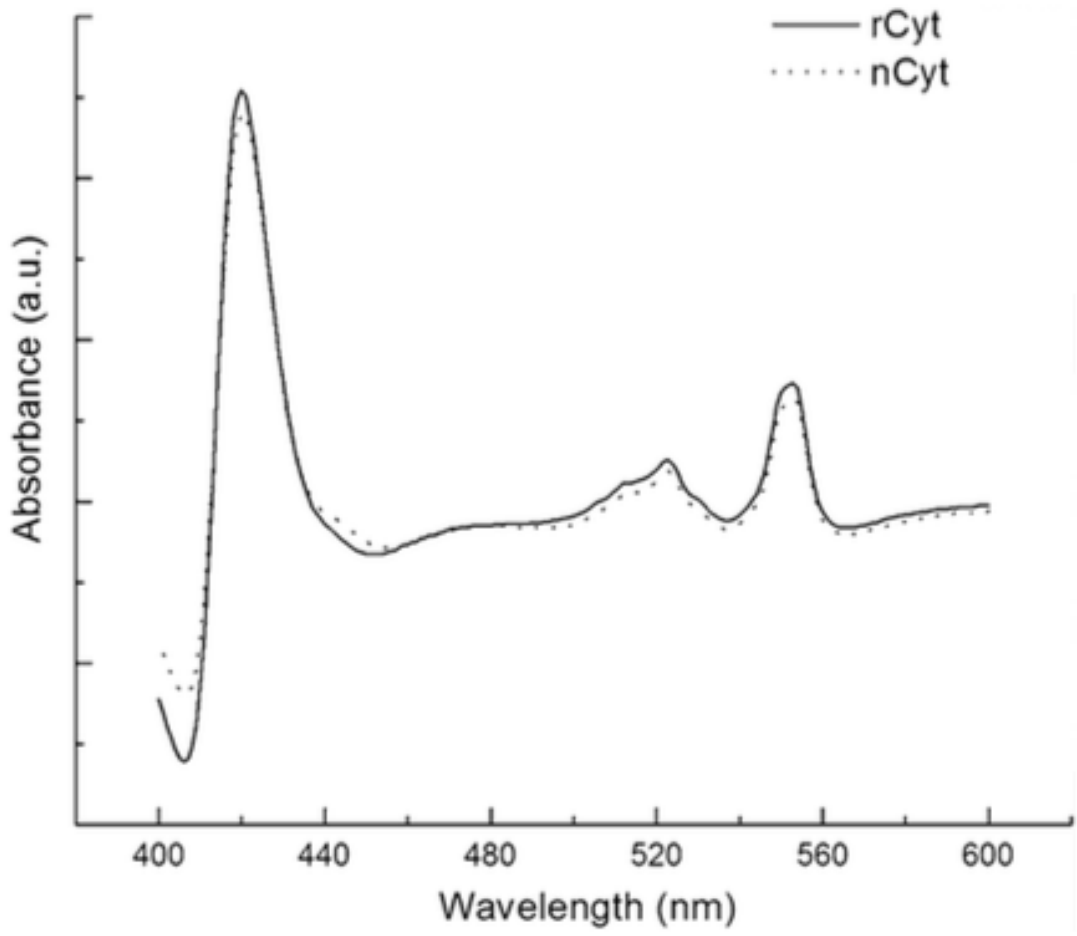

2.2: UV-Visible Difference Spectra. Reduced-minus-oxidized difference spectra of recombinant cyt c553 (solid) and native cyt c553 (dotted) at room temperature. Samples were diluted to 1 lM, based on heme concentration. Separate spectra were collected for reduced (excess dithionite) or oxidized (air purified) conditions, and the oxidized spectrum was subtracted from the reduced spectrum.

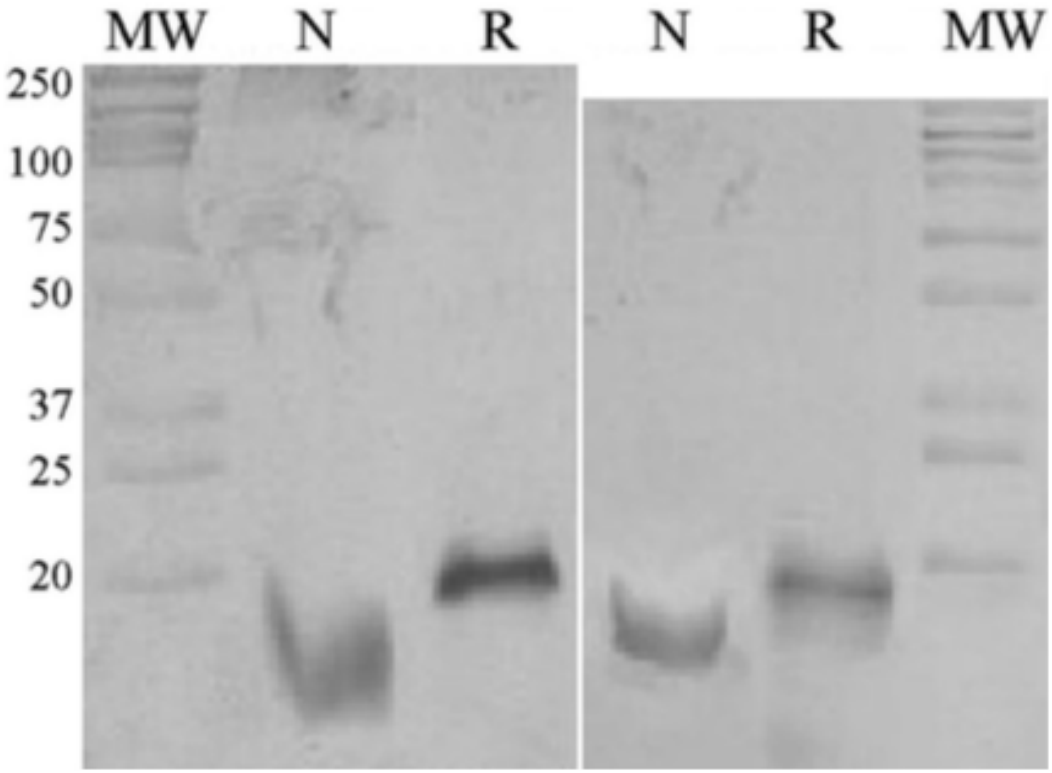

2.3: SDS-PAGE Analysis of Cyt c553 From H. modesticaldum. Equal amounts (equivalent to 125 ng of heme) of native cytochrome c553 (left lane; ‘‘N’’) and recombinant cyt c553 (right lane; ‘‘R’’) were run on 20 % SDS-PAGE gels. Gels were subsequently silver-stained (a) or stained for heme (b)

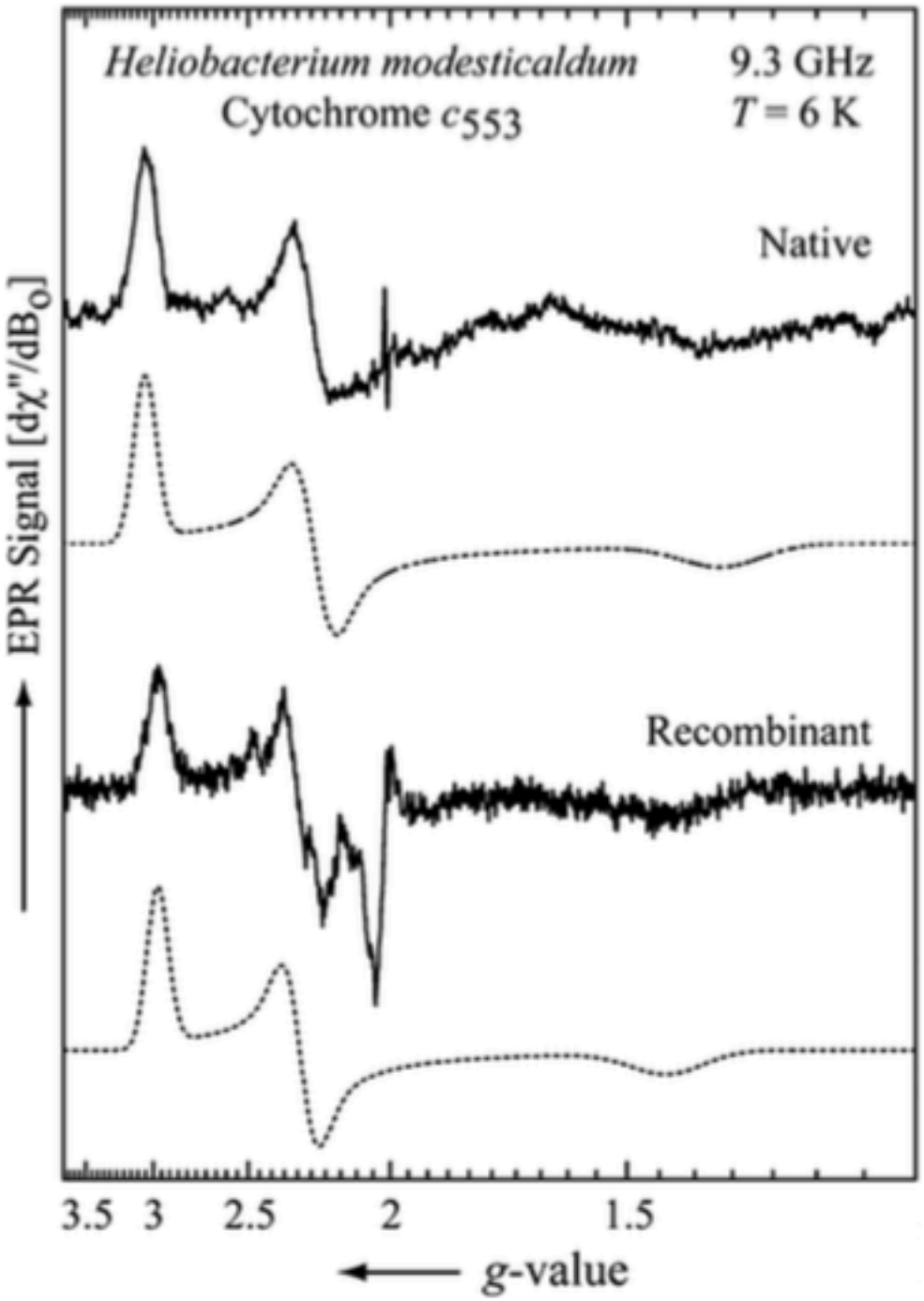

2.4: EPR Spectra of Native and Recombinant Cyt c553. Oxidized- minus-reduced difference cw-EPR spectra of recombinant cytochrome (bottom) and native cytochrome

(top) at 6 K. Microwave frequency and power were 9.337 GHz and 0.2 mW, respectively; field modulation frequency and amplitude were 100 kHz and 2 mT, respectively. Simulations are shown below each spectrum as dotted lines.

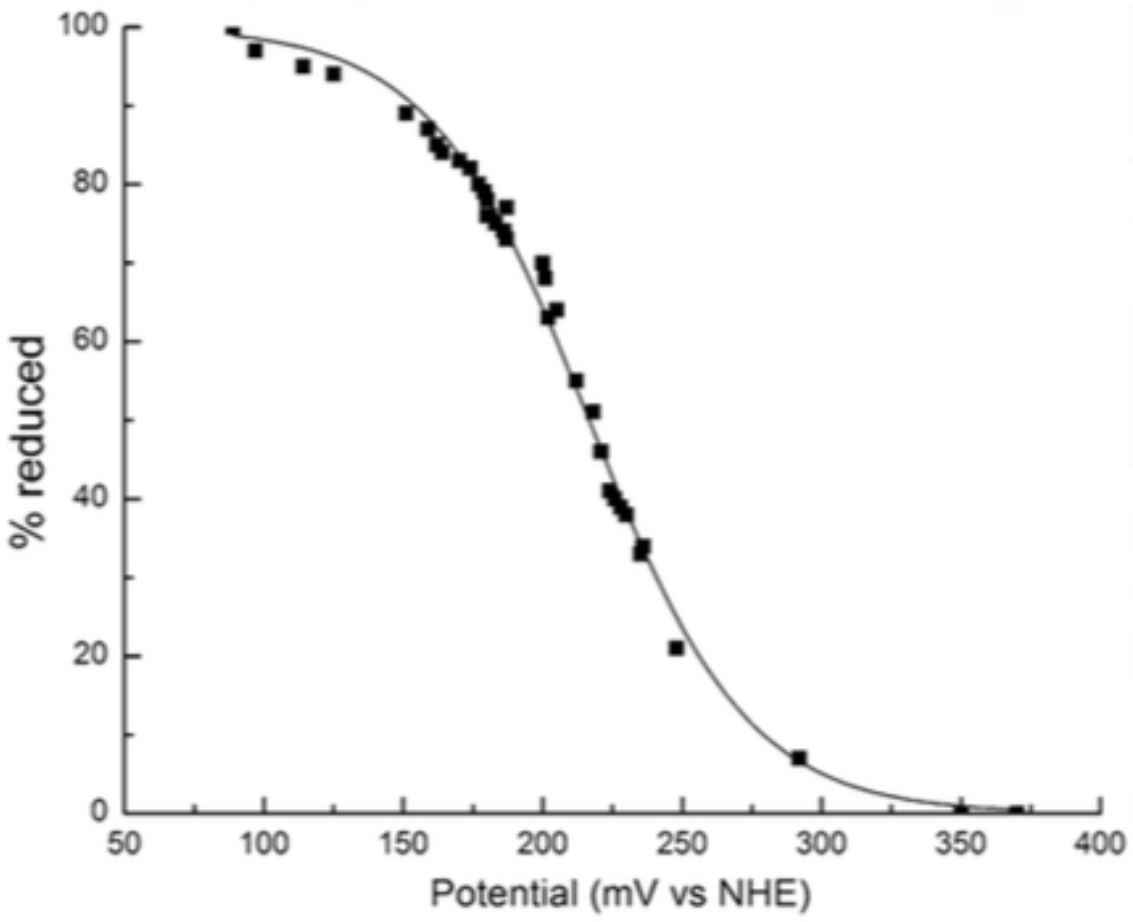

2.5: Potentiometric Titration of Recombinant Cyt c553. Squares are the measured data, and the line represents the best fit to the Nernst equation with no constraints, which yielded E_m = +217 ± 0.6 mV and n = 0.91

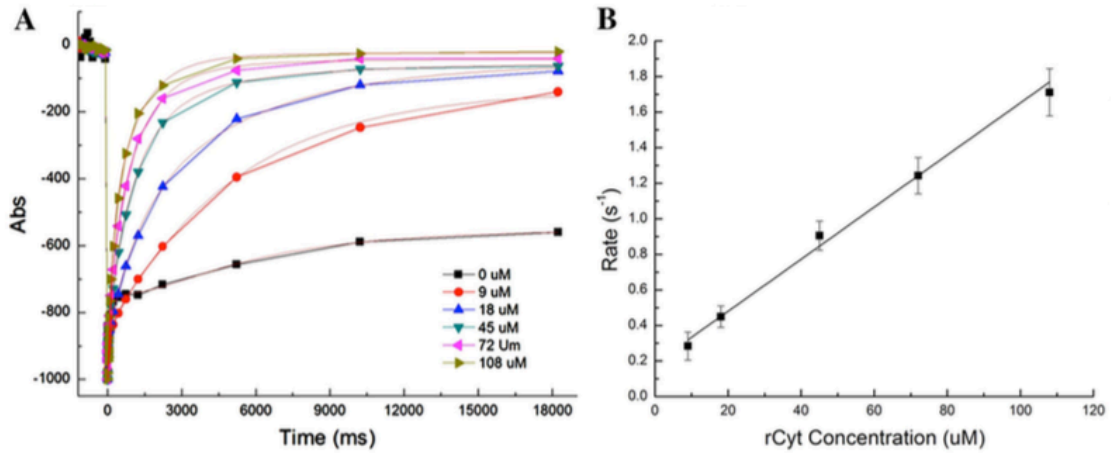

2.6: Use of Recombinant Cyt $_{c553}$ as Electron Donor to $P800^{+}$. HbRCs (at 0.5 lM) were given a saturating 532-nm laser flash (30 mJ, 6-ns duration), and absorption was monitored at 803 nm using 10-ls flashes from an LED. Ascorbate (10 mM) was used as a sacrificial electron donor, and BV (5 mM) was used as an artificial electron acceptor. Panel A shows the raw data of P800 photobleaching and recovery at each cyt c553 concentration, along with the three- component fitting (see text for details). In panel B, the calculated rate of $P800^{+}$ reduction by cyt c553 is plotted vs cyt c553 concentration

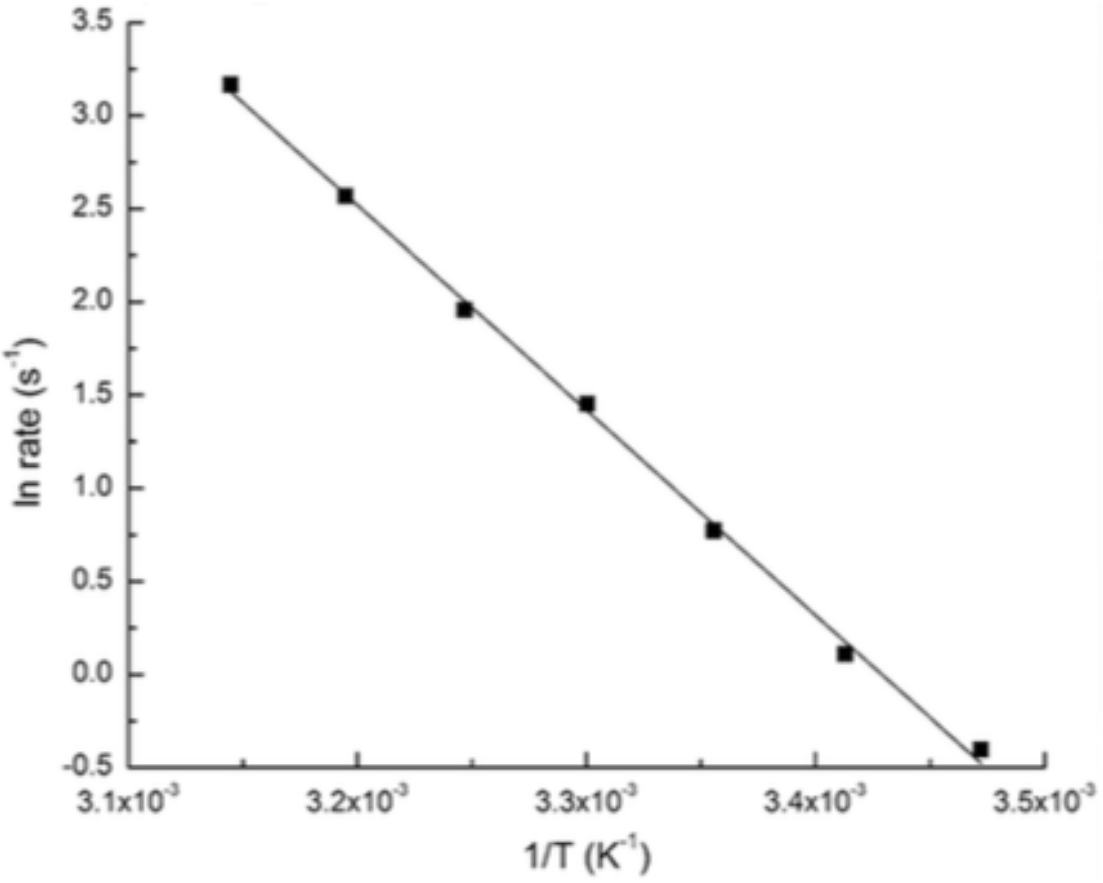

2.7: Arrhenius Plot of Reduction of $P800^+$ by Recombinant Cyt $c553$. The anaerobic cuvette was equilibrated at temperatures varying from 10 to 40 °C, and the reduction of $P800^+$ by cyt $c553$ was followed as in Fig 2.6. The calculated E_a was 91.4 kJ mol^{-1}

CHAPTER 3

LIGHT-DRIVEN QUINONE REDUCTION IN MEMBRANES OF HELIOBACTERIA

Manuscript In Preparation :

Trevor S. Kashey, Dustin D. Luu, John C. Cowgill, and Kevin E. Redding
"Light-driven quinone reduction in membranes of heliobacteria"

ABSTRACT

Photosynthetic reaction centers (RCs) evolved >3 billion years ago and have diverged into Type II RCs reducing quinones and Type I RCs reducing soluble low-potential acceptors via iron-sulfur clusters. Like Photosystem I (PSI), the Type I RC of heliobacteria contains two embedded menaquinones (MQ); unlike PSI, it does not use MQ in forward electron transfer. We found that illumination of heliobacterial membranes resulted in light-dependent reduction of MQ to menaquinol (MQH_2). The MQ/MQH_2 ratio seems to result from competition between the heliobacterial RC and MQH_2 oxidation by the cytochrome b_6c complex. The HbRC may represent a functional intermediate between type II RCs and PSI, preferentially reducing soluble acceptors via its iron-sulfur cluster but reducing its bound MQ in their absence, potentially driving an alternate cyclic electron transfer pathway.

Main text

All known RCs have a common architecture in which 5 transmembrane helices each from two similar (or identical) membrane-embedded polypeptides bind the cofactors required for light-driven electron transfer (ET) through the complex. The type II RCs are

heterodimeric and the two cofactor branches are functionally asymmetric, with one specialized for charge separation and electron transfer to the quinone on the other side (Q_B), which becomes fully reduced to a quinol after two light-driven ET events and can then diffuse into the membrane as the terminal product. In Photosystem I (PSI), the best understood type I RC, there is an iron-sulfur cluster shared between polypeptides called F_X, and the quinone of either branch can be used as an ET intermediate to it from the chlorins (where charge separation takes place). The other known type I RCs are homodimeric and are found in phototrophic bacteria that use them to drive cyclic photophosphorylation. Among these are the Heliobacteria, the only phototrophic member of the Firmicutes. Although the heliobacterial RC (HbRC) possesses two embedded MQs, they are poorly bound (like Q_B) and are not used as intermediates in ET to the F_X cluster (*87*) .This cluster has recently been shown to be the terminal acceptor in the HbRC and is capable of reducing a variety of soluble acceptor proteins (*53, 56, 88*). Although the HbRC contains up to 2 bound MQ, the quinones are bound rather loosely and fall out easily (*87, 89*). Moreover, although some EPR experiments have been interpreted as providing evidence for the involvement of a semiquinone species during forward ET within the HbRC (*90*) ,optical studies have found no signs of such a species (*91*) (*92*), and HbRCs lacking MQ or membranes depleted of MQ by ether extraction are not blocked in ET to the F_X cluster. This indicates that ET within the HbRC is very different from the case in PSI and raises the question: what is the role of the quinone within the HbRC?

Heliobacteria use MQ exclusively as their quinone (*33*). In *Heliobacterium*

modesticaldum, the major quinone found is MQ-9 with a smaller amount of MQ-9; the MQ pool is ~50% reduced in membranes prepared anoxically (*25*). However, if the membranes were exposed to air in the dark during the wash step, the quinone pool was subsequently found to be almost completely oxidized (Table 3.1**).** This is unsurprising, as the genome encodes a cytochrome *bd*-type quinol oxidase complex, which should be capable of reducing O_2 to water using MQH_2 as reductant (*23, 93*). Such air-treated membrane preparations were used for all further studies described here. The genome also encodes a NAD(P)H:MQ oxidoreductase (*23, 93*), which is expected to take part in cyclic electron flow (*64*). Incubation of membranes with 0.5 mM NADH (or NADPH) for 10 minutes resulted in reduction of MQ, such that MQH_2 constituted ~45% of the pool (i.e. a ~15-fold rise in MQH_2 content). Ascorbate did not reduce MQ, but very slow MQ reduction occurred in the dark, such that ~8% MQH_2 was attained after 24 hours. This is likely due to reduction by H_2 present in the glovebox (~5% of the atmosphere), perhaps due to the action of membrane-bound NiFe hydrogenases (*23, 93*). Thus, all experiments employed membranes within 2 hours of thawing.

To test the hypothesis that the activity of the HbRC could result in the reduction of the quinone pool, we exposed membranes to light from a 532-nm laser immediately before extraction. We found that even a few seconds of light was sufficient to observe significant reduction of the quinone pool (Fig. 3.1). The time resolution of our experiments was limited, but we found that after 1 s of illumination (the shortest time we could measure accurately), the MQH_2 level was more or less constant thereafter (not shown).

The MQH_2 level increased with increasing laser power (Fig 3.2), consistent with a role for the HbRC. Since reduction of MQ to MQH_2 is a 2-electron process, it would require a first charge separation to generate the $P_{800}^{+}F_x^{-}$ state, followed by re-reduction of P_{800}^{+} to allow a second charge separation. Charge recombination of the $P_{800}^{+}F_x^{-}$ state occurs with a decay time of ~15 ms (*46*), but the membrane-attached cyt c_{553} can reduce P_{800}^{+} in less than ~1 ms (*63, 94*). It is therefore expected that photo-accumulation of the reduced F_X cluster (F_X^{-}) could occur efficiently in illuminated membranes containing reduced cyt c_{553} but lacking soluble acceptors to the F_X cluster. As the cyt *c* was largely oxidized after exposure to air, ascorbate was added as a sacrificial electron donor to cyt c_{553} (*60*); we had previously established that it could not reduce MQ directly. Quinone reduction was blocked in the absence of ascorbate (Fig. 3.2). The membranes should also be largely devoid of soluble electron carriers that could direct electrons away from the HbRC after a single turnover. Consistent with this, washing of the membranes with 0.1 M Na_2CO_3 buffer at pH 11, which should remove all extrinsic proteins, did not significantly affect MQ reduction levels in the light (Table 3.1). Not only are soluble electron acceptors unnecessary for MQ reduction, one might expect that an acceptor from F_X would compete with MQ for electrons. To test this hypothesis, benzyl viologen (BV) was added to the membrane preparations. BV can act as an acceptor from F_X, but it does not re-reduce P_{800}^{+}, so it would not compete with endogenous cyt c_{553} (*60, 95*). As predicted, the addition of BV inhibited reduction of MQ to MQH_2 in a concentration-dependent manner (Fig. 3.2). This is attributed to a decrease in the steady-state level of F_X^{-}, consistent with excitation of a center in the $P_{800}F_X^{-}$ state being required for production of MQH_2.

Modulating the pH of the samples before light exposure should bias MQ reduction and MQH_2 oxidation in a predictable manner, as protons are consumed by the former and produced by the latter, leading one to expect MQ reduction to be favored (and MQH_2 oxidation to be disfavored) as protons become more abundant. Indeed, higher MQH_2 levels were obtained as pH was lowered (Fig. 3.4). Varying temperature could affect the speed at which MQH_2 and MQ can dissociate from and associate with their binding pockets, affecting the rate of reduction by the HbRC and the rate of its reoxidation by other membrane complexes. Raising the temperature resulted in a higher level of MQH_2 at steady state (Fig. 3.4). Thus, while one would expect that both MQ reduction and oxidation would be accelerated by an increase in temperature, the former process must be more temperature dependent.

The fact that the quinone reduction levels obtained in our experiments were both time-independent (after ~1 s) and very reproducible suggested that the steady-state level of quinol was determined by a competition between reduction by the HbRC and oxidation by other complexes. The cyt b_6c complex is expected to be the major (and perhaps only) contributor to MQH_2 oxidation in the light, as the HbRC would constantly oxidize cyt c_{553}, the electron acceptor of the cyt b_6c complex. We tested this hypothesis by addition of an inhibitor of the cyt b_6c complex. Although stigmatellin is a potent inhibitor of the Q_o site of the cyt b_6c complex in H. *modesticaldum* (*94, 95*), it has become difficult to obtain, prompting us to find an alternative. Making use of an assay for cyt c_{553} re-reduction (Fig. 3.7), we identified azoxystrobin as a relatively potent inhibitor of cyt b_6c activity ($K_{1/2} \approx 5$ μM; Fig. 3.7). The addition of 100 μM azoxystrobin to the light-driven

MQ reduction assay resulted in a doubling of the MQH_2 reduction level (55% vs 26% MQH_2; Table 3.1).

By the same logic, an inhibitor of MQ reduction by the HbRC would be expected to have the opposite effect. Competitive inhibitors that act at the Q_B site have been useful in the analysis of type II RCs. There are no known inhibitors that bind at the phylloquinone-binding site of PSI, which is unsurprising given that the PhQ is tightly bound in the pocket and serves as an intermediate in ET to F_X, not as an exchangeable acceptor. One only sees exchange of the quinone from this site with exogenous quinones if it has become doubly reduced (*96*), or removed by solvent extraction and replaced with a foreign quinone (*97-99*). If MQ is fully reduced to quinol by the HbRC and then exchanges with the MQ pool in the membrane, then the quinone-binding site of the HbRC would be somewhat analogous to the Q_B site in type II RCs. Terbutryn is an inhibitor of the Q_B site in both the purple bacterial RC and PSII (*100*) and blocks light-driven quinone reduction *in vivo* and *in vitro*. We tested its effects on MQ photoreduction in heliobacterial membranes. Addition of 6 μM, 60 μM, and 600 μM terbutryn resulted in a 30%, 70%, and 80% decrease in MQH_2 level respectively. We observed no effect of terbutryn upon P_{800} photo-oxidation yields or upon the rate of decay of P_{800}^+ by charge recombination of $P_{800}^+F_X^-$ with a single laser flash (**data not shown**), consistent with the lack of effect upon charge separation in heliobacterial membranes (*87*) and isolated HbRC (*89*) after quinone removal.

Live heliobacteria exhibit fluorescence induction and the $P_{800}F_X^-$ state has been identified as the one emitting fluorescence, presumably after charge separation and recombination

of the $P_{800}^{+}A_0^{-}F_X^{-}$ state (*94*). When illuminated strongly, the electron acceptor for the HbRC within heliobacteria becomes exhausted in a manner of seconds, leading to a coordinated rise of F_X^{-} and fluorescence. If MQ can serve as an alternate electron acceptor from the HbRC, then one would expect that MQ reduction would quench fluorescence emission; blocking MQ reduction should therefore lead to higher fluorescence emission. We found that addition of terbutryn at lower levels (10-90 μM) to living *H. modesticaldum* cells led to an increase of fluorescence induced by strong actinic light (Fig. 3.3), consistent with the idea that terbutryn inhibits a process leading to oxidation of F_X^{-} (or prevention of F_X reduction). Addition of a soluble acceptor from F_x (BV) also inhibits fluorescence induction (*95*), showing that this is a general effect. Higher terbutryn concentrations (>100 μM) led to a drop in the fluorescence rise, which can be explained as an effect upon the cyt b_6c complex, as terbutryn is known to occupy the Q_o site at lower affinity than the Q_B site of type II RCs.We confirmed this by assessing its effect upon the cyt c_{553} re-reduction rate in heliobacterial membranes, and found that it inhibited cyt *c* re-reduction with a $K_{1/2}$ of ~100 μM (Fig 3.8). This explains the decrease in variable fluorescence, as we have shown that cyt *bc* inhibitors inhibit fluorescence emission by lowering the amount of reduced cyt *c*. RCs containing P_{800}^{+} are unable to perform CS and thus cannot undergo charge recombination and emit fluorescence (*94*).

(Fig. 3.5) Shows the time course of P_{800}^{+} re-reduction after the laser flash. It can be described adequately as the sum of 3 exponential decays with lifetimes of 4.5±0.6 ms (50%), 18± ms (43%), and 1.85±0.37 s (7.5%). The first is assigned to re-reduction by

the membrane-associated cyt c_{553}, the second is due to charge recombination of $P_{800}^{+}F_X^{-}$ (*94*), and the last represents slow reduction by ascorbate. The first assignment is confirmed by the cyt c_{553} kinetics. It is oxidized with a lifetime of 4.6±0.4 ms, identical to the fastest phase of P_{800}^{+} re-reduction. Re-reduction of oxidized cyt *c* is described by two kinetic components – a major component (84%) with a decay time of 150±42 ms and a minor component (15%) with a decay time of ~1 s. The latter is likely due to re-reduction by ascorbate, while the major component is assigned to re-reduction by the cyt b_6c complex, likely due to the reaction between the Rieske FeS cluster and the diheme cyt *c*, since the mobile cyt c_{553} and the diheme cyt *c* have similar spectra (*60, 67*) With this assay in hand, we screened known cyt *bc* Q_o-site inhibitors for their effect upon the rate of c_{553} re-reduction after a laser flash. Results with representative inhibitors present at 40 μM are shown in (Fig. 3.6). Based on these results, we tested azoxystrobin more carefully, as it appeared to be the most potent inhibitor that we tested. A titration of azoxystrobin allowed estimation of the efficacy of the inhibitor (Fig. 3.7). The decay time of cyt c_{553} re-reduction was increased ~30-fold by addition of azoxystrobin at 100 μM. The $K_{1/2}$ for azoxystrobin (i.e. the concentration at which the rate of cyt *c* reduction was reduced by half) was calculated to be ~5 μM. Based on the effects of terbutryn upon fluorescence induction kinetics (Fig 3.3), we hypothesized that at high concentrations this molecule is able to bind at the Q_o site and inhibit the cyt b_6c complex. To test this hypothesis, we used the cyt *c* re-reduction assay. Indeed, at concentrations in the range of hundreds of μM, terbutryn did inhibit the activity of the cyt b_6c complex (Fig 3.3) Based on the titration data, we could estimate a $K_{1/2}$ of ~100 μM for terbutryn. This value is

consistent with the range of terbutryn (above ~100 μM) that caused a decrease in fluorescence, such as was previously observed with stigmatellin, a potent Q_o site inhibitor (*94*).

MATERIALS AND METHODS

Cells and materials: The Ice1 strain of *Heliobacterium modesticaldum* (*17*), generously provided by Prof. Michael Madigan (Southern Illinois Univ.), was used for all studies. Liquid cultures of *H. modesticaldum* were grown anaerobically to late exponential phase in PYE medium (*17*). Benzyl viologen (1,10-dibenzyl-4,40-bipyridinium dichloride), NADH, and azoxystrobin were purchased from Sigma-Aldrich. Terbutryn was a generous gift from Dr. James Allen (Arizona State University).

Isolation of membranes: Late-log cells were harvested by centrifugation at 5000 x*g* and resuspended in 50 mM MOPS (pH 7.0) under an atmosphere of 95% N_2/5% H_2. Lysozyme was added to 100 μg/mL and after 30 min incubation at room temperature cells were lysed by sonication on ice in the dark on the bench (*i.e.* under air). The lysate was monitored by light microscopy every 5 cycles (1 minute at 12 W interspersed with 4 minutes on ice) until cells were fully lysed. Unbroken cells and cell wall material were removed by centrifugation at 12500 x*g* for 5 minutes. The supernatant was transferred to ultracentrifuge tubes in the glovebox and all subsequent steps were performed anoxically under very low green light. Membranes were pelleted by centrifugation at 200,000 x*g* for 30 minutes. Membranes were resuspended in the anaerobic chamber in 50 mM MES (pH 6.0) with 20% glycerol to a final concentration of 38 μM BChl *g*. The BChl *g*

concentration in acetone extracts of membranes was determined via visible spectrophotometry using a gas-tight cuvette and e_{788} = 76 mM^{-1} cm^{-1} at 788 nm (*25*). Membrane aliquots were stored under liquid nitrogen.

MQ reduction assay: All manipulations were performed in an anaerobic chamber in the dark. Unless otherwise noted, membrane samples were diluted to 15 µM BChl *g* in a buffer containing 50 mM MES (pH 6.0), 20 mM ascorbate, and 20 mM $MgSO_4$. Each sample was exposed to light for 5 seconds and immediately extracted by addition of 20 volumes of degassed acetone. After vigorous mixing, they were promptly centrifuged at 14200 x*g* for 1 minute, loaded into a gas-tight Hamilton syringe, removed from the glovebox and immediately loaded onto the HPLC. Sample illumination was provided by a frequency-doubled continuous wave Nd-YAG laser (532 nm) operated in a modulated manner using a TTL pulse generator. It was typically run in pulsed mode at 1 kHz with a 500-µs pulse length (*i.e.* 50% power); maximum output of the laser was 860 mW. The pulse lengths were shortened to lower power further (*e.g.* 10% power, or 86 mW average power, corresponded to using 100-µs pulses at 1 kHz). Temperature was controlled by water bath incubation for 10 minutes followed by immediate laser exposure. The pH was changed by washing and resuspending membranes in the following buffers: pH 5 (50 mM acetate), pH 6 (50 mM MES), pH 7 (50 mM MOPS), pH 8 (50 mM Tricine). After addition of inhibitors (BV, azoxystrobin, terbutryn), membranes were allowed to incubate at room temperature in the dark for 20 minutes before illumination to allow equilibration with the added reagent.

Pigment analysis: Samples were injected into a Quaternary Gradient LC-2000plus-LPG

HPLC (Jasco) using a C-18 Column (Phenomenex Ultrasphere 250 mm L x 4.6 mm ID packed with 5-µm particles). Pigments were eluted isocratically using 17:1 methanol/hexane at a flow rate of 1.5 mL min^{-1}. Integration of the peaks in the chromatograms allowed calculation of the number of pigments per HbRC. The abundance of each pigment was calculated from the area of the peak at 750 nm for BChl g, 246 nm for MQH_2, 260 nm for MQ and normalized to 22 BChl *g* per RC, using the extinction coefficients of these pigments at those wavelengths (76 mM^{-1} cm^{-1}, 15 cm^{-1} mM^{-1} and 45 cm^{-1} mM^{-1}, respectively (*101*)). The integrated MQ and MQH_2 peak areas were used to calculate the ratio of MQH_2 to MQ in the extract. Peaks associated with MQ and MQH_2 were assigned based on their UV-visible absorbance spectrum, as per (*25*).

Cyt c *re-reduction assay:*

An assay was developed to examine the efficacy of potential cyt *bc* inhibitors in the membranes by monitoring cyt c_{553} oxidation and reduction. The assay consisted of membranes (50 µM BChl *g*) suspended in a buffer containing 50 mM MOPS (pH 7), 10 mM $MgSO_4$, 20 µM benzyl viologen, 500 µM NADH in a 10-mm anaerobic cuvette. Benzyl viologen was used to accept electrons from F_X^-, thus preventing charge recombination from the $P_{800}^+F_X^-$ state and ensuring that P_{800} would be re-reduced by cyt c_{553}. NADH was added to donate electrons to the menaquinone pool (via the NADH dehydrogenase). A 6-ns saturating (~25 mJ) laser flash from a frequency-double NdYAG laser (532 nm; Continnum Minilite) was used to photo-oxidize P_{800}. Oxidation and re-reduction of P_{800} was followed with 10-µs flashes at 805 nm, while cyt c_{553} was monitored at 554 nm.

Evolutionary and physiological implications

The striking structural similarity between the core of PSI, PSII, and the purple bacterial RC has led to the conclusion that the type I and type II RCs share a common evolutionary origin (*102*) (*103*) (*104*). That is, the RC has evolved only once on this planet and the original RC was almost surely homodimeric. All known type II RCs (PSII, and the RCs of purple proteobacteria and Chloroflexi) are heterodimeric, as their function dictates a specialization of the two cofactor branches: one for charge separation, and one for stabilization of the semiquinone anion (i.e. preventing charge recombination before the second electron arrives to fully reduce it to a quinol). Although PSI is also a heterodimer, it has been shown that it is functionally symmetric at the core, in that both cofactor branches are used for ET to the F_X cluster (*105*). Although the phylloquinone cofactor of PSI has a headgroup (2-methylnaphthoquinone) identical to that of MQ, differing only in the isoprenoid tail substituent, it is not normally reduced to a quinol. However, PSI can reduce the embedded quinone when the latter is replaced with a quinone of higher potential (*96*), albeit very inefficiently. It is thought that PSI has evolved to use the embedded 2-methylnaphthoquinone exclusively as an ET intermediate to the F_X cluster and its structure and function prohibits double reduction of the quinone to quinol (*106*).

All of the other type I RCs are homodimeric and exist in anoxygenic phototrophic bacteria (Heliobacteria, Chlorobi, Chloroacidobacteria) that presumably employ cyclic photophosphorylation using ferredoxin as RC electron acceptors and either ferredoxins or NAD(P)H as electron donors to a complex I-like enzyme that pumps protons across the membrane as the electrons are transferred to the MQ pool. Our results suggest that the

HbRC represents a functional hybrid between PSI and the type II RCs, preferentially reducing soluble (one-electron) acceptors when they are available, and reducing their embedded quinones when they are such soluble acceptors are limiting. Thus, there might be two possible electron transport pathways in heliobacteria – a longer one using complex I under conditions when the soluble acceptor pool is oxidized and a shorter one resembling the cycle in purple bacteria when the acceptor pool becomes reduced. Although the shorter cycle would pump fewer protons per electron than the longer cycle, some pumping is better than nothing

REFERENCES

17. L. K. Kimble, L. Mandelco, C. R. Woese, M. T. Madigan, Heliobacterium modesticaldum, sp. nov., a thermophilic heliobacterium of hot springs and volcanic soils. *Arch Microbiol* **163**, 259-267 (1995).

23. W. M. Sattley *et al.*, The genome of Heliobacterium modesticaldum, a phototrophic representative of the Firmicutes containing the simplest photosynthetic apparatus. *J Bacteriol* **190**, 4687-4696 (2008).

25. I. Sarrou *et al.*, Purification of the photosynthetic reaction center from *Heliobacterium modesticaldum*. *Photosynth Res* **111**, 291-302 (2012).

33. A. Hiraishi, Occurrence of menaquinone is the sole isoprenoid quinone in the photosynthetic bacterium *Heliobacterium chlorum*. *Arch Microbiol* **151**, 378-379 (1989).

46. M. Heinnickel, R. Agalarov, N. Svensen, C. Krebs, J. H. Golbeck, Identification of F_X in the Heliobacterial Reaction Center as a [4Fe-4S] Cluster with an S = 3/2 Ground Spin State. *Biochemistry* **45**, 6756-6764 (2006).

53. S. P. Romberger, C. Castro, Y. Sun, J. H. Golbeck, Identification and characterization of PshBII, a second F_A/F_B-containing polypeptide in the photosynthetic reaction center of *Heliobacterium modesticaldum*. *Photosynth Res* **104**, 293-303 (2010).

56. S. P. Romberger, J. H. Golbeck, The F_X iron-sulfur cluster serves as the terminal bound electron acceptor in heliobacterial reaction centers. *Photosynth Res* **111**, 285-290 (2012).

60. T. S. Kashey, J. B. Cowgill, M. D. McConnell, M. Flores, K. E. Redding, Expression and characterization of cytochrome c_{553} from *Heliobacterium modesticaldum*. *Photosynth Res* **120**, 291-299 (2014).

63. H. Oh-oka, M. Iwaki, S. Itoh, Electron donation from membrane-bound cytochrome *c* to the photosynthetic reaction center in whole cells and isolated membranes of *Heliobacterium gestii*. *Photosynthesis Research* **71**, 137-147 (2002).

64. D. M. Kramer, B. Schoepp, U. Liebl, W. Nitschke, Cyclic electron transfer in *Heliobacillus mobilis* involving a menaquinol-oxidizing cytochrome *bc* complex and an RCI-type reaction center. *Biochemistry* **36**, 4203-4211 (1997).

67. H. Yue, Y. Kang, H. Zhang, X. Gao, R. E. Blankenship, Expression and characterization of the diheme cytochrome *c* subunit of the cytochrome *bc*

complex in *Heliobacterium modesticaldum*. *Arch Biochem Biophys* **517**, 131-137 (2012).

87. F. A. Kleinherenbrink, I. Ikegami, A. Hiraishi, S. C. M. Otte, J. Amesz, Electron transfer in menaquinone-depleted membranes of *Heliobacterium chlorum*. *Biochim Biophys Acta* **1142**, 69-73 (1993).

88. S. P. Romberger, J. H. Golbeck, The bound iron-sulfur clusters of type-I homodimeric reaction centers. *Photosynth Res* **104**, 333-346 (2010).

89. A. Chauvet *et al.*, Temporal and spectral characterization of the photosynthetic reaction center from *Heliobacterium modesticaldum*. *Photosynth Res* **116**, 1-9 (2013).

90. R. Miyamoto, H. Mino, T. Kondo, S. Itoh, H. Oh-Oka, An electron spin-polarized signal of the $P_{800}^{+}A_1(Q)^{-}$ state in the homodimeric reaction center core complex of *Heliobacterium modesticaldum*. *Biochemistry* **47**, 4386-4393 (2008).

91. K. Brettel, W. Leibl, U. Liebl, Electron transfer in the heliobacterial reaction center: evidence against a quinone-type electron acceptor functioning analogous to A1 in photosystem I. *Biochimica et Biophysica Acta* **1363**, 175-181 (1998).

92. S. Lin, H. C. Chiou, R. E. Blankenship, Secondary electron transfer processes in membranes of *Heliobacillus mobilis*. *Biochemistry* **34**, 12761-12767 (1995).

93. W. M. Sattley, R. E. Blankenship, Insights into heliobacterial photosynthesis and physiology from the genome of Heliobacterium modesticaldum. *Photosynth Res* **104**, 113-122 (2010).

94. K. E. Redding *et al.*, Modulation of the fluorescence yield in heliobacterial cells by induction of charge recombination in the photosynthetic reaction center. *Photosynth Res* **120**, 221-235 (2014).

95. A. M. Collins, K. E. Redding, R. E. Blankenship, Modulation of fluorescence in *Heliobacterium modesticaldum* cells. *Photosynth Res* **104**, 283-292 (2010).

96. M. D. McConnell, J. B. Cowgill, P. L. Baker, F. Rappaport, K. E. Redding, Double reduction of plastoquinone to plastoquinol in photosystem 1. *Biochemistry* **50**, 11034-11046 (2011).

97. J. Biggins, Evaluation of selected benzoquinones, naphthoquinones, and anthraquinones as replacements for phylloquinone in the A1 acceptor site of the photosystem I reaction center. *Biochemistry* **29**, 7259-7264 (1990).

98. T. W. Johnson *et al.*, Recruitment of a foreign quinone into the A(1) site of photosystem I - I. Genetic and physiological characterization of phylloquinone

biosynthetic pathway mutants in Synechocystis sp PCC 6803. *Journal of Biological Chemistry* **275**, 8523-8530 (2000).

99. T. W. Johnson *et al.*, Recruitment of a foreign quinone into the A(1) site of photosystem I - Invivo replacement of plastoquinone-9 by media- supplemented naphthoquinones in phylloquinone biosynthetic pathway mutants of synechocystis sp PCC 6803. *Journal of Biological Chemistry* **276**, 39512-39521 (2001).

100. C. R. Lancaster, M. V. Bibikova, P. Sabatino, D. Oesterhelt, H. Michel, Structural basis of the drastically increased initial electron transfer rate in the reaction center from a Rhodopseudomonas viridis mutant described at 2.00-A resolution. *J Biol Chem* **275**, 39364-39368. (2000).

101. A. Kroger, V. Dadak, On the Role of Quinones in Bacterial Electron Transport. *European Journal of Biochemisty* **11**, 328-340 (1969).

102. A. Amunts, O. Drory, N. Nelson, The structure of a plant photosystem I supercomplex at 3.4 A resolution. *Nature* **447**, 58-63 (2007).

103. E. P. Morris, B. Hankamer, D. Zheleva, G. Friso, J. Barber, The three-dimensional structure of a photosystem II core complex determined by electron crystallography. *Structure* **5**, 837-849 (1997).

104. J. Deisenhofer, O. Epp, K. Miki, R. Huber, H. Michel, X-ray structure analysis of a membrane protein complex. Electron density map at 3 A resolution and a model of the chromophores of the photosynthetic reaction center from Rhodopseudomonas viridis. *J Mol Biol* **180**, 385-398 (1984).

105. M. Guergova-Kuras, B. Boudreaux, A. Joliot, P. Joliot, K. Redding, Evidence for two active branches for electron transfer in photosystem I. *Proc Natl Acad Sci U S A* **98**, 4437-4442. (2001).

106. N. Srinivasan, I. Karyagina, R. Bittl, A. van der Est, J. H. Golbeck, Role of the hydrogen bond from Leu722 to the A1A phylloquinone in photosystem I. *Biochemistry* **48**, 3315-3324 (2009).

TABLES

Condition	Laser Power	% Reduction	% Error
No Ascorbate	22 mW	3.2	2.1
	430 mW	3.6	1.3
	860 mW	3.4	1.7
Dark Control	-	2.8	3.5
Buffer Control	-	27.8	1.9
DMSO Control	-	26.4	2.8
Carbonate Washed	-	22.32	1.2
Laser Power	22 mW	17.5	1.1
	430 mW	28.1	2.5
	860 mW	59.5	6
Temperature			
21C	-	28.1	2.5
30C	-	40.9	4.7
40C	-	50.8	2.5
pH			
5 Acetate	-	51.9	2.5
6 MES	-	46.7	0.2
7 MOPS	-	39.7	2.2
8 Tricine	-	26.3	0.7
Terbutryn Note that full laser power was used (860 mW) in order to maximize the MQ reduction signal.			
6 µM	860 mW	42	3.8
60 µM	860 mW	18	2.6
600 µM	860 mW	12	5.2
Benzyl Viologen			
10 µM	-	27	1.6
50 µM	-	16.77	2.8
5 mM	-	11.1	1
Azoxystrobin			
100 µM	-	54.9	4.1

3.1: Summary of Parameters Used in the MQ Reduction Assay on Isolated Heliobacterial Membranes. Unless otherwise noted, all samples were pH 6, and exposed to 430 mW laser power.

FIGURES

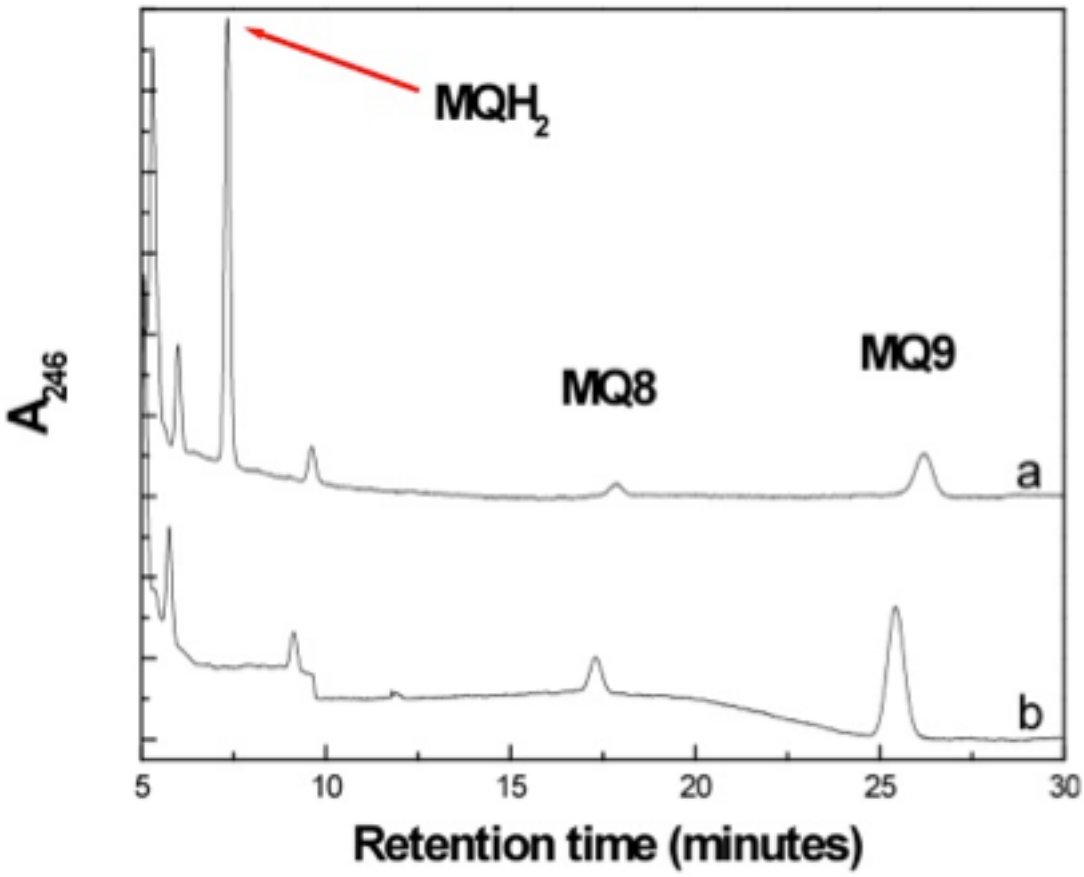

3.1: HPLC Chromatograph of an Acetone Extract of Heliobacterial Membranes Monitored at 246 nm. Membranes had been exposed to light (top) or maintained in the dark (bottom). Elution times of MQH2-9 (7 min), MQ-8 (17 min), and MQ-9 (26 min) are indicated.

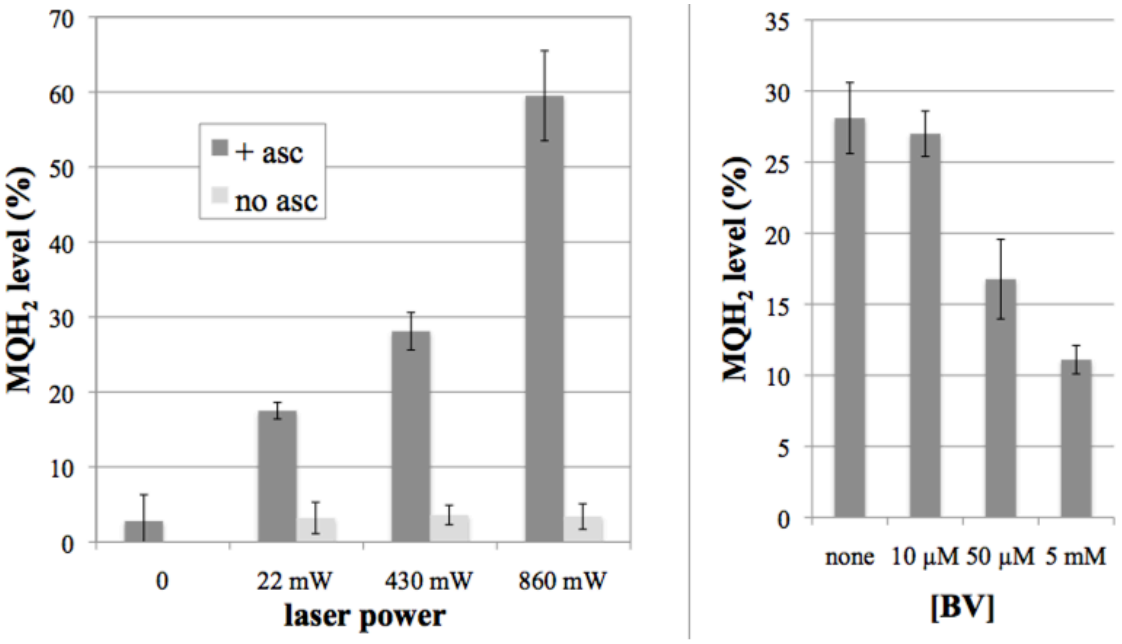

3.2: **A:** MQH_2 Level After Exposure to Increasing Laser Intensity in the Presence (dark) or Absence (light) of ascorbate. **B:** MQ photoreduction in membranes incubated with various amounts of benzyl viologen.

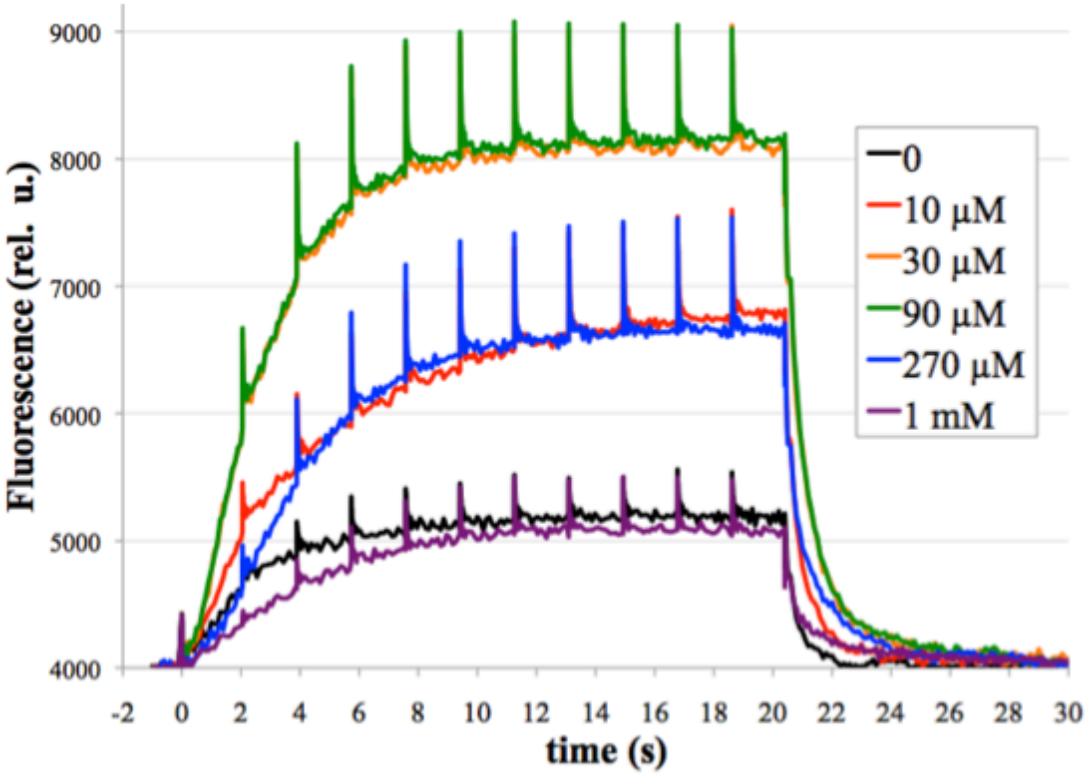

3.3: **A:** MQH_2 Level After Exposure to Increasing Laser Intensity In the Presence (dark) or Absence (light) of ascorbate. **B:** MQ photoreduction in membranes incubated with various amounts of benzyl viologen.

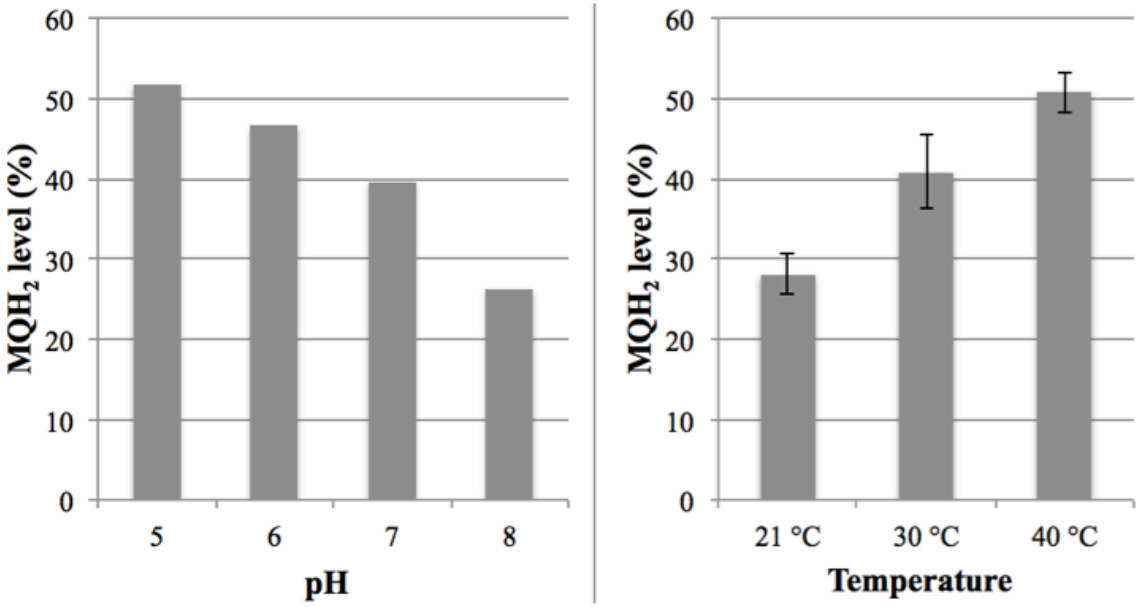

3.4: Isolated Heliobacterial Membranes Were Exposed To Varying Temperatures (A) and pH's(B). Via HPLC, the integrated MQ and MQH_2 peak areas were used to calculate the ratio of MQH_2 to MQ in the extract to determine the % of the pool reduced to MQH_2. MQ and MQH_2 peaks were assigned based on their UV-visible absorbance spectrum

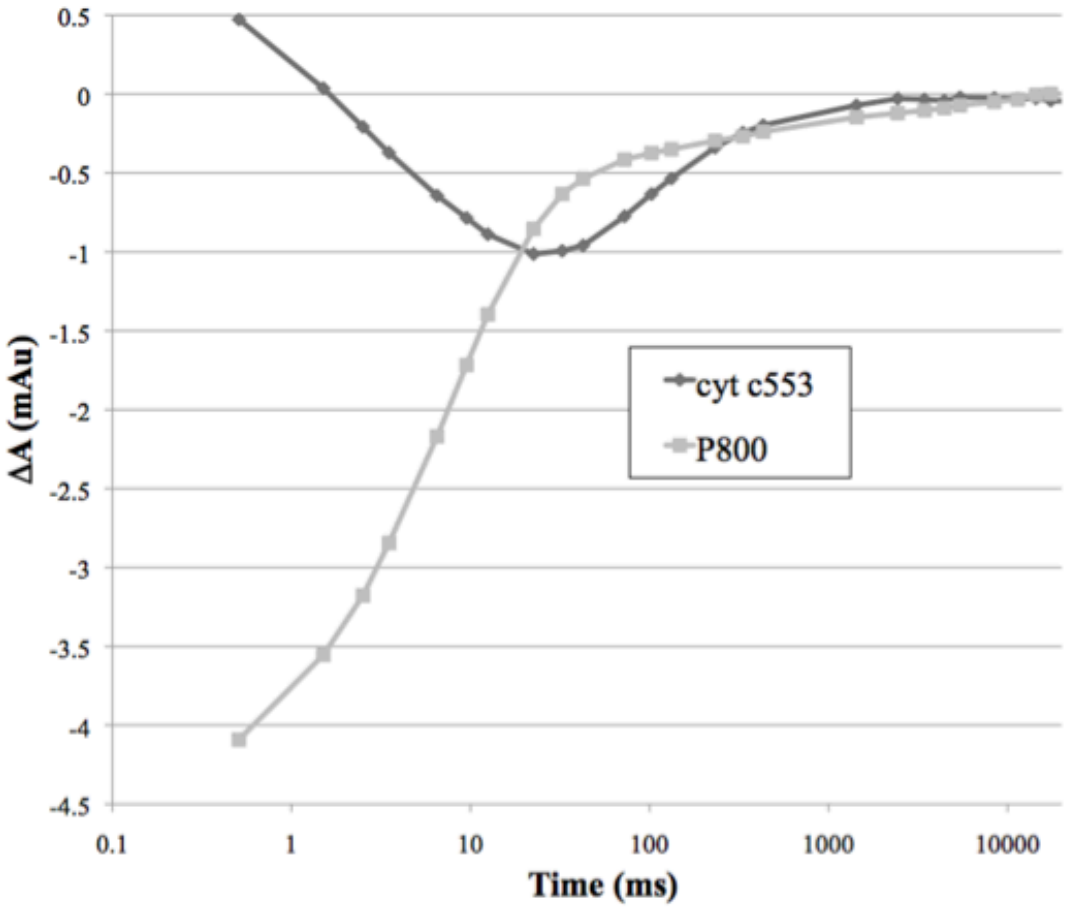

3.5: Measuring cyt c_{553} Re-reduction Kinetics. Isolated heliobacterial membranes incubated with 0.5 mM NADH for 15 minutes were given a saturating 532-nm laser flash (25mJ, 6 ns duration). Absorption was monitored at 803 nm (P800, gray curve) or 554 nm (cyt c_{553}, black curve) using 10 µs flashes from an LED before and after the saturating laser flash at 532 nm at time 0. Time after the flash is plotted on a log scale (the first point is 500 µs after the flash).

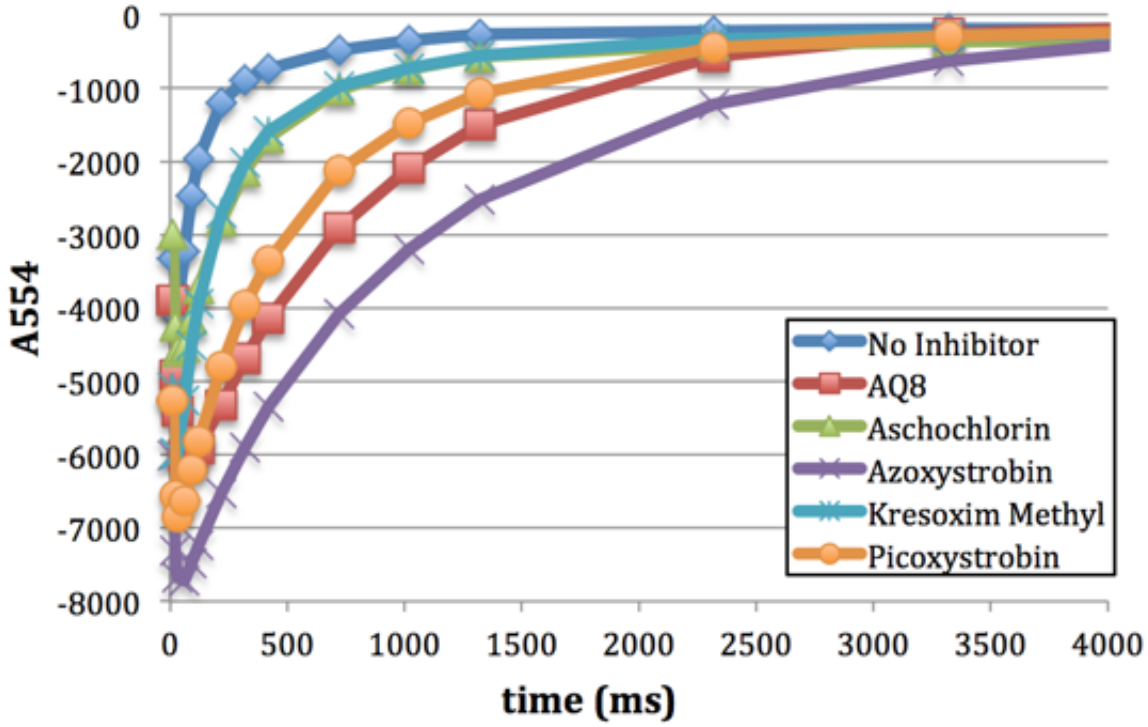

3.6: Measuring cyt c_{553} Re-reduction Kinetics with Candidate Inhibitors: Anthroquinone-8 (red squares), Aschochlorin (green triangles), Azoxystrobin (purple x's), kresoxim methyl (blue x's) and picoxystrobin (orange circles) were add to isolated heliobacterial membranes to a final concentration of 40 µM and incubated for 20 minutes in order to test their effect upon cyt c_{553} re-reduction.

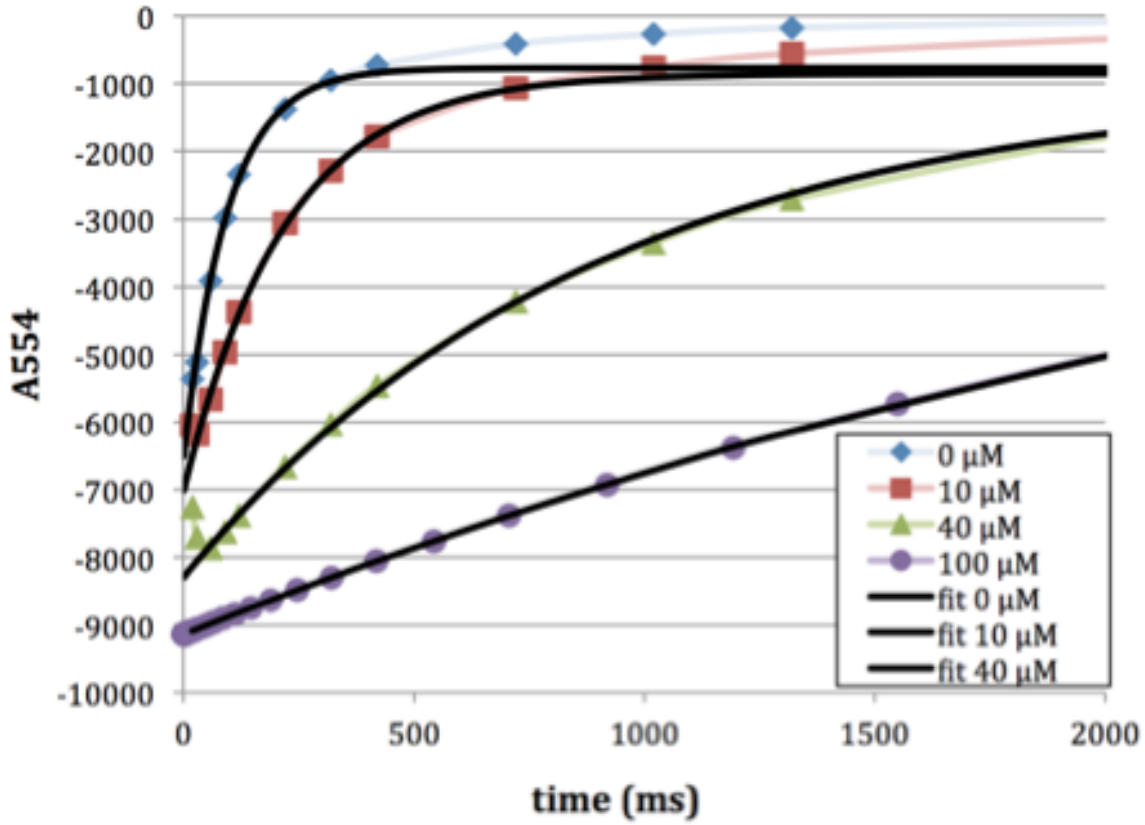

3.7: Effect of Titrating of Azoxystrobin on cyt c_{553} Re-reduction Kinetics. Re-reduction of cyt *c* was observed after a saturating single turnover laser flash in membranes that had been equilibrated with varying concentrations of azoxystrobin: 0 (blue diamonds), 10 µM (red squares), 40 µM (green triangles), and 100 µM (purple circles). Black lines are fits to a single exponential decay.

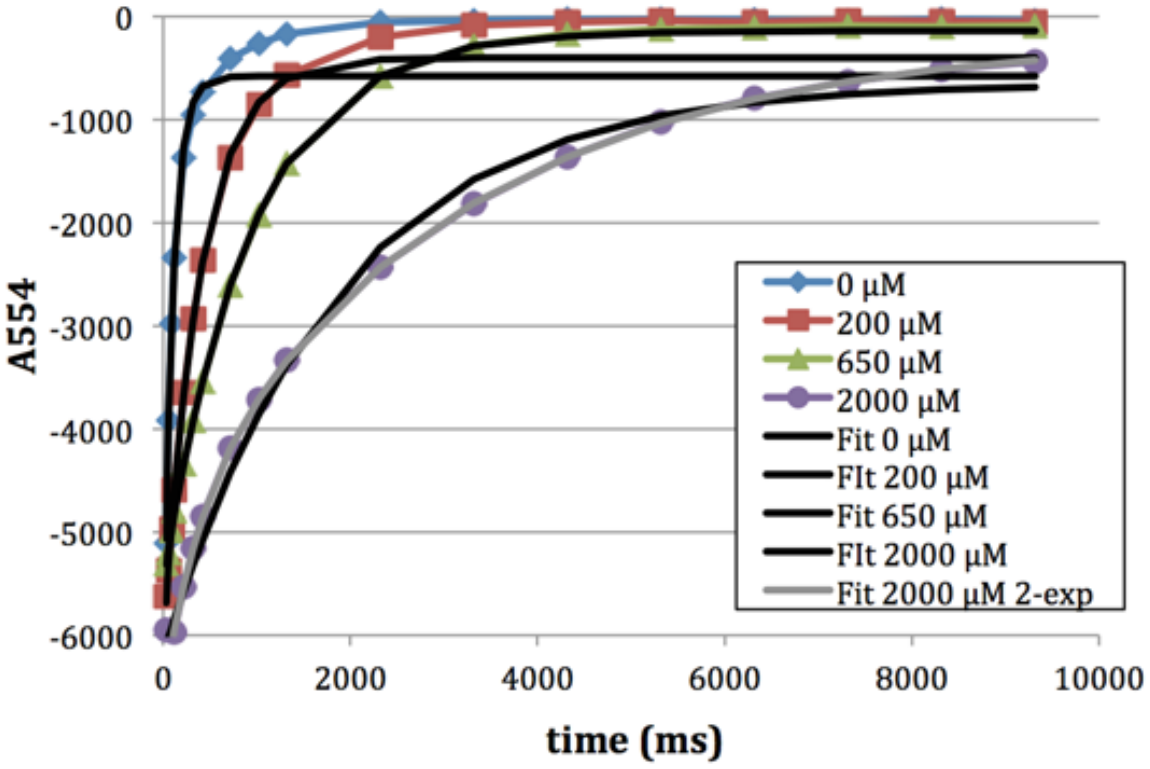

3.8: Effect of Titrating of Terbutryn on cyt c_{553} Re-Reduction Kinetics. Re-reduction of cyt *c* was observed after a saturating single turnover laser flash in membranes that had been equilibrated with varying concentrations of terbutryn: 0 (blue diamonds), 200 µM (red squares), 650 µM (green triangles), and 2 mM (purple circles). Black lines are fits to a single exponential of the first 90% of decay.

CHAPTER 4

THE FE-S CLUSTER FX REDUCES ENDOGENOUS NIF-SPECIFIC FERREDOXIN FDXB

Abstract

Heliobacteria contain the most elemental photosynthetic reaction centers known. Their Type 1 reaction center (HbRC) consists solely of 2 PshA proteins with a homodimeric structure. In algal and cyanobacterial photosystem I (PSI) the terminal acceptor F_A/F_B protein (PsaC) is strongly adhered to the P_{700} core. Heliobacteria contain two known F_A/F_B proteins, PshB I and PshB II, that act as endogenous acceptors to the HbRC core. However, these acceptors are not tightly bound and have since been considered soluble acceptors instead of subunits. These paralogous F_A/F_B proteins are now thought to accept electrons from the HbRC and subsequently reduce other proteins involved in downstream metabolism. If this were the case, they would be analogous to flavodoxin and ferredoxin in PSI. When HbRC cores are isolated, they do not contain the soluble acceptors PshBI and PshBII.There is preliminary evidence showing the direct reduction of another endogenous (but recombinant in E.*coli*) 2[4Fe-4S] acceptor. The presence of an Fe/S cluster verified by UV-Vis Clarified lysate containing FdxB accepts electrons without the use of PshBI or PshBII acting as intermediate electron transfer agents. This is contrary to PSI, where PsaC is required for the reduction of endogenous electron acceptors. This preliminary data may imply the HbRC core may be able to reduce a variety of soluble acceptors.

Introduction

Photosynthetic reaction centers (RC) are made up of a large family of widespread pigment containing membrane-bound complexes. These pigment-protein complexes are distributed amongst many species and participate in the process of converting light energy into chemical energy. Currently, there are two known types of RC's that utilize charge separation as their driving force for photosynthesis. Type I reactions centers, like the homodimeric reaction centers present in heliobacteria, reduce a terminal [4Fe-4S] cluster (*88*). Type II reactions centers, like Photosystem II, and reaction centers present in purple bacteria reduce quinones as their terminal electron acceptors. Heliobacteria are a photoheterotrophic, gram-positive group of strict anaerobes (*15*). They are unique in that they produce a brownish-green pigment bacteriochlorophyll *g* (BChl *g)* (*27*). The HbRC is considered the simplest Type I reaction center. Originally purified by Trost et al in 1989, there were no antenna complexes(*47*). The HbRC is absent of any bound cytochromes or antenna machinery (*26, 107*). Highly purified HbRC consist of two identical PshA peptides arranged in homodimeric fashion, and earlier purification methods yielded bound proteins PhsBI and II, containing 2 4[Fe/4s] (*25, 74*).
The membrane-embedded PshA homodimer houses approximately 22 BChl *g* antenna molecules, along with the primary donor P_{800} , primary acceptor A_0, and the terminal acceptor F_x. Once the reaction center absorbs a photon, a charge separated state is formed. P_{800} (BChl *g*') acts as the primary donor of this energy to the primary acceptor of

this exciton A_0 (*108*). From A_0, the electron is transferred to the [4Fe-4S] cluster F_x (*43*) that is bound between the PshA peptides. The participation of a menaquinone cofactor between A_0 and F_x is still debated , but it has been well established that it does not have any effect on forward electron transfer when removed (*87, 90, 109-112*). Extrinsically, there are loosely bound F_A/F_B containing proteins, PshB I and PshB II (*53, 56, 74*). PshB I and PshB II share 62% sequence identity, but similar size with the same amino acid count (54 a.a.). When examining the primary structure, they are related to other bacterial ferredoxins in total mass and proposed tertiary construction (*56*). The Golbeck group had first published their opinion of the mobile electron acceptor hypothesis that was further corroborated by Romberger et al in 2012 (*56, 88*). Upon optimization of HbRC purification procedures, no extrinsic PshB proteins were co-purifying with the PshA homodimers (*25*). Unsurprisingly, there is a large pool of studies that probe the HbRC on the acceptor side and intrapeptide electron transfer (*69, 77*). Relative to the acceptor side of the HbRC, there isn't much information on the donor side of that specifically study forward electron transfer beyond the RC itself. Romberger et al. produced a compelling argument for the HbRC's capacity to donate electrons to water soluble redox proteins without PshB I or II acting as an intermediary (*56*). This study is partly corroborated by the interaction of HbRC particles with clarified cell lysates that include recombinant FdxB, a 2[4Fe-4S] protein found in the polycistronic nitrogen fixation operon in *H. modesticaldum.* Romberger et al. used a cyanobacterial flavodoxin, which would be an exogenous acceptor, but otherwise a good model protein for this study because its low molecular weight, and its ease of spectroscopic measurement as compared to soluble Fe/S

redox proteins. The flavin mononucleotide is quite easily measured between 450 and 650 nm. Bacterial ferredoxins give an un unassuming shoulder in the 400-450 nm (Fig. 4.1) range with minimal shifting regardless of oxidation state. Moreover, it is exceedingly difficult to determine competition with endogenous PshBI and PshBII proteins with a tertiary endogenous ferredoxin-like protein. Romberger et al was able to show that HbRC (sans PshB proteins) were able to reduce the soluble electron acceptor flavodoxin, which was concomitantly inhibited by the reintroduction of PshB I and II. That previous work, combined with preliminary data from the lysates containing FdxB provide strong argument for the HbRC's role in donating electrons to a pool of soluble electron acceptors, that include PshB I and PshB II.

Materials and Methods:

Construction of the recombinant His6-tagged fdxb:

The recombinant *fdxb* was designed by taking the matured gene sequence and adding a hexahistidine tag on the 5' end. The synthesized sequence (Genscript) was cloned into pET30a (Novagen) using the Nde1 and Xho1 restriction sites, which were introduced at the 5' and 3' ends of the synthesized DNA, respectively. The resulting plasmid, called pET30a-fdxB replaces the multicloning site of pET30a with the synthetic H6-FdxB gene, putting it under control of the T7 promoter.

Strain construction and protein expression:

The pET30a-FdxB plasmid was transformed into BL21(DE3) cells (Invitrogen) and grown on Luria-Bertani (LB) plates containing 50 mg L^{-1} kanamycin (Fisher Scientific). A single colony was picked to inoculate a 10-mL starting culture in 50 mg L^{-1} kanamycin. The starter culture was grown aerobically, overnight, spinning at 250 RPM, and used to inoculate 1 L of LB broth containing 50 mg L^{-1} kanamycin. At the time of inoculation, the culture was supplemented with 2 mM cysteine (Sigma-Aldrich) and 2 mM Ferric Ammonium Citrate (Fisher Scientific).

The culture was grown at 37^{O}C at 200 RPM until OD_{600} = 0.55. When cells reached OD_{600} = 0.55, isopropyl b-D-1-thio-galactopyranoside (IPTG) (Goldbio) was added to a final concentration of 400mM. Post induction, the culture was transferred to 500 mL centrifuge tubes and placed in an anaerobic chamber (coy) with a 5% hydrogen 95% hydrogen atmosphere. After the culture was relocated to the glove box, there was an addition of 1.7mM sodium hydrosulfite (Fluka) in order to help shift the culture to anaerobic conditions. The culture grew in anaerobic conditions for 20 hours before cell harvesting. The culture was harvested anaerobically by centrifugation for 10 minutes at 5000 x *g*. Pellets had a dark grey appearance, and cells were resuspended in anaerobic 50 mM Tris pH 8.0 by vortexing. The final cell suspension remained dark grey. Cell suspensions were flash frozen in liquid nitrogen and placed in -80^{O}C without glycerol to aid in cell disruption.

Preparation of clarified FdxB cell lysates and attempted nickel column purification:

Cell suspensions were thawed on ice and lysozyme powder (sigma) was added to a final concentration of 1 mg per mL cell suspension and allowed to incubate for 30 minutes. After the incubation period the cells were sonicated with a Microson XL 2000 on ice for 10 rounds of 1 min at 50 % power with 1 min between each round. The cell lysate was centrifuged at 25,000g for 30 min at 4 °C, and the supernatant was re-spun under the same conditions. The resulting supernatant was passed through a 0.22 micrometer syringe filter, producing clarified lysate.

His60 Ni Super-flow resin (Clontech) was packed at 0.5 mL resin per liter of induced culture and washed with with 10 column volumes of anaerobic 50 mM Tris pH 8.0. After wash, the column was equilibrated with 10 column volumes of equilibration buffer (50 mM Tris pH 8.0 + 200 mM NaCl + 10 mM Imidazole). After equilibration, the clarified lysate was added to the column and the column had appeared to turn almost completely brown. After washing with 10 column volumes of wash buffer (50 mM Tris pH 8.0 + 200 mM NaCl + 30 mM Imidazole) the column turned back to the typical bluish green color. After washing, the protein was “eluted” by the addition of 5 mL elution buffer (50 mM Tris pH 8.0 + 200 mM NaCl + 300 mM Imidazole).

Note: the brown material had washed off the column during the purification likely contained the FdxB protein. This implies that the holoprotein did not bind to the column.

2 other constructs have been created with the *fdxb* gene that included an N-terminal strep tag and an N-terminal MBP fusion. Interestingly, The strep-tagged construct (which included the apoprotein) did not bind either, and the Factor Xa cleavage of the fused MBP protein was both inefficient and cost prohibitive.

It has been advised that a tagless purification approach utilizing a combination of both ion exchange and size exclusion may be the next best route to take. All further experiments are done on clarified cell lysate (sonicated, double spun, and filtered).

UV-Vis spectroscopy:

UV-Visible spectrum of the clarified FdxB lysate was collected by using uninduced lysate as a blank. Spectra were taken on a Lamba35 spectrometer, which scanned from 300 nm to 600 nm.

Transient absorption spectroscopy:

Transient absorption spectroscopy was performed with a JTS-10 transient spectrometer (Bio-Logic). Pre-purified HbRC samples were diluted to 500 nanomolar (based on a normalized count of 22 BChl *g* per homodimer) in a buffer that contained 50 mM MOPS at pH 7.0, m MM $MgSO_4$, 10 mM ascorbate and 0.03% *n*-dodecyl -D- maltoside. The sample was loaded into an anaerobic cuvette (1-cm pathlength). A baseline was taken for 1.2 s before the exciting laser flash. Linear regression was utilized to subtract any

baseline shifts. A frequency-doubled Nd:YAG laser (Surlite Mini-Lite, Continuum) delivered a 6-ns saturating flash (20 mJ at 532 nm) to generate the P_{800}^{+} cation. The redox state of the primary electron donor was interrogated 10 microsecond LED flashes that were centered at 803 nm. The probing LED flashes started 350 microseconds after the excitation flash. A 780 nm high-pass filter and a 532 nm notch filter were placed in front of the measurement and reference detectors. The filters served to minimize the effects of the actinic flash. The concentration of FdxB was essentially calculated based off of the method from (Malkin et al.) and was added in an anaerobic fashion to the HbRC sample from 10 nm to 1 mM. The sample was allowed to equilibrate for 1 minute after the addition of more FdxB lysate before each transient experiment, and between each transient experiment.

Results:

Attempted purification and UV-Visible spectra

Using the published genome sequence (*23*), The FdxB apoprotein that is normally made in *H. modesticaldum* was codon optimized for *E. coli* and overexpressed in BL21(DE3) cells. *E. coli* cells were grown in the presence of cysteine and ferric ammonium citrate, then protein expression was induced by IPTG. The iron-sulfur clusters were inserted into the peptide using an *in vivo* technique wherein the induced cells spontaneously insert the clusters after being forced into anaerobic conditions. Despite multiple constructs, there was no success in getting the protein to bind to commercial biotinylated or nickel chelated resin. The Fe/S proteins have similar absorbance spectra with a broad shoulder

in the 400 nm region (Fig. 4.1). EPR and transient kinetic data is yet to be collected on fully purified apoprotein.

Transient absorption spectroscopy:

To determine whether the reconstituted HbRC complex is functional at room temperature, the kinetics between P_{800}^{+} and F_X^{-} were measured with time resolved spectroscopy via the JTS-10 spectrometer. When originally studied, enriched HbRC particles had biphasic kinetics. There was a 15-millisecond phase assigned to recombination from the P_{800}^{+} / F_X^{-} state, and the second 75-ms phase that was assigned to the back reaction from the P_{800}^{+} / $[F_A/F_B]^{-}$ state (*44*). Highly purified HbRC particles have monophasic kinetics; a ~15-ms phase that comes from charge recombination between P_{800}^{+} and F_X^{-} after an excitation flash. Our lab has shown these kinetic phases are conserved in carbonate washed membranes as well. The ratio of these kinetic phases in unwashed membranes is about equal in detergent solubilized membranes and enriched HbRC preparations (*44*). In future preparations the HbRC particles were determined to have monophasic kinetics. The 75-ms charge recombination component was no longer visualized (*25*) (*56*), this would indicate that the PhB proteins had been removed during the anion exchange chromatography step of the purification process. When endogenous PshB proteins are added back to purified reaction center cores the charge recombination kinetics return to a biphasic state (*74*). Clarified FdxB lysate undergoes a single electron reduction that results in a change in P_{800}^{+} recovery kinetics. Similar to benzyl viologen (*60*), increasing amounts of soluble electron acceptor lead to larger gaps in P_{800}^{+} recovery

times. Under the conditions of a single excitation flash, the soluble electron acceptor is reduced by F_x and it creates a long lived P_{800}^+ that is slowly reduced by ascorbate (>1 min). As the stoichiometry between donor and acceptor changes, the more lysate that's added, the longer the recovery time takes. No substantial changes in recovery time are noted when uninduced extract is added as a control.

Discussion:

The purpose of this study was to look through the genome of *H. modesticaldum* and find potential soluble electron acceptors with similar characteristics as PshB I and PshB II. Once a candidate was identified, it would be expressed and purified in order characterize its functional capacity with the HbRC. Currently, no other proteins have been considered integral to the quaternary structure of the HbRC, as PshA is the sole structural protein in the HbRC (*25*). When pigments are normalized to a single carotenoid, the PshA homodimer coordinates all 20 of the surrounding antenna Bchl *g* molecules, the special pair P_{800}, the primary electron acceptor A_0, and the terminal acceptor F_x(*25*). Originally, the F_A/F_B protein (later dubbed PshB I and PshB II) was considered the terminal electron acceptor (*48*). Upon further characterization of the highly purified reaction center particles (*25, 56*). The PshA homodimer is considered the sole protein in the HbRC. Not only did the highly purified particles lack the once bound F_A/F_B protein, but addition of an exogenous acceptor actually competed with it when they were added together (*56*). It would appear that there is no functional PsaC analog in HbRC. After looking through the published *H. modesticaldum* genome (*23*), a putative ferredoxin like protein, FdxB, was identified. This gene had been codon optimized for *E. coli*, cloned into an expression

vector, and produced recombinantly. Affinity chromatography was unsuccessful in isolating the overexpressed FdxB protein. The product of this recombinant expression has a characteristic visible spectrum of the studied dicluster ferredoxin like proteins, as well as possible interaction with the reaction center with no intermediary electron transfer cofactor past F_x. To date, there is no reliable EPR spectra that would further corroborate this interaction with the HbRC or likeness to the PhsB proteins. The clarified FdxB lysate was found to participate in laser-flash mediated electron transfer with the purified HbRC particles, and did so in a concentration dependent manner. At an 81 to 1 stoichiometry, the clarified lysate containing FdxB decreased the number of recombination events in HbRC particles by approximately 40% compared to 3% in control. That is to say, F_X^- was oxidized before it could quench P_{800}^+ cation. Despite multiple constructs, the FdxB peptide has not yet been successfully isolated. The original construction consisted of an N-terminal MPB fusion. This hybrid peptide did bind to the amylose resin, but the Factor Xa enzymatic cleavage was terribly inefficient and not economically feasible. Second, an N-terminal strep tag was added. Interestingly, this peptide did not bind to the biotinylated resin at all, it is possible that, under the chromatography conditions, the peptide folded in such a way that hid the tag internally. Lastly, an N-terminal hexahistidine tag was added to the FdxB peptide and the refolded holoprotein does not bind to the nickel column for reasons unknown. There are still options for attempting purification of this protein. First, using the *in vivo* reconstitution protocol on the strep-tagged construct. Second, purify the unfolded, hexahistidine tagged, peptide with the Clontech nickel-chelated resin. Third, to overexpress the FdxB peptide, refold it *in vivo* and then attempt consecutive ion exchange

chromatography and size exclusion chromatography. Once the protein has been completely isolated, a more fastidious study can be done with the HbRC to determine kinetic rate values and ascertain intelligible EPR spectra.

The calculated PI of FdxB is 5.29 with a molecular weight that's predicted to be 9.8 kDa (90 amino acids) . The calculated PI of PshB is 4.06 with a predicted molecular weight of 5.4 kDa (54 amino acids). These are compared with PsaC which has a calculated PI of 5.5 and a predicted molecular weight of 8.8 kDa. All three proteins are low molecular weight, acidic, and contain the double CxxCxxCxxxC motif indicative of [4Fe-4S] clusters. Neither PshB or FdxB Contain the C-terminal extension that is implicated for PsaC binding to PSI (*113*). Since this sequence does not exist in PshB or FdxB, there must be a different mechanism of interface with the HbRC. The only way know for sure is to get adequate resolution with x-ray diffraction techniques while the proteins are bound to the HbRC.

Summary:

This section had shown the synthesis and insertion of the *fdxB* gene into a vector, and that it can highly expressed in *E. coli* and refolded *in vivo* (as evidenced by heavy discoloration after reconstitution). Fe/S clusters were reconstituted by having cells grow up in media that contained an iron (ferric ammonium citrate) and sulfur (cysteine) source followed by a shift to anaerobic conditions. Even though the protein has not been purified, the clarified lysate containing *fdxB* does interact with HbRC cores. FdxB shows little primary structure homology with either of the endogenous PshB proteins but still

remained a prime candidate for this project because of the relatively small size (90 amino acids), the double CxxCxxCxxxC motif that is found within the sequence indicating Fe/S cluster binding, and the location in the genome (in the nitrogen fixation operon). Because of these initial characteristics, there was reason to believe that FdxB may act as a nitrogen fixation pathway specific ferredoxin that acted as a soluble electron acceptor to the HbRC. Preliminary results to show that FdxB may interact the reaction center as a mobile acceptor of electrons but it is unclear as to whether or not it just adds to the acceptor pool or is specifically donating electrons to any component proteins in the nitrogen fixation pathway. Currently, two experiments, UV-Vis and transient spectroscopy seem to show this protein is comparable to the HbRC's typical acceptors. EPR and Cyclic voltammetry were both unsuccessful due to issues with sample amount and purity. The Z-loop and C-terminal extension, both required for binding of PsaC in PSI are missing from the PshB proteins and FdxB. Since these portions of the protein are not in the sequence, HbRC may in fact be considerably different than PSI when it comes to protein stability and function.

REFERENCES

15. H. Gest, J. L. Favinger, Heliobacterium chlorum, an anoxygenic brownish-green bacterium containing a `new' form of bacteriochlorophyll. *Arch Microbiol* **136**, 11-16 (1983).

23. W. M. Sattley *et al.*, The genome of Heliobacterium modesticaldum, a phototrophic representative of the Firmicutes containing the simplest photosynthetic apparatus. *J Bacteriol* **190**, 4687-4696 (2008).

25. I. Sarrou *et al.*, Purification of the photosynthetic reaction center from *Heliobacterium modesticaldum*. *Photosynth Res* **111**, 291-302 (2012).

26. J. Amesz, The antenna-reaction center complex of heliobacteria. *Advances in Photosynthesis* **2**, 687-697 (1995).

27. H. Brockmann, A. Lipinski, Bacteriochlorophyll g. A new bacteriochlorophyll from Heliobacterium chlorum. *Arch Microbiol* **136**, 17-19 (1982).

43. F. A. M. Kleinherenbrink, H.-C. Chiou, R. LoBrutto, R. E. Blankenship, Spectroscopic evidence for the presence of an iron-sulfur center similar to FX of photosystem I in *Heliobacillus mobilis*. *Photosynthesis Research* **41**, 115-123 (1994).

44. M. Heinnickel, G. Shen, R. Agalarov, J. H. Golbeck, Resolution and reconstitution of a bound Fe-S protein from the photosynthetic reaction center of Heliobacterium modesticaldum. *Biochemistry* **44**, 9950-9960 (2005).

47. J. T. Trost, R. E. Blankenship, Isolation of a photoactive photosynthetic reaction center-core antenna complex from *Heliobacillus mobilis*. *Biochemistry* **28**, 9898-9904 (1989).

48. W. Nitschke, P. Setif, U. Liebl, U. Feiler, A. W. Rutherford, Reaction center photochemistry of *Heliobacterium chlorum*. *Biochemistry* **29**, 11079-11088 (1990).

53. S. P. Romberger, C. Castro, Y. Sun, J. H. Golbeck, Identification and characterization of PshBII, a second F_A/F_B-containing polypeptide in the photosynthetic reaction center of *Heliobacterium modesticaldum*. *Photosynth Res* **104**, 293-303 (2010).

56. S. P. Romberger, J. H. Golbeck, The F_X iron-sulfur cluster serves as the terminal bound electron acceptor in heliobacterial reaction centers. *Photosynth Res* **111**, 285-290 (2012).

60. T. S. Kashey, J. B. Cowgill, M. D. McConnell, M. Flores, K. E. Redding, Expression and characterization of cytochrome c_{553} from *Heliobacterium modesticaldum*. *Photosynth Res* **120**, 291-299 (2014).

69. H. Oh-oka, Type 1 reaction center of photosynthetic heliobacteria. *Photochem Photobiol* **83**, 177-186 (2007).

74. M. Heinnickel, G. Shen, J. H. Golbeck, Identification and characterization of PshB, the dicluster ferredoxin that harbors the terminal electron acceptors F(A) and F(B) in *Heliobacterium modesticaldum*. *Biochemistry* **46**, 2530-2536 (2007).

77. C. Azai, Y. Tsukatani, S. Itoh, H. Oh-oka, C-type cytochromes in the photosynthetic electron transfer pathways in green sulfur bacteria and heliobacteria. *Photosynth Res* **104**, 189-199 (2010).

87. F. A. Kleinherenbrink, I. Ikegami, A. Hiraishi, S. C. M. Otte, J. Amesz, Electron transfer in menaquinone-depleted membranes of *Heliobacterium chlorum*. *Biochim Biophys Acta* **1142**, 69-73 (1993).

88. S. P. Romberger, J. H. Golbeck, The bound iron-sulfur clusters of type-I homodimeric reaction centers. *Photosynth Res* **104**, 333-346 (2010).

90. R. Miyamoto, H. Mino, T. Kondo, S. Itoh, H. Oh-Oka, An electron spin-polarized signal of the $P_{800}^{+}A_1(Q)^{-}$ state in the homodimeric reaction center core complex of *Heliobacterium modesticaldum*. *Biochemistry* **47**, 4386-4393 (2008).

107. S. Neerken, T. J. Aartsma, J. Amesz, Pathways of Energy Transformation in Antenna Reaction Center Complexes of Heliobacillus mobilis. *Biochemistry* **39**, 3297-3303 (2000).

108. M. Kobayashi *et al.*, Bacteriochlorophyll *g* epimer as a possible reaction center component of heliobacteria. *Biochim Biophys Acta* **1057**, 89-96 (1991).

109. S. Lin, H.-C. Chiou, F. A. M. Kleinherenbrink, R. E. Blankenship, Time-resolved spectroscopy of energy and electron transfer processes in the photosynthetic bacterium Heliobacillus mobilis. *Biophysical Journal* **66**, 437-445 (1994).

110. K. Brettel, W. Leibl, U. Liebl, Electron transfer in the heliobacterial reaction center: evidence against a quinone-type electron acceptor functioning analogous to A1 in photosystem I. *Biochim Biophys Acta* **1363**, 175-181 (1998).

111. A. van der Est, C. Hager-Braun, W. Leibl, G. Hauska, D. Stehlik, Transient electron paramagnetic resonance spectroscopy on green-sulfur bacteria and heliobacteria at two microwave frequencies. *Biochim Biophys Acta* **1409**, 87-98 (1998).

112. I. P. Muhiuddin, S. E. Rigby, M. C. Evans, J. Amesz, P. Heathcote, ENDOR and special TRIPLE resonance spectroscopy of photoaccumulated semiquinone electron acceptors in the reaction centers of green sulfur bacteria and heliobacteria. *Biochemistry* **38**, 7159-7167 (1999).

113. N. Fischer, M. Hippler, P. Setif, J. P. Jacquot, J. D. Rochaix, The PsaC subunit of photosystem I provides an essential lysine residue for fast electron transfer to ferredoxin. *Embo J* **17**, 849-858 (1998).

FIGURES

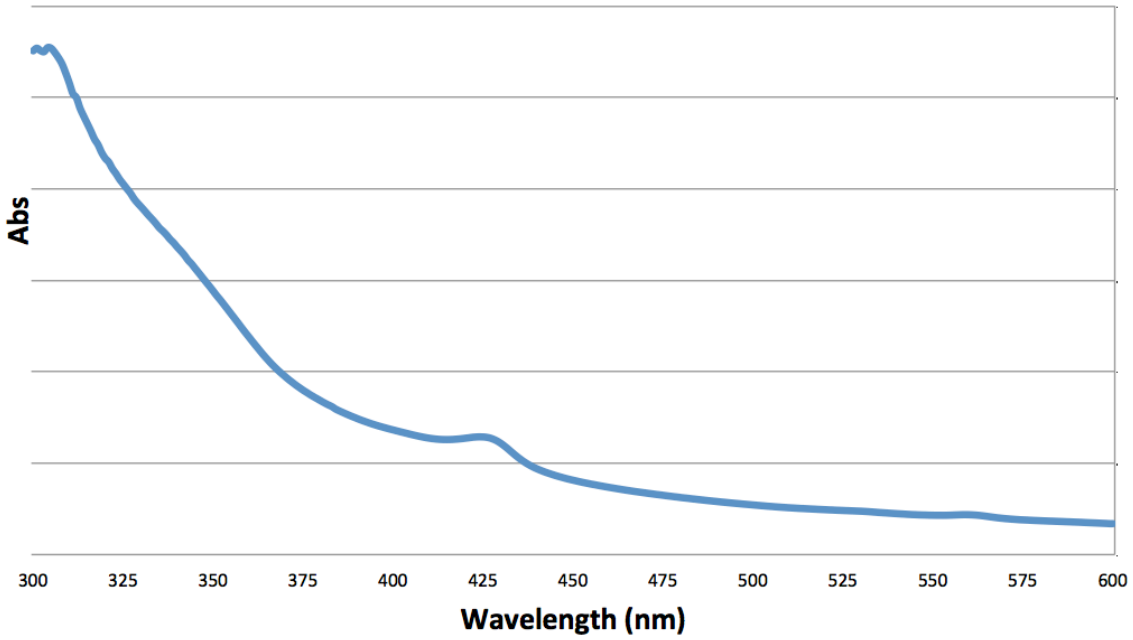

4.1: UV-Visible Spectrum of Fully-Oxidized Clarified Lysate Containing Overexpressed FdxB with *In Vivo* Fe/S Cluster Formation.

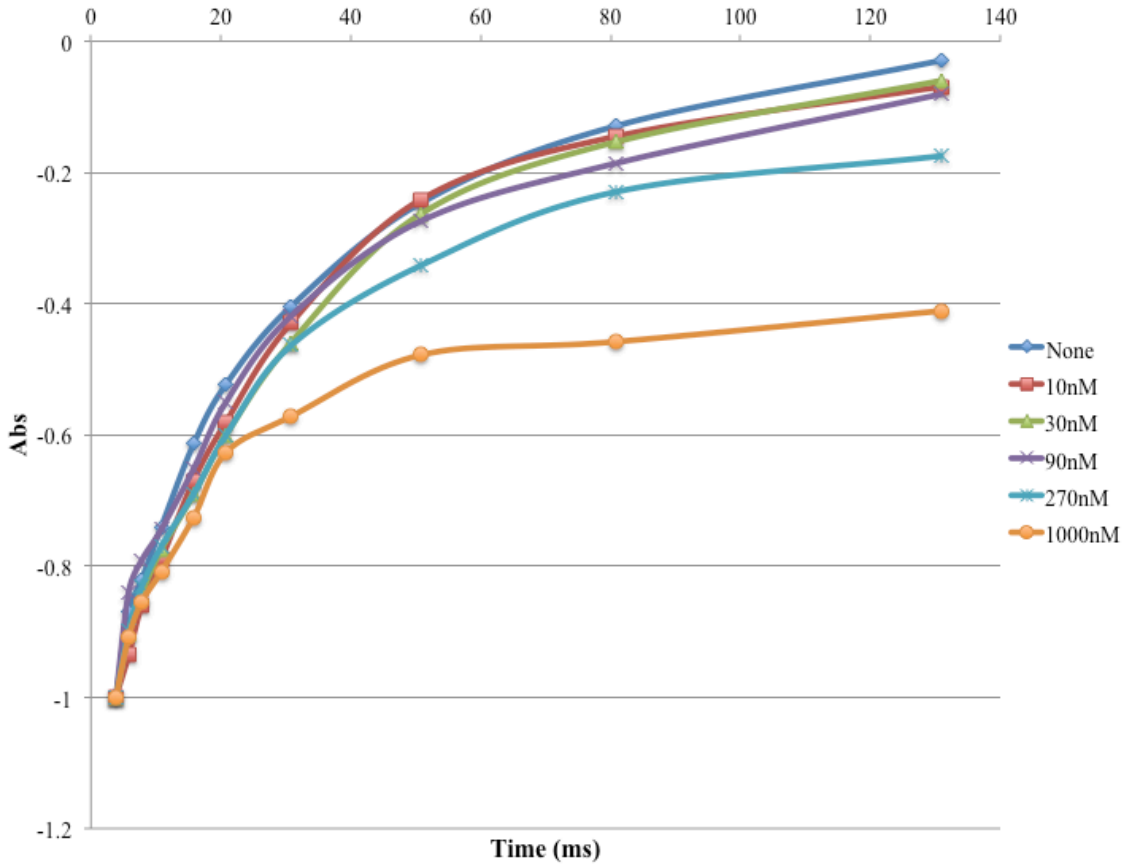

4.2: P_{800} Photobleaching and Recovery at Each Calculated Concentration of Unpurified FdxB. Lysate containing overexpressed FdxB was used as an electron acceptor to F_X^-. HbRCs were given a saturating 532-nm laser flash (30 mJ, 6-ns duration), and absorption was monitored at 803 nm using 10-µs flashes from an LED. Ascorbate (10 mM) was used as a sacrificial electron donor.

MASTER REFERENCE LIST

1. R. E. Blankenship, *Molecular Mechanisms of Photosynthesis*. (Blackwell Science Ltd, Oxford, 2002), pp. 321.

2. J. Deisenhofer, H. Michel, Nobel lecture. The photosynthetic reaction centre from the purple bacterium Rhodopseudomonas viridis. *Embo J* **8**, 2149-2170 (1989).

3. K. Brettel, W. Leibl, Electron transfer in photosystem I. *Biochimica Et Biophysica Acta-Bioenergetics* **1507**, 100-114 (2001).

4. V. P. Shinkarev, B. Zybailov, I. R. Vassiliev, J. H. Golbeck, Modeling of the P700+ charge recombination kinetics with phylloquinone and plastoquinone-9 in the A1 site of photosystem I. *Biophysical Journal* **83**, 2885-2897 (2002).

5. M. G. Müller, C. Slavov, R. Luthra, K. E. Redding, A. R. Holzwarth, Independent initiation of primary electron transfer in the two branches of the photosystem I reaction center. *Proc Natl Acad Sci U S A* **107**, 4123-4128 (2010).

6. S. Neerken, J. Amesz, The antenna reaction center complex of heliobacteria: composition, energy conversion and electron transfer. *Biochimica et Biophysica Acta* **1507**, 278-290 (2001).

7. G. Hauska, T. Schoedl, H. Remigy, G. Tsiotis, The reaction center of green sulfur bacteria. *Biochimica et Biophysica Acta* **1507**, 260-277 (2001).

8. D. A. Bryant *et al.*, Candidatus Chloracidobacterium thermophilum: an aerobic phototrophic Acidobacterium. *Science* **317**, 523-526 (2007).

9. G. Hauska, T. Schoedl, H. Remigy, G. Tsiotis, The reaction center of green sulfur bacteria. *Biochimica et Biophysica Acta* **1507**, 260-277 (2000).

10. M. Kobayashi *et al.*, The primary electron acceptor of green sulfur bacteria, bacteriochlorophyll 663, is chlorophyll a esterified with D2,6-phytadienol. *Photosynthesis Research* **63**, 269-280 (2000).

11. M. Büttner *et al.*, The photosystem I-like P840-reaction center of green S-bacteria is a homodimer. *Biochimica et Biophysica Acta* **1101**, 154-156 (1992).

12. J. S. Okkels *et al.*, A membrane-bound monoheme cytochrome c551 of a novel type is the immediate electron donor to P840 of the Chlorobium vibrioforme photosynthetic reaction center complex. *Journal of Biological Chemistry* **267**, 21139-21145 (1992).

13. H. P. Permentier *et al.*, Reaction center complexes of green sulfur bacteria. *Photosynthesis: Mechanisms and Effects, Proceedings of the International Congress on Photosynthesis, 11th, Budapest, Aug. 17-22, 1998* **1**, 527-530 (1998).

14. G. Hauska, T. Schoedl, H. Remigy, G. Tsiotis, The reaction center of green sulfur bacteria(1). *Biochimica et Biophysica Acta* **1507**, 260-277 (2001).

15. H. Gest, J. L. Favinger, Heliobacterium chlorum, an anoxygenic brownish-green bacterium containing a `new' form of bacteriochlorophyll. *Arch Microbiol* **136**, 11-16 (1983).

16. L. K. Kimble, A. K. Stevenson, M. T. Madigan, Chemotrophic growth of heliobacteria in darkness. *FEMS Microbiol Lett* **115**, 51-55 (1994).

17. L. K. Kimble, L. Mandelco, C. R. Woese, M. T. Madigan, Heliobacterium modesticaldum, sp. nov., a thermophilic heliobacterium of hot springs and volcanic soils. *Arch Microbiol* **163**, 259-267 (1995).

18. P. Beer-Romero, H. Gest, Heliobacillus mobilis, a peritrichously flagellated anoxyphototroph containing bacteriochlorophyll g. *FEMS Microbiology Letters* **41**, 109-114 (1987).

19. A. K. Stevenson, L. K. Kimble, C. R. Woese, M. T. Madigan, Characterization of new phototrophic heliobacteria and their habitats. *Photosynthesis Research* **53**, 1-12 (1997).

20. I. A. Bryantseva, V. M. Gorlenko, E. I. Kompantseva, L. A. Achenbach, M. T. Madigan, Heliorestis daurensis, gen. nov. Sp. Nov., An alkaliphilic rod-to-coiled-shaped phototrophic heliobacterium from a siberian soda lake. *Arch Microbiol* **172**, 167-174 (1999).

21. M. T. Madigan, J. G. Ormerod, Taxonomy, physiology and ecology of heliobacteria. *Advances in Photosynthesis* **2**, 17-30 (1995).

22. M. W. Pickett, M. P. Williamson, D. J. Kelly, An enzyme and 13C-NMR of carbon metabolism in heliobacteria. *Photosynth Res.* **41**, 75-88 (1994).

23. W. M. Sattley *et al.*, The genome of Heliobacterium modesticaldum, a phototrophic representative of the Firmicutes containing the simplest photosynthetic apparatus. *J Bacteriol* **190**, 4687-4696 (2008).

24. L. Kimble, M. T. Madigan, Nitrogen fixation and nitrogen metabolism in heliobacteria. *Archives of Microbiology* **158**, 155-161 (1992).

25. I. Sarrou *et al.*, Purification of the photosynthetic reaction center from *Heliobacterium modesticaldum*. *Photosynth Res* **111**, 291-302 (2012).

26. J. Amesz, The antenna-reaction center complex of heliobacteria. *Advances in Photosynthesis* **2**, 687-697 (1995).

27. H. Brockmann, A. Lipinski, Bacteriochlorophyll g. A new bacteriochlorophyll from Heliobacterium chlorum. *Arch Microbiol* **136**, 17-19 (1982).

28. M. Kobayashi *et al.*, Light-independent isomerization of bacteriochlorophyll g to chlorophyll a catalyzed by weak acid in vitro. *Analytica Chimica Acta* **365**, 199-203 (1998).

29. R. C. Prince, H. Gest, R. E. Blankenship, Thermodynamic properties of the photochemical reaction center of Heliobacerium chlorum. *FEBS Lett* **182**, 345-349 (1985).

30. A. M. Nuijs, R. J. Van Dorssen, L. N. M. Duysens, J. Amesz, Excited states and primary photochemical reactions in the photosynthetic bacterium Heliobacterium chlorum. *Proceedings of the National Academy of Sciences of the United States of America* **82**, 6965-6968 (1985).

31. E. J. Van de Meent *et al.*, Identification of 81-hydroxychlorophyll a as a functional reaction center pigment in heliobacteria. *Biochimica et Biophysica Acta* **1058**, 356-362 (1991).

32. E. J. van de Meent, M. Kobayashi, C. Erkelens, P. A. van Veelen, J. Amesz, Identification of 8^1-hydroxychlorophyll *a* as a functional reaction center pigment in heliobacteria. *Biochim Biophys Acta* **1058**, 356-362 (1991).

33. A. Hiraishi, Occurrence of menaquinone is the sole isoprenoid quinone in the photosynthetic bacterium *Heliobacterium chlorum*. *Arch Microbiol* **151**, 378-379 (1989).

34. M. B. Hale, R. E. Blankenship, R. C. Fuller, Menaquinone is the sole quinone in the facultatively aerobic green photosynthetic bacterium *Chloroflexus aurantiacus*. *Biochim Biophys Acta* **723**, 376-382 (1983).

35. A. Vermeglio, Secondary electron transfer in reaction centers of Rhodopseudomonas sphaeroides. Out-of-phase periodicity of two for the formation of ubisemiquinone and fully reduced ubiquinone. *Biochim Biophys Acta* **459**, 516-524 (1977).

36. H.-U. Schoeder, W. Lockau, Phylloquinone copurifies with the large subunit of photosystem I. *FEBS Lett.* **199**, 23-27 (1986).

37. R. E. Blankenship *et al.*, Primary photochemistry in the facultative green photosynthetic bacterium Chloroflexus aurantiacus. *J Cell Biochem* **22**, 251-261 (1983).

38. J. T. Trost, D. C. Brune, R. E. Blankenship, Protein sequences and redox titrations indicate that the electron acceptors in reaction centers from heliobacteria are similar to photosystem I. *Photosynthesis Research* **32**, 11-22 (1992).

39. I. P. Muhiuddin, S. E. J. Rigby, M. C. W. Evans, J. Amesz, P. Heathcote, ENDOR and Special TRIPLE Resonance Spectroscopy of Photoaccumulated Semiquinone Electron Acceptors in the Reaction Centers of Green Sulfur Bacteria and Heliobacteria. *Biochemistry* **38**, 7159-7167 (1999).

40. F. A. M. Kleinherenbrink, J. Amesz, Stoichiometries and rates of electron transfer and charge recombination in *Heliobacterium chlorum*. *Biochimica et Biophysica Acta* **1143**, 77-83 (1993).

41. U. Liebl *et al.*, Single core polypeptide in the reaction center of the photosynthetic bacterium Heliobacillus mobilis: structural implications and relations to other photosystems. *Proceedings of the National Academy of Science, U.S.A.* **90**, 7124-7128 (1993).

42. F. A. Kleinherenbrink, H. C. Chiou, R. LoBrutto, R. E. Blankenship, Spectroscopic evidence for the presence of an iron-sulfur center similar to Fx of Photosystem I in Heliobacillus mobilis. *Photosynthesis Research* **41**, 115-123 (1994).

43. F. A. M. Kleinherenbrink, H.-C. Chiou, R. LoBrutto, R. E. Blankenship, Spectroscopic evidence for the presence of an iron-sulfur center similar to FX of photosystem I in *Heliobacillus mobilis*. *Photosynthesis Research* **41**, 115-123 (1994).

44. M. Heinnickel, G. Shen, R. Agalarov, J. H. Golbeck, Resolution and reconstitution of a bound Fe-S protein from the photosynthetic reaction center of Heliobacterium modesticaldum. *Biochemistry* **44**, 9950-9960 (2005).

45. K. G. Parrett, T. Mehari, P. G. Warren, J. H. Golbeck, Purification and properties of the intact P-700 and Fx-containing Photosystem I core protein. *Biochim Biophys Acta* **973**, 324-332 (1989).

46. M. Heinnickel, R. Agalarov, N. Svensen, C. Krebs, J. H. Golbeck, Identification of F_X in the Heliobacterial Reaction Center as a [4Fe-4S] Cluster with an S = 3/2 Ground Spin State. *Biochemistry* **45**, 6756-6764 (2006).

47. J. T. Trost, R. E. Blankenship, Isolation of a photoactive photosynthetic reaction center-core antenna complex from *Heliobacillus mobilis*. *Biochemistry* **28**, 9898-9904 (1989).

48. W. Nitschke, P. Setif, U. Liebl, U. Feiler, A. W. Rutherford, Reaction center photochemistry of *Heliobacterium chlorum*. *Biochemistry* **29**, 11079-11088 (1990).

49. B. Jagannathan, J. H. Golbeck, Understanding of the binding interface between PsaC and the PsaA/PsaB heterodimer in photosystem I. *Biochemistry* **48**, 5405-5416 (2009).

50. P. Jordan *et al.*, Three-dimensional structure of cyanobacterial photosystem I at 2.5 A resolution. *Nature* **411**, 909-917. (2001).

51. M. L. Antonkine *et al.*, Assembly of protein subunits within the stromal ridge of photosystem I. Structural changes between unbound and sequentially PS I-bound polypeptides and correlated changes of the magnetic properties of the terminal iron sulfur clusters. *J Mol Biol* **327**, 671-697 (2003).

52. P. Fromme, H. Bottin, N. Krauss, P. Setif, Crystallization and electron paramagnetic resonance characterization of the complex of photosystem I with its natural electron acceptor ferredoxin. *Biophysical Journal* **83**, 1760-1773 (2002).

53. S. P. Romberger, C. Castro, Y. Sun, J. H. Golbeck, Identification and characterization of PshBII, a second F_A/F_B-containing polypeptide in the photosynthetic reaction center of *Heliobacterium modesticaldum*. *Photosynth Res* **104**, 293-303 (2010).

54. A. Hatano, K. Inoue, D. Deo, H. Sakurai, Isolation and partial characterization of two ferredoxins from the photosynthetic bacterium Heliobacillus mobilis. *Journal of Photoscience* **9**, 388-390 (2002).

55. I. R. Vassiliev, M. L. Antonkine, J. H. Golbeck, Iron-sulfur clusters in type I reaction centers. *Biochimica Et Biophysica Acta-Bioenergetics* **1507**, 139-160 (2001).

56. S. P. Romberger, J. H. Golbeck, The F_X iron-sulfur cluster serves as the terminal bound electron acceptor in heliobacterial reaction centers. *Photosynth Res* **111**, 285-290 (2012).

57. S. Takaichi *et al.*, The major carotenoid in all known species of heliobacteria is the C30 carotenoid 4,4'-diaponeurosporene, not neurosporene. *Arch Microbiol* **168**, 277-281 (1997).

58. M. Heinnickel, J. H. Golbeck, Heliobacterial photosynthesis. *Photosynth Res* **92**, 35-53 (2007).

59. E. J. van de Meent, F. A. M. Kleinherenbrink, J. Amesz, Purification and properties of an antenna-reaction center complex from heliobacteria. *Biochimica et Biophysica Acta* **1015**, 223-230 (1990).

60. T. S. Kashey, J. B. Cowgill, M. D. McConnell, M. Flores, K. E. Redding, Expression and characterization of cytochrome c_{553} from *Heliobacterium modesticaldum*. *Photosynth Res* **120**, 291-299 (2014).

61. I. Albert, A. W. Rutherford, H. Grav, J. Kellermann, H. Michel, The 18-kDa cytochrome c_{553} from *Heliobacterium gestii*: gene sequence and characterization of the mature protein. *Biochemistry* **37**, 9001-9008 (1998).

62. D. W. Lee, Y. Ozturk, A. Osyczka, J. W. Cooley, F. Daldal, Cytochrome bc1-cy fusion complexes reveal the distance constraints for functional electron transfer between photosynthesis components. *J Biol Chem* **283**, 13973-13982 (2008).

63. H. Oh-oka, M. Iwaki, S. Itoh, Electron donation from membrane-bound cytochrome *c* to the photosynthetic reaction center in whole cells and isolated membranes of *Heliobacterium gestii*. *Photosynthesis Research* **71**, 137-147 (2002).

64. D. M. Kramer, B. Schoepp, U. Liebl, W. Nitschke, Cyclic electron transfer in *Heliobacillus mobilis* involving a menaquinol-oxidizing cytochrome *bc* complex and an RCI-type reaction center. *Biochemistry* **36**, 4203-4211 (1997).

65. W. Nitschke *et al.*, Membrane-bound c-type cytochromes in Heliobacillus mobilis. Characterization by EPR and optical spectroscopy in membranes and detergent-solubilized material. *European Journal of Biochemistry* **242**, 695-702 (1996).

66. A. L. Ducluzeau, E. Chenu, L. Capowiez, F. Baymann, The Rieske/cytochrome *b* complex of Heliobacteria. *Biochim Biophys Acta* **1777**, 1140-1146 (2008).

67. H. Yue, Y. Kang, H. Zhang, X. Gao, R. E. Blankenship, Expression and characterization of the diheme cytochrome *c* subunit of the cytochrome *bc* complex in *Heliobacterium modesticaldum*. *Arch Biochem Biophys* **517**, 131-137 (2012).

68. S. Junemann, P. Heathcote, P. R. Rich, On the mechanism of quinol oxidation in the bc1 complex. *J Biol Chem* **273**, 21603-21607 (1998).

69. H. Oh-oka, Type 1 reaction center of photosynthetic heliobacteria. *Photochem Photobiol* **83**, 177-186 (2007).

70. M. T. Madigan, J. G. Ormerod, in *Anoxygenic Photosynthetic Bacteria,* R. E. Blankenship, M. T. Madigan, C. E. Bauer, Eds. (Kluwer Academic Publishers, Dordrecht, The Netherlands, 1995), pp. 17-30.

71. W. Nitschke, U. Liebl, K. Matsuura, D. M. Kramer, Membrane-Bound c-Type Cytochromes in Heliobacillus mobilis. In Vivo Study of the Hemes Involved in Electron Donation to the Photosynthetic Reaction Center. *Biochemistry* **34**, 11831-11839 (1995).

72. R. E. Feissner *et al.*, Recombinant cytochromes c biogenesis systems I and II and analysis of haem delivery pathways in Escherichia coli. *Mol Microbiol* **60**, 563-577 (2006).

73. J. H. Morrissey, Silver stain for proteins in polyacrylamide gels: a modified procedure with enhanced uniform sensitivity. *Anal Biochem* **117**, 307-310 (1981).

74. M. Heinnickel, G. Shen, J. H. Golbeck, Identification and characterization of PshB, the dicluster ferredoxin that harbors the terminal electron acceptors F(A) and F(B) in *Heliobacterium modesticaldum*. *Biochemistry* **46**, 2530-2536 (2007).

75. N. Tamura, S. Itoh, Y. Yamamoto, M. Nishimura, Electrostatic Interaction between Plastocyanin and P700 in the Electron Transfer Reaction of Photosystem I-Enriched Particles. *Plant and Cell Physiol.* **22**, 603-612 (1981).

76. F. Drepper, P. Mathis, Structure and function of cytochrome c2 in electron transfer complexes with the photosynthetic reaction center of Rhodobacter sphaeroides: optical linear dichroism and EPR. *Biochemistry* **36**, 1428-1440 (1997).

77. C. Azai, Y. Tsukatani, S. Itoh, H. Oh-oka, C-type cytochromes in the photosynthetic electron transfer pathways in green sulfur bacteria and heliobacteria. *Photosynth Res* **104**, 189-199 (2010).

78. H. Oh-oka, M. Iwaki, S. Itoh, Membrane-bound cytochrome c_z couples quinol oxidoreductase to the P840 reaction center complex in isolated membranes of the green sulfur bacterium *Chlorobium tepidum*. *Biochemistry* **37**, 12293-12300 (1998).

79. P. L. Dutton, K. M. Petty, H. S. Bonner, S. D. Morse, Cytochrome c2 and reaction center of Rhodospeudomonas spheroides Ga. membranes. Extinction coefficients, content, half-reduction potentials, kinetics and electric field alterations. *Biochim Biophys Acta* **387**, 536-556 (1975).

80. N. Okumura, K. Shimada, K. Matsuura, Photo-oxidation of membrane-bound and soluble cytochrome c in the green sulfur bacterium Chlorobium tepidum. *Photosynthesis Research* **41**, 125-134 (1994).

81. R. C. Prince, H. Gest, R. E. Blankenship, Thermodynamic properties of the photochemical reaction center of Heliobacerium chlorum. *FEBS Letters* **182**, 345-349 (1985).

82. A. Nakamura, T. Suzawa, Y. Kato, T. Watanabe, Species dependence of the redox potential of the primary electron donor p700 in photosystem I of oxygenic photosynthetic organisms revealed by spectroelectrochemistry. *Plant Cell Physiol* **52**, 815-823 (2011).

83. H. Oh-oka, M. Iwaki, S. Itoh, Viscosity dependence of the electron transfer rate from bound cytochrome c to P840 in the photosynthetic reaction center of the green sulfur bacterium *Chlorobium tepidum*. *Biochemistry* **36**, 9267-9272 (1997).

84. Y. Ozturk *et al.*, Soluble variants of Rhodobacter capsulatus membrane-anchored cytochrome cy are efficient photosynthetic electron carriers. *J Biol Chem* **283**, 13964-13972 (2008).

85. H. Oh-oka *et al.*, Highly purified photosynthetic reaction center (PscA/cytochrome c551)2 complex of the green sulfur bacterium *Chlorobium limicola*. *Biochemistry* **34**, 13091-13097 (1995).

86. S. Wang, X. Li, J. C. Williams, J. P. Allen, P. Mathis, Interaction between cytochrome c2 and reaction centers from purple bacteria. *Biochemistry* **33**, 8306-8312 (1994).

87. F. A. Kleinherenbrink, I. Ikegami, A. Hiraishi, S. C. M. Otte, J. Amesz, Electron transfer in menaquinone-depleted membranes of *Heliobacterium chlorum*. *Biochim Biophys Acta* **1142**, 69-73 (1993).

88. S. P. Romberger, J. H. Golbeck, The bound iron-sulfur clusters of type-I homodimeric reaction centers. *Photosynth Res* **104**, 333-346 (2010).

89. A. Chauvet *et al.*, Temporal and spectral characterization of the photosynthetic reaction center from *Heliobacterium modesticaldum*. *Photosynth Res* **116**, 1-9 (2013).

90. R. Miyamoto, H. Mino, T. Kondo, S. Itoh, H. Oh-Oka, An electron spin-polarized signal of the $P_{800}^{+}A_1(Q)^{-}$ state in the homodimeric reaction center core complex of *Heliobacterium modesticaldum*. *Biochemistry* **47**, 4386-4393 (2008).

91. K. Brettel, W. Leibl, U. Liebl, Electron transfer in the heliobacterial reaction center: evidence against a quinone-type electron acceptor functioning analogous to A1 in photosystem I. *Biochimica et Biophysica Acta* **1363**, 175-181 (1998).

92. S. Lin, H. C. Chiou, R. E. Blankenship, Secondary electron transfer processes in membranes of *Heliobacillus mobilis*. *Biochemistry* **34**, 12761-12767 (1995).

93. W. M. Sattley, R. E. Blankenship, Insights into heliobacterial photosynthesis and physiology from the genome of Heliobacterium modesticaldum. *Photosynth Res* **104**, 113-122 (2010).

94. K. E. Redding *et al.*, Modulation of the fluorescence yield in heliobacterial cells by induction of charge recombination in the photosynthetic reaction center. *Photosynth Res* **120**, 221-235 (2014).

95. A. M. Collins, K. E. Redding, R. E. Blankenship, Modulation of fluorescence in *Heliobacterium modesticaldum* cells. *Photosynth Res* **104**, 283-292 (2010).

96. M. D. McConnell, J. B. Cowgill, P. L. Baker, F. Rappaport, K. E. Redding, Double reduction of plastoquinone to plastoquinol in photosystem 1. *Biochemistry* **50**, 11034-11046 (2011).

97. J. Biggins, Evaluation of selected benzoquinones, naphthoquinones, and anthraquinones as replacements for phylloquinone in the A1 acceptor site of the photosystem I reaction center. *Biochemistry* **29**, 7259-7264 (1990).

98. T. W. Johnson *et al.*, Recruitment of a foreign quinone into the A(1) site of photosystem I - I. Genetic and physiological characterization of phylloquinone biosynthetic pathway mutants in Synechocystis sp PCC 6803. *Journal of Biological Chemistry* **275**, 8523-8530 (2000).

99. T. W. Johnson *et al.*, Recruitment of a foreign quinone into the A(1) site of photosystem I - Invivo replacement of plastoquinone-9 by media- supplemented naphthoquinones in phylloquinone biosynthetic pathway mutants of synechocystis sp PCC 6803. *Journal of Biological Chemistry* **276**, 39512-39521 (2001).

100. C. R. Lancaster, M. V. Bibikova, P. Sabatino, D. Oesterhelt, H. Michel, Structural basis of the drastically increased initial electron transfer rate in the reaction center from a Rhodopseudomonas viridis mutant described at 2.00-A resolution. *J Biol Chem* **275**, 39364-39368. (2000).

101. A. Kroger, V. Dadak, On the Role of Quinones in Bacterial Electron Transport. *European Journal of Biochemisty* **11**, 328-340 (1969).

102. A. Amunts, O. Drory, N. Nelson, The structure of a plant photosystem I supercomplex at 3.4 A resolution. *Nature* **447**, 58-63 (2007).

103. E. P. Morris, B. Hankamer, D. Zheleva, G. Friso, J. Barber, The three-dimensional structure of a photosystem II core complex determined by electron crystallography. *Structure* **5**, 837-849 (1997).

104. J. Deisenhofer, O. Epp, K. Miki, R. Huber, H. Michel, X-ray structure analysis of a membrane protein complex. Electron density map at 3 A resolution and a model

of the chromophores of the photosynthetic reaction center from Rhodopseudomonas viridis. *J Mol Biol* **180**, 385-398 (1984).

105. M. Guergova-Kuras, B. Boudreaux, A. Joliot, P. Joliot, K. Redding, Evidence for two active branches for electron transfer in photosystem I. *Proc Natl Acad Sci U S A* **98**, 4437-4442. (2001).

106. N. Srinivasan, I. Karyagina, R. Bittl, A. van der Est, J. H. Golbeck, Role of the hydrogen bond from Leu722 to the A1A phylloquinone in photosystem I. *Biochemistry* **48**, 3315-3324 (2009).

107. S. Neerken, T. J. Aartsma, J. Amesz, Pathways of Energy Transformation in Antenna Reaction Center Complexes of Heliobacillus mobilis. *Biochemistry* **39**, 3297-3303 (2000).

108. M. Kobayashi *et al.*, Bacteriochlorophyll *g* epimer as a possible reaction center component of heliobacteria. *Biochim Biophys Acta* **1057**, 89-96 (1991).

109. S. Lin, H.-C. Chiou, F. A. M. Kleinherenbrink, R. E. Blankenship, Time-resolved spectroscopy of energy and electron transfer processes in the photosynthetic bacterium Heliobacillus mobilis. *Biophysical Journal* **66**, 437-445 (1994).

110. K. Brettel, W. Leibl, U. Liebl, Electron transfer in the heliobacterial reaction center: evidence against a quinone-type electron acceptor functioning analogous to A1 in photosystem I. *Biochim Biophys Acta* **1363**, 175-181 (1998).

111. A. van der Est, C. Hager-Braun, W. Leibl, G. Hauska, D. Stehlik, Transient electron paramagnetic resonance spectroscopy on green-sulfur bacteria and heliobacteria at two microwave frequencies. *Biochim Biophys Acta* **1409**, 87-98 (1998).

112. I. P. Muhiuddin, S. E. Rigby, M. C. Evans, J. Amesz, P. Heathcote, ENDOR and special TRIPLE resonance spectroscopy of photoaccumulated semiquinone electron acceptors in the reaction centers of green sulfur bacteria and heliobacteria. *Biochemistry* **38**, 7159-7167 (1999).

113. N. Fischer, M. Hippler, P. Setif, J. P. Jacquot, J. D. Rochaix, The PsaC subunit of photosystem I provides an essential lysine residue for fast electron transfer to ferredoxin. *Embo J* **17**, 849-858 (1998).